

Education: that which reveals to the wise, and conceals from the stupid,  
the vast limits of their knowledge—Mark Twain.

I may not have gone where I intended to go, but I think I have ended  
up where I needed to be—Douglas Adams.



**University of Alberta**

A Sedimentologic and Ichnologic Facies Model for Mud-Dominated Inner-Estuarine  
Deposits, Mary's Point and the Shepody River, Bay of Fundy, New Brunswick, Canada

By

Nadine Jennipher Pearson



A thesis submitted to the Faculty of Graduate Studies and Research in partial fulfillment  
of the requirements for the degree of Master of Science

Department of Earth and Atmospheric Sciences

Edmonton, Alberta

Spring 2006



Library and  
Archives Canada

Bibliothèque et  
Archives Canada

Published Heritage  
Branch

Direction du  
Patrimoine de l'édition

395 Wellington Street  
Ottawa ON K1A 0N4  
Canada

395, rue Wellington  
Ottawa ON K1A 0N4  
Canada

*Your file* *Votre référence*  
*ISBN: 0-494-13871-8*  
*Our file* *Notre référence*  
*ISBN: 0-494-13871-8*

**NOTICE:**

The author has granted a non-exclusive license allowing Library and Archives Canada to reproduce, publish, archive, preserve, conserve, communicate to the public by telecommunication or on the Internet, loan, distribute and sell theses worldwide, for commercial or non-commercial purposes, in microform, paper, electronic and/or any other formats.

The author retains copyright ownership and moral rights in this thesis. Neither the thesis nor substantial extracts from it may be printed or otherwise reproduced without the author's permission.

**AVIS:**

L'auteur a accordé une licence non exclusive permettant à la Bibliothèque et Archives Canada de reproduire, publier, archiver, sauvegarder, conserver, transmettre au public par télécommunication ou par l'Internet, prêter, distribuer et vendre des thèses partout dans le monde, à des fins commerciales ou autres, sur support microforme, papier, électronique et/ou autres formats.

L'auteur conserve la propriété du droit d'auteur et des droits moraux qui protègent cette thèse. Ni la thèse ni des extraits substantiels de celle-ci ne doivent être imprimés ou autrement reproduits sans son autorisation.

---

In compliance with the Canadian Privacy Act some supporting forms may have been removed from this thesis.

Conformément à la loi canadienne sur la protection de la vie privée, quelques formulaires secondaires ont été enlevés de cette thèse.

While these forms may be included in the document page count, their removal does not represent any loss of content from the thesis.

Bien que ces formulaires aient inclus dans la pagination, il n'y aura aucun contenu manquant.

  
**Canada**

This thesis is dedicated to the amazing silt and clay particles found in the upper portion of the Chignecto Bay estuary, without which none of this research would have been possible.

## ABSTRACT

Studies of fine-grained clastic sediments deposited in the macrotidal inner-estuarine mouth of Chignecto Bay, Bay of Fundy, New Brunswick, Canada cataloged the sedimentologic and ichnologic characteristics of tidal point bars and adjacent tidal flats. The aim of the study was to establish an ichnological model for application to the geological record.

Within the study area, the distribution of ichnological structures and sedimentary characteristics such as grain-size distribution and organic content are associated with bank bathymetry, tidal-bank slope, and the local hydraulic processes. The distribution of traces is associated with the duration of intertidal exposure and sedimentation rates. The seasonality of the depositional setting favors opportunistic fauna and thereby contributes to an impoverished brackish-water trace assemblage.

Bedding mimics the dip of the depositional surface. Variations in laminae thickness are attributed to spring-neap variation in tidal-current strength and an intercalation of laminated and burrowed beds represent seasonal variations in the depositional system.

## ACKNOWLEDGMENTS

The last three and a half years have certainly been unforgettable... whether its been wading through tidal creeks in Willapa Bay, Washington; standing thigh deep in mud in the Bay of Fundy; bush-whacking through jungle in New Zealand; running across outcrop between waves in New South Wales, Australia; or just simply hanging out at the Power Plant with colleagues/friends it has all been fantastic and thanks for all of the memories.

Thanks to Murray Gingras for initially asking me “how would you like to work in mud?” and for not being put off when I asked “are you serious?” For providing me with guidance in my research, encouragement when I needed it, help on those black days when I thought I would never finish, feedback on my writing, and for making me laugh (whether at myself, or directed at you). Thanks for being a person I could sit, relax and share a beer with.

Thanks to George “Jedi” Pemberton for the initial inspiration to begin a master’s degree at the University of Alberta. For encouraging and believing in me, and for making me believe that I could excel in the research arena.

I’m indebted to my husband, Andrew Pearson, without whose support and encouragement this work would not have been possible. Thanks for always being there for me when I was discouraged, for finding constructive ways for me to deal with the day-to-day stresses that my research provided, and for loving me.

Thanks to my parents, Daniel and Charlotte Watson, for always pushing me to do my best. Without your teachings I would never have come to this place in life. You have molded me into the person that I am today.

Thanks to my in-laws, Sharon and Dietmar Seibt, for providing support (whether financial or emotional) whenever I needed it. For caring for me like a daughter and providing me with my drive for excellence in everything I do. You always had faith in me and I truly appreciate it.

Thanks to Craig Madill, Darren Demaine, Mark Darrah and John Middleton for introducing me to a world in which I could escape. Without our late night gaming sessions I think I would have succumbed to the stresses of academic life a long time ago.

Thanks to Nerissa Harvey, Robert Grover, Patrick Nicoll, Kelli Fraser, Lynn Reich, Curtis Lettley, Keltie Elder, Shannon Galloway, Cameron and Victoria Webb, and Kathleen Gaylynn for providing ample distractions from my research. Whether you were there when I needed to go out, when I needed to vent or when I just wanted to go out and party. Without friends like you I do not think life would be the same.

Thanks to Nerissa Harvey, Shahin Dashtgard, Kerrie Bann and Tyler Hauck for outstanding field assistance and scientific guidance. A special thanks is given to Ian Armitage for commencing research at Mary's Point and the Shepody River locales.

And lastly, I would like to thank the Natural Science and Engineering Research Council (NSERC), BP Canada, ConocoPhillips Houston, Devon Energy, Nexen Energy, Petro Canada, and Talisman Energy for their financial support.

## Table of Contents

<b>1.0 INTRODUCTION</b>	<b>1</b>
1.1 Introduction	1
1.1.1 Thesis Outline	1
1.2 Study Area	2
1.2.1 Bay of Fundy	2
1.2.2 Mary's Point	3
1.2.3 Shepody River	4
1.3 Geological History	4
1.4 References	7
<b>2.0 AN ICHNOLOGICAL AND SEDIMENTOLOGICAL FACIES MODEL FOR MUDDY POINT-BAR DEPOSITS</b>	<b>10</b>
2.1 Introduction	10
2.1.1 Research Rationale	10
2.1.2 Methods	12
2.1.3 Geological Setting	14
2.2 Main Channel Point-bar Deposits	16
2.2.1 General Sedimentology and Ichnology of the Study Area	16
2.2.2 Detailed Sedimentology and Ichnology of the Cut-bank Sections	20
2.2.3 Total Organic Carbon and Grain-size Analysis	23
2.3 Interpretations	25
2.3.1 Preservation of a Tidal Signature	25
2.3.2 The Significance of Convolute Bedding and Pebbly Lags	26

2.3.3	Mud Deposition at the Shepody River	27
2.3.4	Interpretation of IHS Sedimentological and Ichnological Variability	29
2.4	Summary	32
2.5	References	34

### **3.0 AN ICHNOLOGICAL AND SEDIMENTOLOGICAL FACIES MODEL FOR**

	<b>MUD-FLAT DEPOSITS</b>	<b>40</b>
3.1	Introduction	40
3.1.1	Research Rationale	40
3.1.2	Methods	41
3.1.3	Geological Setting	44
3.2	Tidal-Flat and Tidal-Creek Point-Bar Deposits	46
3.2.1	General Sedimentology and Ichnology of the Study Area	46
3.2.2	Detailed Sedimentology and Ichnology of the Cut-bank and Mud-flat Sections	54
3.2.3	Total Organic Carbon and Grain-size Analysis	57
3.3	Interpretations	59
3.3.1	Preservation of a Tidal Signature	59
3.3.2	The Significance of Convolute Bedding and Pebbly Lags	60
3.3.3	Deposition and Accumulation of Muddy Sediment at Mary's Point	61
3.3.4	Morphology of the Mud Flat	62
3.3.5	Sedimentologic and Ichnologic Variability at Mary's Point	63

3.4 Summary	66
3.5 References	68
<b>4.0 THE SIGNIFICANCE OF ATLANTIC STURGEON FEEDING EXCAVATIONS, MARY'S POINT, BAY OF FUNDY, NEW BRUNSWICK, CANADA</b>	<b>75</b>
4.1 Introduction	75
4.1.1 Research Rationale	75
4.1.2 Methods	76
4.1.3 Geological Setting	77
4.2 The Atlantic Sturgeon ( <i>Acipenser oxyrhynchus</i> )	79
4.3 Feeding Excavations of <i>Acipenser oxyrhynchus</i>	80
4.4 Organism and Trace Distribution	84
4.4.1 Observations	85
4.4.2 Interpretations	85
4.5 Orientation and Time of Excavation	86
4.5.1 Observations	86
4.5.2 Interpretations	92
4.6 Bioerosion and Redeposition Capabilities	92
4.7 Discussion	94
4.8 Conclusions	95
4.9 References	97
<b>5.0 CONCLUSIONS</b>	<b>100</b>

## List of Figures

<b><u>Description:</u></b>	<b><u>Page:</u></b>
<b>Figure 1-1:</b> Location map of Chignecto Bay, Mary's Point and the Shepody River, Bay of Fundy, New Brunswick, Canada. (A) Map of Canada with the Bay of Fundy marked by the solid box. (B) Schematic diagram of Chignecto Bay. The solid box marks the Shepody River locale, and the dashed box identifies the Mary's Point locale.	3
<b>Figure 1-2:</b> Post-glacial relative sea-level changes from 13000 BP to present. Originally modified and adapted from Shaw and Courtney (2002).	6
<b>Figure 2-1:</b> Location map of Chignecto Bay in the Bay of Fundy, New Brunswick, Canada. (A) Map of Canada with the Bay of Fundy identified by the solid box. (B) Schematic diagram of Chignecto Bay with the study area marked by the dashed box. The star identifies the most basinward station. (C) Air photo of the Shepody River in 2001.	11
<b>Figure 2-2:</b> Bioturbation intensity (BI). Measurement of the intensity of bioturbation in the Shepody River deposits; originally adapted and modified from Reineck (1963), Taylor et al. (2003), and Bann et al. (2004).	14

**Figure 2-3:** Different scales of view for muddy, main channel point bars. (A) Point-bar deposits exposed during low tide. (B) Side profile of Shepody most basinward (cut bank) exposure. Deposits are stepped and each step represents a single (seasonal) unit. (C) Front view of Shepody outcrop. Deposits are laterally continuous across the point bar. 16

**Figure 2-4:** Schematic diagram of an intertidal point-bar assemblage (substrate silty- to sandy-mud) at Shepody River. The trace assemblage shown represents the dominant bioturbators present in an intertidal point bar within the Shepody River. The upper-intertidal zone is characterized by the activity of the nereid worm *Nereis virens* and *diversicolor* and the bivalve *Macoma balthica*. *Nereis* produces *Polykladichnus*, *Palaeophycus*, and *Planolites* traces; while *Macoma* makes *Siphonichnus* burrow forms. The middle-intertidal zone is dominated by the amphipod *Corophium volutator*, which creates the traces *Arenicolites* and *Diplocraterion*. The upper-subtidal to lower-intertidal zones are typified by *Polykladichnus* and *Skolithos* burrows, which are the result of the work of the capitellid polychaete *Heteromastus*. The lower, more stressed portion of the point bar has the highest preservation potential. 17

**Figure 2-5:** Traces observed in the Shepody River sediments. (A) *Skolithos* (Sk) and *Polykladichnus* (Pk), made by *Heteromastus*, vertical face, scale in centimetres. (B) *Siphonichnus* (Si), created by *Macoma balthica* (shown), vertical face, scale in centimetres. (C) Fin trace (?*Undichnia*), plan view, scale = 2.5 cm (quarter). (D) *Arenicolites* (Ar), generated by *Corophium volutator*, plan view, scale = 3 cm. (E) *Palaeophycus* (Pa), produced by *Nereis virens*, plan view, scale = 1.8 cm (dime).

19

**Figure 2-6:** Vertical section of Shepody low-tide exposure showing the sedimentological and ichnological characteristics. Base is at lower-left and top at the upper-right. Note massive versus laminated interbeds—these are interpreted to be the result of variable seasonal processes.

20

**Figure 2-7:** Seasonal deposits of the Shepody River. (A) Spring deposits typified by parallel-laminated silty mud and little or no bioturbation (BI 0 to 1). Arrows highlight the variation in laminae thickness. (B) Transition from spring to summer deposition with variable bioturbation intensities (BI 0 to 3, typically 2). (C) Summer and fall deposits characterized by pervasive bioturbation (BI 2 to 6, commonly 5). Scale is in centimetres.

22

- Figure 2-8:** Typical grain diameter distribution found in a single seasonal deposit (summer to fall) in the Shepody River. 23
- Figure 2-9:** Vertical section of Shepody outcrop shows the distribution of total organic carbon (TOC) and grain-size. Note while TOC decreases, the proportion of silt and sand increases upwards. See Fig. 2-8 for typical grain distribution. 24
- Figure 2-10:** Total organic carbon scatter plot. Note the initial increase in TOC values up the exposure but as grain-size increases up section the TOC percentages decrease. 25
- Figure 2-11:** Schematic diagram showing the facies transition within a Shepody low-tide exposure. Note the vertical trends in the sedimentology, ichnology, and TOC values. 31
- Figure 3-1:** Schematic diagram of the sampling transects across Mary's Point. (A) Diagram shows the locations of the 26 exposures that were examined for the sedimentological and ichnological characteristics. These sections lie on 7 transects completed across the intertidal flat. (B) Diagram displays the location of the 38 stations that TOC and grain-size data was gathered. These lie on 4 transects completed across the intertidal flat. Note that the map grid was taken from an NTS map, each Square is 100 X 100 m. 41

**Figure 3-2:** Bioturbation intensity (BI). Measurement of the intensity of bioturbation in the Mary's Point deposits; adapted and modified from Reineck (1963), Taylor et al. (2003), and Bann et al. (2004). 43

**Figure 3-3:** Location map of Chignecto Bay and Mary's Point, Bay of Fundy, New Brunswick, Canada. (A) Map of Canada with the Bay of Fundy marked by the solid box. (B) Schematic diagram of Chignecto Bay, and the location of the study identified by the dashed box. 44

**Figure 3-4:** Sedimentary structures present in the deposits at Mary's Point. (A) Cut bank exposure showing the transition from horizontal, planar-bedded deposits in the upper point bar down into the low-angle, planar-bedded deposits of the lower point bar. The dashed line marks the transition point between these deposits. Scale = 2 m (ruler). (B) Lower point-bar deposits characterized by low-angle, planar-bedding. (C) Upper point-bar deposits typified by horizontal, planar bedding. Units found in this section display a seasonal nature, which is marked by the transition from laminated (early winter and (primarily) spring) to bioturbated (summer to fall). 46

**Figure 3-5:** Different scales of view for convoluted bedding found at Mary's Point. (A) Large-scale deformation found in the upper portion of a point bar. Shovel for scale. (B) Small-

scale deformation found in a laminated deposit. Most beds at Mary's Point display this scale of deformation. Scale is in centimetres. (C) Deformation marked by the presence of the patchy pebble/gravel lag. Note the wavy nature of the deformation. The pebble/gravel clasts are accumulating in the synclines of the deformed sediment. (D) Placement of the pebble/gravel lags tends to occur above the bioturbated and below the laminated beds. The arrow points to the pebble/gravel clasts in the syncline of the deformed sediment.

47

**Figure 3-6:** Morphological features of Mary's Point. (A) Photo shows a shallow, tidal creek in the upper-intertidal zone. Within this zone tidal creeks have broad meanders and creek depths ranging up to 17 cm. Note the right-angle meander-bends and small point bars developed in the foreground. (B) Photo of a tidal creek in the middle-intertidal zone. Noteworthy is the difference in channel depth and width observed from the upper-intertidal to the middle-intertidal zones. Within this zone, tight meanders and channel depths greater than 1.4 m characterize the tidal creeks. Arrows point to areas displaying rotational slumping. (C) Down channel view of a tidal creek in the middle-intertidal zone. Arrows highlight areas where slumping is common. Note that in areas near the creek bend slumping increases and displays characteristics of rotational slumping.

48

**Figure 3-7:** Infaunal traces observed in the Mary's Point sediment. (A) *Polykladichnus* (Pk), made by *Nereis virens*, vertical face, scale = 3 cm. (B) Surface trace made by *Macoma balthica* while interface feeding. The 'star-like' appearance of this trace is the result of the *Macoma's* siphon probing the sediment (shown in photo). Image is in plan view; scale = 3 cm. (C) Extensive horizontal network of *Nereis virens*. The traces resemble the ichnogenera *Planolites* (Pl) and *Palaeophycus* (Pa). Image is in plan view, scale is in centimetres. (D) Surface trace made by *Corophium volutator* while interface feeding. The grooves leading to the burrow opening are the result of *Corophium* scraping the sediment with their antennae. Arrows point to individual examples of this trace. Image is in plan view, scale = 3 cm. (E) *Diplocraterion* (Di), generated by *Corophium volutator*, vertical face, scale = 3 cm. (F) *Siphonichnus* (Si), generated by *Macoma balthica* (shown), vertical face, scale is in centimetres.

51

**Figure 3-8:** Schematic diagram of an intertidal point-bar assemblage (substrate is silty- to sandy-mud) at Mary's Point. The trace assemblage shown represents the dominant bioturbators present in an intertidal point bar within Mary's Point. (A) The lower-intertidal zone is typified by *Polykladichnus*, *Palaeophycus*, *Planolites* and *Skolithos* burrows. These are the work of *Heteromastus*, *Nereis virens*, *Cerebratulus lacteus*, and *Glycera dibranchiata*. (B) The middle-intertidal

zone is dominated by the amphipod *Corophium volutator*, which creates the traces *Arenicolites* and *Diplocraterion*. Other bioturbators present within this zone are *Nereis virens* and *N. diversicolor*, which make *Polykladichmus*, *Planolites*, and *Palaeophycus*; and the bivalve *Macoma balthica*, which produces the trace *Siphonichmus*. (C) The upper-intertidal zone is characterized by the activity of *Nereis virens* and *diversicolor*, *Macoma balthica*, and *Corophium volutator*. *Nereis* produces *Polykladichmus*, *Palaeophycus*, and *Planolites* traces; *Macoma balthica* makes *Siphonichmus* burrow forms; and *Corophium* generates *Arenicolites* and *Diplocraterion* traces.

52

**Figure 3-9:** Traces found on the depositional surface at Mary's Point. (A) *Undichnia* (Und), made by a flatfish, scale is in centimetres. (B) *Piscichnus*, made by an Atlantic sturgeon, scale = 5 cm. The position of the snout impression in relation to the excavation pit correlates to the anatomical arrangement of the Atlantic sturgeon's snout and protractile mouth. (C) *Piscichnus* (Psc) and *Undichnia* (Und), made by a flatfish, scale = 5 cm. (D) *Undichnia* (Und), made by an Atlantic sturgeon, scale in centimetres. (E) The trackway of a Great Heron, scale = 15 cm (pencil).

53

**Figure 3-10:** Seasonal deposits at Mary's Point. (A) Spring deposits typified by horizontal, planar laminated silty- and sandy-mud, and little or no bioturbation (BI 0-2, typically 1). (B) Laminated unit characterized by horizontal, planar-bedding. Within this unit alternations in individual bed thickness were documented; thinner deposits are characteristic of neap tidal cycles (shown), while thicker deposits are from spring tidal cycles (shown). (C) Summer to fall deposits characterized by pervasive bioturbation (BI 2-6, commonly 5).

54

**Figure 3-11:** Isolated occurrences of current ripples on the present day intertidal surface. (A) Sand lens found on the foreground of a point bar. This sand was likely transported from the supratidal zone by ice rafting in the early spring. Ripple foresets dip to the west indicating flood-dominated transport. Scale = 20 cm (arrow). (B) Coarse silt lens found on the intertidal flat. Ripple foresets dip to the southwest indicating flood-dominated transport.

55

**Figure 3-12:** TOC and grain-size trends measured on the present day intertidal surface at Mary's Point. Note the arrow pointing in the direction of fetch. (A) TOC values. There is an increase in TOC values in the landward direction, with the larger values occurring in areas sheltered from wave action. (B) Mean grain-size values. There is a decrease in grain-size

in the landward direction, with the larger values found in areas dominated by wave reworking. Note that the TOC contours occur in the same areas as the mean grain-size contours. (C) Modal grain-size values. Similar to the mean grain-size values these values also decrease in the landward direction and are greatest in areas characterized by wave action. 58

**Figure 4-1:** Typical sturgeon feeding excavation. The shallow, crescent-shaped snout-impression houses the preserved barbel impression and is closely followed by the cylindrical plug-shaped excavation. Substrate is silty- to sandy-mud and excavations are usually 2 to 6 cm in depth. Note that bay water is impounded within the cylindrical excavation. Scale is 10 cm. 75

**Figure 4-2:** Location map of Chignecto Bay and Mary's Point, Bay of Fundy, New Brunswick, Canada. (A) Map of Canada with the Bay of Fundy identified by the solid box. (B) Schematic diagram of Chignecto Bay, and the location of the study area (dashed box). 78

**Figure 4-3:** Sketch of the Atlantic Sturgeon, *Acipenser oxyrinchus*. Sketch by Karmen Zivkovic. 79

**Figure 4-4:** Infaunal community present within the intertidal sediment at Mary's Point. (A) *Corophium volutator*, scale = 1 cm. (C) *Nereis diversicolor*, scale in centimetres. (C) *Cerebratulus lacteus*, scale = 3 cm. (D) *Glycera dibranchiata*, scale = 3 cm. (E) *Nereis virens*, scale = 3 cm. (F) *Macoma balthica*, scale = 3 cm. (G) *Heteromastus*, scale = 3 cm.

80

**Figure 4-5:** A comparison between the intertidal mud flat surfaces between May 2003 and July 2004. Arrows highlight individual examples of the sturgeon traces. Note that bay water is pooling in many of the excavations. (A) Sturgeon feeding at the height of spawning season. The intertidal mud flat is completely reworked by their foraging activity. Both the banks of the intertidal creek and the mud flat surfaces adjacent to it are littered with traces. Photo taken in May 2003. (B) Sturgeon feeding frenzy on the bank of the intertidal creek. On this bank there are over 400 individual excavations present. Noteworthy is the lack of feeding pits on the mud flat surfaces adjacent to the intertidal creek. Photo taken in July 2004.

82

**Figure 4-6:** Atlantic sturgeon fin-trace (*Undichnia*), scale in centimetres.

83

**Figure 4-7:** Atlantic sturgeon fecal material. (A) Example of fecal material broken up by tidal processes. It usually takes at least two tidal cycles to break up this material. Arrows point to shell debris contained in expelled sediment. Scale is in centimetres. (B) Example of fecal material not broken up by tidal processes. Scale is 15 cm.

83

**Figure 4-8:** Schematic diagram showing infaunal distribution and Atlantic sturgeon feeding trends across Mary's Point. (A) Infaunal distribution across Mary's Point. Letters indicate dominant food source for the Atlantic sturgeon at each stations. C= *Corophium volutator*, M= *Macoma balthica*, and P= polychaetes. In instances where the dominant food source is more than one organism both are included. Subdivision of the intertidal mud flat through the distribution of dominant benthos is shown. UIZ= Upper Intertidal Zone, MIZ= Middle Intertidal Zone, and LIZ= Lower Intertidal Zone. (B) Atlantic sturgeon feeding trace distribution across Mary's Point. The number of sturgeon excavations found at each station is shown. (C) This diagram highlights general areas of high (>50 traces / 100 m<sup>2</sup>) and low (<50 traces / 100 m<sup>2</sup>) trace abundance. Note that areas of high sturgeon trace abundance are loosely correlated with areas dominated by the amphipod *Corophium volutator*. The grid was taken from a NTS map, each square is 100 X 100 m.

84

**Figure 4-9:** Schematic representation of average orientation trends at each station at Mary's Point. Arrows highlight the directions the fish are aligning. The grid was taken from a NTS map, each square is 100 X 100 m.

86

**Figure 4-10:** Rose diagrams constructed for the sturgeon-snout orientations with 10° petals. Letters correspond to individual stations at Mary's Point (inset map). Each rose diagram corresponds to an area of 100 m<sup>2</sup>. The grid for the inset map was taken from a NTS map, each square is 100 X 100 m.

88

**Figure 4-11:** Schematic diagram demonstrating dominant current directions during the subsequent stages of the tidal cycle at Mary's Point. (A) At rising tide, flood currents (~45°) are dominant on the intertidal flat. Expected sturgeon-snout orientations are parallel but opposite to this direction (200° to 260°). (B) During slack-water conditions minimal current energy is observed. This stage is short (~30 minutes) and orientations of the traces can be in any direction. (C) Initial stages of falling tide are characterized by tidal currents in the ebb direction (~225°). Under these circumstances sturgeon-snout orientations will be parallel but opposite to this direction (20° to 80°). (D) The final stages of falling tide are dominated by local currents directed towards the intertidal creeks. During this phase, trace orientations are found in many directions but can be grouped into the following orientations: 0° to 20°, 80° to 200°, and 260°

to 360°. The sturgeon-snout orientations will depend on position near the intertidal creek, tidal creek morphology and which intertidal creek observations are made at. Note: Slack-water phase at low-tide is not depicted.

## **1.0 INTRODUCTION**

### **1.1 Introduction**

Research from Mary's Point and the Shepody River in the Bay of Fundy, New Brunswick, Canada documents the sedimentological and ichnological characteristics of the fine-grained deposits found in the inner portion of the Chignecto Bay estuary. This study provides the criteria for identifying both point-bar and mud-flat deposits in the modern and ancient sedimentary record. Much of the previous research within estuaries has been focused on systems that are dominated by sand (Amos 1987; Amos 1988; Dalrymple et al. 1991; Nio and Yang 1991; Clifton 1997; Allen and Duffy 1998; Gingras et al. 1999; Gingras et al. 2002; Choi et al. 2004). Notably, there is a lack of research on the mud-dominated estuarine environments within the literature. These muddy deposits are common in many ancient sedimentary successions but so far lack an integrated sedimentological and ichnological model to use in paleoenvironmental reconstruction. In order to advance understanding of depositional conditions within the inner estuary a more thorough treatment of mud-dominated sedimentary accumulations is required.

In general, the Shepody River and Mary's Point sediments comprise fine-grained (mud-dominated), tidally derived sediment. To capture a range of sedimentary environments observations were gathered within an intertidal mud flat (Mary's Point) and a tidal-channel complex (Shepody River) (Fig. 1.1). Both of these locales are characterized by point-bar and tidal-flat deposits, however Shepody has first-order tidal channel point bars and Mary's Point does not.

#### **1.1.1 Thesis Outline**

Chapter 2 scrutinizes the sedimentology and ichnology of first order tidal point-bar deposits using the Shepody River as the main dataset. The main foci of this chapter are characterizing the sedimentologic and ichnologic trends found within an intertidal point bar, relating these trends to the environmental conditions at the time of deposition,

and resolving the temporal nature of the tidal deposits.

Chapter 3 examines the sedimentology and ichnology of tidal-creek point-bar and tidal-flat deposits using Mary's Point as the primary dataset. This chapter provides a detailed description of the lateral trends in sedimentology and ichnology across the intertidal-flat surface, the morphologic features present within a mud flat environment, and the temporal nature of the tidal deposits.

Chapter 4 documents the occurrence and potential significance of Atlantic sturgeon (*Acipenser oxyrinchus*) feeding traces that were observed on the intertidal mud flats of Mary's Point. This chapter documents the trends in trace and infaunal abundance across the intertidal-flat surface, and the contribution that the foraging/feeding behavior of the sturgeon have on bioerosion and substrate cohesiveness.

## **1.2 STUDY AREA**

### **1.2.1 Bay of Fundy**

The Bay of Fundy is a macrotidal estuary on the southeastern coast of New Brunswick, Canada (Fig. 1-1A). It is a funnel-shaped bay that is 270 km in length and 80 km in width at its head. The Bay of Fundy tides have been well described in Amos et al. (1991), and Desplanque and Mossman (2001) as the largest documented tides in the world. The extreme tidal characteristics are the result of a combination of diurnal and semidiurnal tides. The tidal range within the upper reaches of the Bay of Fundy was documented to exceed 14 m (mean values: spring 11.3 m and neap 7.2 m), and as such is classified as macrotidal (Amos et al. 1991; Desplanque and Mossman 2001) or even in some instances as hypertidal (Allen and Duffy 1998). These large tides are attributed to the Bay's near resonance with the tides in the Atlantic Ocean (Desplanque and Mossman 2001).

The Bay of Fundy's head is split into two smaller bays, Chignecto Bay and the Minas Basin. The Minas Basin is dominated by sand accumulation and has been

thoroughly examined by Dalrymple (1979, 1984), Dalrymple et al. (1991), and Amos et al. (1992). Chignecto Bay is a “muddy” estuary due to the nature of its sediment sources, the eroded cliffs that surround the bay and the exhumed seabed. These are composed of Paleozoic mudstone and sandstone, and Holocene silt and clay, respectively (Amos 1987). In comparison to the Minas Basin, very little sedimentological and ichnological research has been conducted within Chignecto bay, barring the research completed by Amos (1987) and Amos et al. (1991).

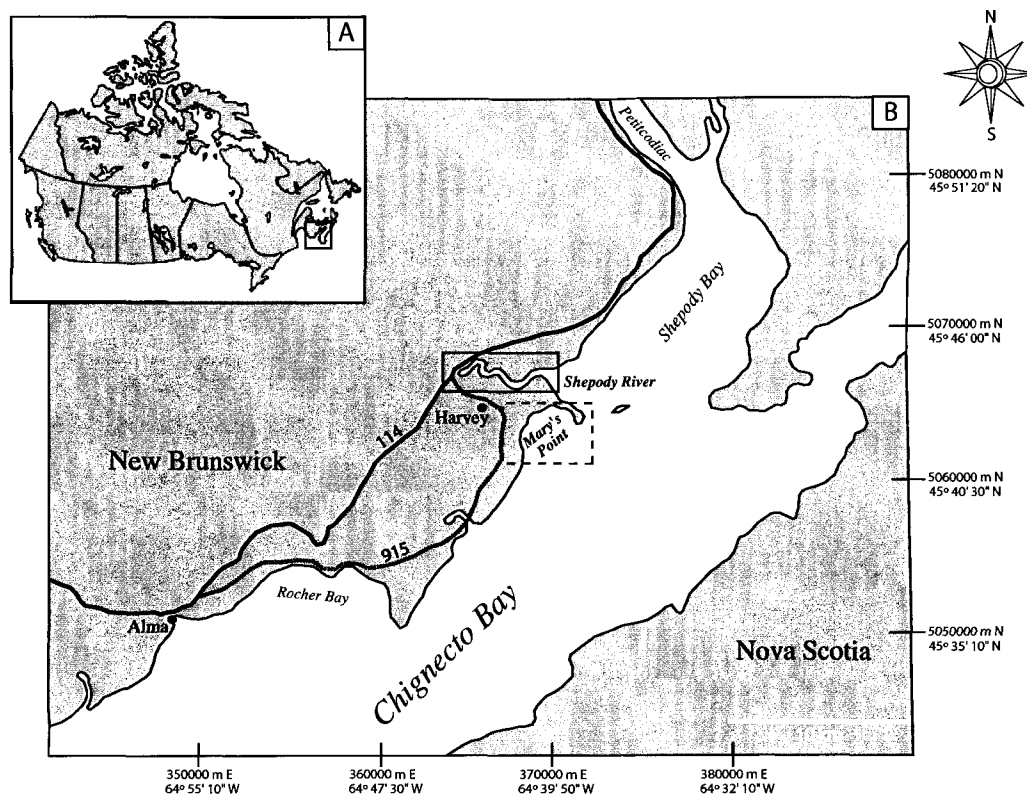


**Figure 1-1:** Location map of Chignecto Bay, Mary’s Point and the Shepody River, Bay of Fundy, New Brunswick, Canada. (A) Map of Canada with the Bay of Fundy marked by the solid box. (B) Schematic diagram of Chignecto Bay. The Shepody River locale is marked by the solid box, and the Mary’s Point locale is identified by the dashed box.

### 1.2.2 Mary’s Point

Mary’s Point (N45°43’45”, W64°39’50”; 5065000 m, 0370000 m: Fig. 1-1B) is located in the northeast portion of Chignecto Bay and covers an area of approximately 12 km<sup>2</sup> at mean high tide. This locale is characterized by an intertidal mud flat surface that

is dissected by numerous tidal creeks. Creek bank exposures were observed to range in height from 0.17 (upper-intertidal) to 1.4 m (lower-intertidal) with widths found in excess of 17 m. Low-tide water depths in the thalweg generally range between 0.10 (upper-intertidal) to 0.75 m (lower-intertidal) at times of low river flow. The sedimentary texture of the deposits is dominated by the accumulation of fine-grained sediment composed dominantly of silt and clay (mean values: 65% silt, 25% clay and 10% sand).

### **1.2.3 Shepody River**

The Shepody River (N45°44'00", W64°43'30"; 5067070 m N, 0369780 m E: Fig. 1-1B) is in the northeast portion of Chignecto Bay and covers an area of approximately 51 km<sup>2</sup> at mean high tide. The Shepody Estuary exhibits a distinctive funnel shape in plan view, an attestation to its tidal dominance. Channel point-bar relief ranges from 6 to 15 m (average 10 m), with low-tide riverbank exposures ranging between 1.7 to 3.2 m. Point-bar deposits are laterally continuous, and occur over distances exceeding 26 m. The current velocities for one tidal cycle were observed to peak at 80 cm/sec (surface-water velocity at center of channel) and are highest during maximum ebb tides. Salinity measurements were taken during rising-tide conditions in the late spring to early summer (April to July), and were taken at two locations within the channel. The values found at these locations ranged from 27 ppt near the study area to 16 ppt at the landward locale. The waters at the Shepody river locale have a high sediment load held in suspension and were found to be in excess of 21 gm / liter. Grain-size analyses show that the typical texture is: silt (66%), clay (24%), and sand (10%).

### **1.3 GEOLOGICAL HISTORY**

The structural Bay of Fundy originated during the Appalachian Orogeny approximately 286 to 360 million years ago (Desplanque and Mossman 2001). This system was largely controlled by the development of the Chignecto-Chedabucto-

Cobequid Fault Zone (C<sup>3</sup>FZ) (Amos et al. 1991). Post Acadian and Appalachian tectonic events (Carboniferous-Permian) along the C<sup>3</sup>FZ resulted in the formation of a series of semi-connected depositional basins infilled with terrestrial, shallow marine and volcanic material (Amos et al. 1991). The bedrock geology expresses Triassic half-graben basinal development, which began 430 million years ago (Amos et al. 1991). This half-graben complex displaces Precambrian volcanics and Paleozoic fluvial and deltaic sediments; the half graben was subsequently infilled during the Triassic Period (Amos et al. 1991). Infilling was followed by a phase of basaltic lava eruptions (Desplanque and Mossman 2001). Clastic sediment deposition resumed late into the Middle Jurassic and was followed by a period of extensive folding, and uplifting of strata (Caledonian Orogeny) (Desplanque and Mossman 2001). The overall orientation of the strata was tilted southwestward into a saucer-shaped structure (Desplanque and Mossman 2001). Sporadic sedimentation continued into the Cretaceous, however, these deposits were only preserved in the lowlands adjacent to the Bay of Fundy (Desplanque and Mossman 2001). Cretaceous strata rest unconformably on Triassic and Carboniferous rocks as a result of Cretaceous and Tertiary fluvial incision events (Amos et al. 1991; Desplanque and Mossman 2001).

Over the last 15000 years, Chignecto Bay has been affected by rapid sea level changes and large changes in the tidal regime (Amos et al. 1991:Fig. 1-2). The submergence of Chignecto Bay through ice loading was greatest (55 m) at approximately 15000 BP (Amos et al. 1991). During this time deltaic deposits were formed along the front of the ice-sheet through melt-out into the inundated Bay of Fundy (Amos et al. 1991). The Chignecto isthmus emerged at 12000 BP and both the Georges and Browns Banks reached maximum emergence around 11000 BP (Shaw and Courtney 2002). Marine reworking and erosion of glacial deposits into gravel beds subsequent to deglaciation (13300 to 10000 BP) is suggestive of strong tidal currents present in Chignecto Bay (Amos et al. 1991). This is tentatively correlated with a brief period of

macrotidal conditions that peaked at 12000 BP as postglacial emergence caused sea level to approach that of today (Amos et al. 1991). Fresh water Holocene deposits found at a depth of 25 m below mean sea level within Chignecto Bay demonstrate that glacial rebound resulted in the relative emergence of the Chignecto Bay system (Amos et al. 1991). From 6000 BP until present the relative sea level rose 15 cm/century causing the submergence of the Georges and Browns Banks (Amos et al. 1991). Their eventual submergence relaxed the limitations they had imposed on the overall tidal regime, and as a result the tidal range increased 30 cm/century (Amos et al. 1991). With the increase in tidal range the Bay of Fundy became increasingly macrotidal (Amos et al. 1991).

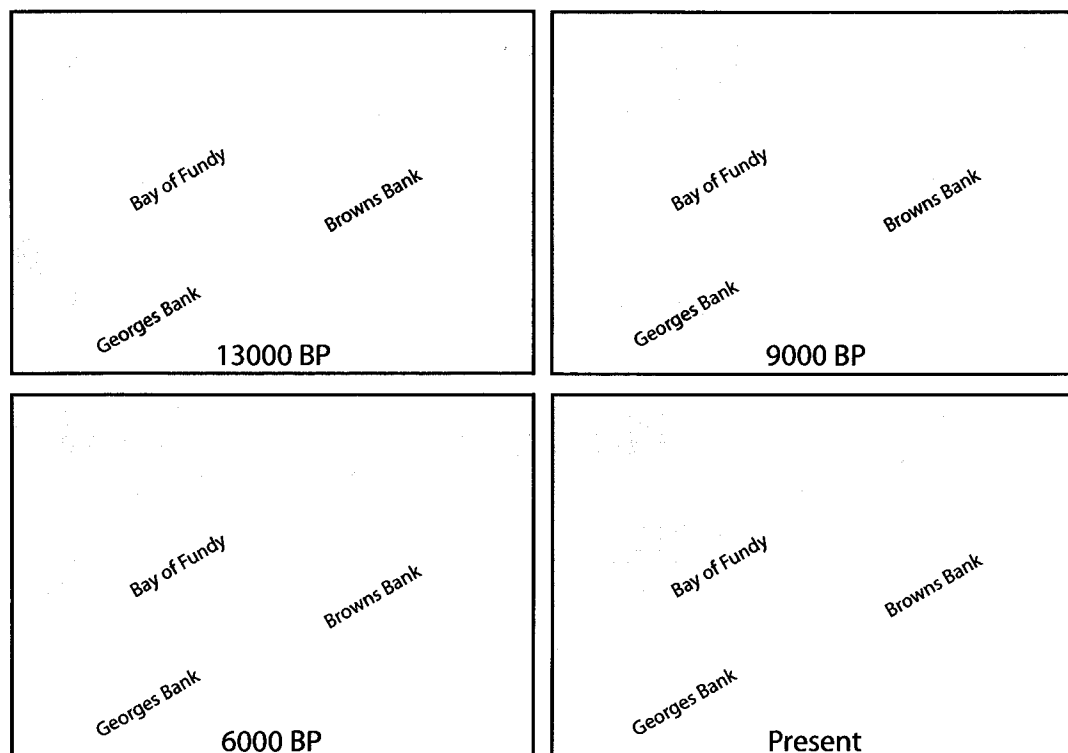


**Figure 1-2:** Post-glacial relative sea-level changes from 13000 BP to present. Modified and adapted from Shaw and Courtney (2002).

#### 1.4 REFERENCES

Allen, J., and Duffy, M., 1986, Medium-term sedimentation on high intertidal mudflats and salt marshes in the Severn estuary, SW Britain: The role of wind and tide: *Marine Geology*, v. 150, p. 1-27.

Allen, J., and Duffy, M., 1998, Temporal and spatial depositional patterns in the Severn Estuary, southwestern Britain: intertidal studies at spring-neap and seasonal scales, 1991-1993: *Marine Geology*, v. 146, p. 147-171.

Amos, C.L., 1987, Fine-grained sediment transport in Chignecto Bay, Bay of Fundy, Canada: *Continental Shelf Research*, v. 7, p. 1295-1300.

Amos, C.L., 1988, The influence of subaerial exposure on the bulk properties of fine-grained intertidal sediment from Minas Basin, Bay of Fundy: *Estuarine, Coastal and Shelf Science*, v. 27, p. 1-13.

Amos, C.L., and Mosher, D.C., 1985, Erosion and deposition of fine-grained sediments from the Bay of Fundy: *Sedimentology*, v. 32, p. 815-832.

Amos, C.L., Tee, K.T., and Zaitlin, B.A., 1991, The post-glacial evolution of Chignecto Bay, Bay of Fundy, and its modern environment of deposition: *Canadian Society of Petroleum Geologists, Memoir 10*, p. 59-90.

Amos, C.L., Daborn, G.R., Christian, H.A., Atkinson, A., and Robertson, A., 1992, In situ erosion measurements on fine-grained sediments from the Bay of Fundy: *Marine Geology*, v. 108, p. 175-196.

Choi, K.S., Dalrymple, R.W., Chun, S.S., and Kim, S.P. 2004, Sedimentology of modern, inclined heterolithic stratification (IHS) in the macrotidal Han River Delta, Korea: *Journal of Sedimentary Research*, v. 74, no. 5, p. 677-689.

Clifton, H.E., 1997, Tidal sedimentation and facies: Canadian Society of Petroleum Geologists Short Course, Supplementary Field Guide.

Dalrymple, R.W., 1979, Wave-induced liquefaction: a modern example from the Bay of Fundy: *Sedimentology*, v. 26, p. 835-844.

Dalrymple, R.W., 1984, Morphology and internal structure of sandwaves in the Bay of Fundy: *Sedimentology*, v. 31, p. 365-382.

Dalrymple, R.W., Makino, Y., and Zaitlin, B.A., 1991, Temporal and spatial patterns of rhythmic deposition on mud flats in the macrotidal Cobequid Bay-Salmon River Estuary, Bay of Fundy, Canada, *in* Smith, D. G., Zaitlin, B. A., Reinson, G. E., & Rahmani, R. A., eds., *Clastic Tidal Sedimentology*, Canadian Society of Petroleum Geologists, Calgary, Alberta, Memoir 16, p. 137-160.

Desplanque, C., and Mossman, D., 2001, Bay of Fundy tides: *Geoscience Canada*, v. 28, p. 1-11.

Gingras, M.K., Pemberton, S.G., Saunders, T., and Clifton, H.E., 1999, The ichnology of modern and Pleistocene brackish-water deposits at Willapa Bay, Washington: variability in estuarine settings: *Palaios*, v. 14, p. 352-374.

Gingras, M.K., Rasanen, M., and Ranzi, A., 2002, The significance of bioturbated

inclined heterolithic stratification in the southern part of the Miocene Solimoes Formation, Rio Acre, Amazonia Brazil: *Palaios*, v. 17, p. 591-601.

Nio, S.D., and Yang, C.S., 1991, Diagnostic attributes of clastic tidal deposits: a review, *in* Smith, D. G., Zaitlin, B. A., Reinson, G. E., & Rahmani, R. A., eds., *Clastic Tidal Sedimentology*, Canadian Society of Petroleum Geologists, Calgary, Alberta, Memoir 16, p. 3-28.

Shaw, J., and Courtney, R.C., 2002, Postglacial coastlines of Atlantic Canada: Geological Survey of Canada, Open File Report 4302, digital images.

## **2.0 AN ICHNOLOGICAL AND SEDIMENTOLOGICAL FACIES MODEL FOR MUDDY POINT-BAR DEPOSITS**

A version of this chapter has been accepted for publication in *The Journal of Sedimentary Research*. Pearson, N.J., and Gingras, M.K. *in press*.

### **2.1 INTRODUCTION**

#### **2.1.1 Research Rationale**

Mud-dominated point bars and intertidal flats are a common and aerially important component of many estuaries, but their physical *and* biological characteristics are seldom studied together. Previous estuarine research (Amos and Mosher 1985; Amos 1987; Dalrymple et al. 1990, 1991, 1992) has shown the importance of the physical sedimentological criteria but generally understates the potential biogenic sedimentary structures have for interpreting marginal-marine deposits. The development of a detailed ichnological characterization of muddy point-bar deposits is desirable if only to produce more-detailed paleogeographic models for application to the sedimentary record. Integration of ichnology into a sedimentological framework allows recognition of lateral variation and identification of key subenvironments within estuarine deposits (Reineck 1963; Howard and Frey 1975; Pemberton et al. 1982; Pemberton and Wightman 1992; MacEachern et al. 1999; Gingras et al. 2002).

Estuarine mudstones, in particular point-bar deposits, are the least understood of brackish-water deposits: this is partly due to a perceived lack of utility for their application to subsurface reservoir rocks. Also, very muddy deposits in modern settings are not the most attractive subjects for study. Due to minimal textural heterogeneity, primary lamination is commonly difficult to observe, and mobility about mud flats is limited by their locally fluid nature. On the other hand, biogenic structures can be easily observed, especially in firmer substrates, and eroded cut banks can reveal sedimentary lamination effectively.

Inclined heterolithic stratification has been a popular subject in recent years, subsequently numerous papers describing IHS in ancient settings (Smith 1987, 1988, 1989; Thomas et al. 1987; Eberth 1996; Gingras et al. 2002; Bann et al. 2004) and to a lesser extent in modern settings (Dalrymple et al. 1991; Choi et al. 2004) has been presented. These data characterize conditions for the deposition of IHS in sand-dominated systems but overall lack reference to mud-dominated systems. Given substantial oil reserves in marginal-marine deposits contained in strata characterized by both sandy- and muddy-IHS end members an understanding of the depositional dynamics of both systems

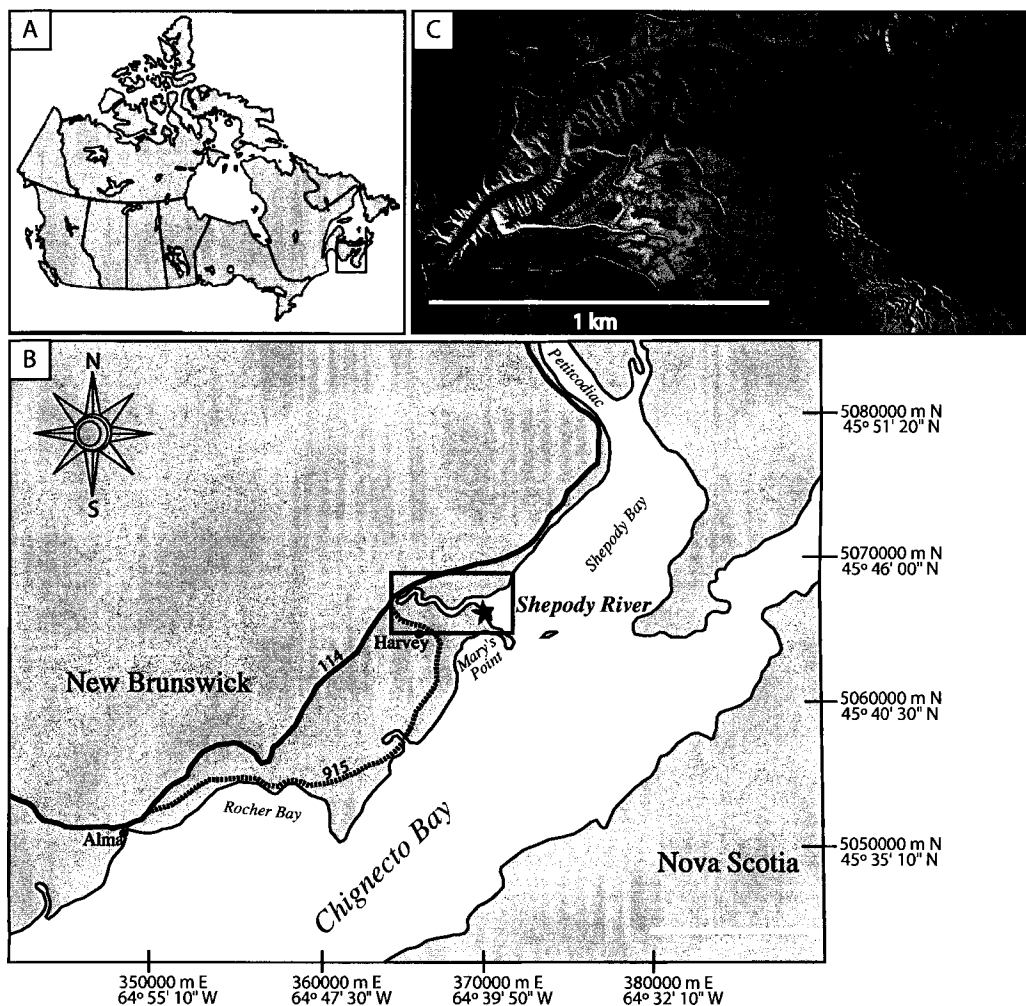


**Figure 2-1:** Location map of Chignecto Bay in the Bay of Fundy, New Brunswick, Canada. (A) Map of Canada with the Bay of Fundy identified by the solid box. (B) Schematic diagram of Chignecto Bay with the study area marked by the dashed box. The star identifies the most basinward station. (C) Air photo of the Shepody River in 2001.

would be a helpful exploration tool.

This study focuses on describing the physical and biological structures found in the transition from the upper-subtidal to upper-intertidal environments associated with point bars along the Shepody-River Estuary, which debouches into the Bay of Fundy (Fig. 2-1). There, rhythmic bedding is exposed where tributaries dissect tidal point bars, exposing IHS. As discussed below, the rhythmic beds represent a composite of tidal and seasonal processes. Although the beds are locally bioturbated, much of the physical sedimentary character is preserved. As such the records of biological and physical processes are available for scrutiny. Furthermore, the variations in bed thickness, both vertically and laterally, are related to the primary hydraulic processes that influence mud deposition within and adjacent to the channel system. The objectives of this paper are to describe the physical and biological structures observed within the tidal deposits, with the aim of identifying significant ichnologic and sedimentologic characteristics for application to the rock record.

### **2.1.2 Methods**

A variety of methods were employed, during the summer field season (June to August 2004), to investigate the point-bar deposits. These included detailed logging of 6 fresh exposures, box coring, salinity measurements and X-ray analysis. The upper portions of the subtidal point-bar deposits were studied during times of extremely low tide, which occurred during spring-tide conditions. The upper- to lower-intertidal point-bar deposits were observed during normal low-tide conditions. X-ray plates were taken from sediment slices 1 cm thick using a Soyee SY-31-100P portable X-ray unit with a fixed time station of 10 milliampere (mA), and 90 kilovolts (kVp) for 0.03 seconds. The mA value represents the quantity of X-rays reaching the X-ray detector, while the kVp value measures the peak power of the X-ray beam. From these datasets the sedimentary texture, sedimentary structures, nature of bedding contacts and lateral variability were

documented. Salinity measurements were taken with the aid of a conductivity salinity meter during the late spring and early summer months of 2002, 2003 and 2004.

Ichnological observations focused on the identification of ichnogenera, the bioturbation intensity, as well as the diversity and abundance of incipient ichnofossils. Other data collected included the presence of plant- and shell-debris (e.g. seaweed, logs, *Macoma balthica* shells, etc.) hosted within the silty or sandy mud laminae, the presence of pebble lags/*in situ* clasts, and the dip angle of bedding.

Collection of the above physical data was limited by the unlithified nature of the sediment. In particular, difficulties arose when trying to identify individual ichnogenera within historical deposits and in tracing bedding contacts. This difficulty was exacerbated within zones dominated by sediment deformation and fluid-mud accumulation.

Some of the ichnological data were subjectively collected, for example: (1) the bioturbation intensity (hereafter denoted as BI) varies from absent to complete, and (2) trace fossil size was recorded as diminutive (1-5 mm) or moderate (5-8 mm). Measurement of the bioturbation intensity was adapted and modified from Reineck 1963; Taylor et al. 2003; and Bann et al. 2004 (Fig. 2-2).

Laboratory work consisted of sample preparation for grain-size determination and the analysis of total organic carbon content (TOC). The process first involved desiccating sediments by heating at 105°C for 24 hours. Disaggregation of the dry samples was accomplished manually using a mortar and pestle. Grain-size analysis was conducted using a Sedigraph 5100. The Sedigraph 5100 measures the grain diameters of the sample using a finely collimated beam of low energy X-rays, which pass through a sample cell. The distribution of particle mass at various points in the cell affects the number of X-ray pulses reaching the detector, which are used to derive the particle-size distribution and is expressed as a percentage mass of assigned particle diameters (Shrader and Monsen 2005). The TOC was determined using the method of Heiri et al. (2001), which consists of: (1) assessing the initial mass of the dried sample; (2) baking samples for 4 hours at

550°C (to incinerate the organic carbon and other volatiles); and (3) measuring the final mass of the sample directly after baking. The difference between the initial and final masses was determined and the result was then recorded as a percentage of the total sample.

Grade	Classification	Visual Representation
0	Bioturbation Absent	
1	Sparse bioturbation, bedding distinct, few discrete traces	
2	Uncommon bioturbation, bedding distinct, low trace density	
3	Moderate bioturbation, bedding boundaries sharp, traces discrete, overlap rare	
4	Common bioturbation, bedding boundaries indistinct, high trace density with common overlap	
5	Abundant bioturbation, bedding completely disturbed (just visible)	
6	Complete bioturbation, total biogenic homogenization of sediment	

**Figure 2-2:** Bioturbation intensity (BI). Measurement of the intensity of bioturbation in the Shepody River deposits; adapted and modified from Reineck (1963), Taylor et al. (2003), and Bann et al. (2004).

### 2.1.3 Geological Setting

The Bay of Fundy is a large, macrotidal estuary on the southeastern coast of New Brunswick, Canada. It is a straight-sided, funnel-shaped bay 270 km in length and 80

km in width at its head. A tidal range that commonly exceeds 13 m and a tidal prism that surpasses 104 km<sup>3</sup> characterizes the bay (Desplanque and Mossman 2001). The bay's head is split into two smaller bays, Chignecto Bay and the Minas Basin. Chignecto, which is adjacent to our study locale, is a "muddy" estuary due to the nature of its sediment sources, the eroded cliffs that surround the bay and the eroded seabed. These are composed of Paleozoic mudstone and sandstone, and Holocene silt and clay, respectively (Amos 1987). The Shepody River is located in the upper (NE) portion of Chignecto Bay (Fig. 2-1B) and covers an area of approximately 51 km<sup>2</sup> at mean high tide.

This study focused on cut-bank exposed sections of modern point bars flanking the Shepody River (5067070m N, 0369780m E; N45°44'00", W64°43'30"). The Shepody Estuary exhibits a distinctive funnel shape in plan view, an attestation to its tidal dominance. Although six exposures were examined in general, the bulk of our detailed measurements for this study focused on the most basinward outcrop (Fig. 2-1B star). Sections are generally well exposed, with channel point-bar relief ranging from 6-15 m (average 10 m), and low-tide riverbank exposures ranging between 1.7 to 3.2 m in relief. The current velocities for one tidal cycle were observed to peak at 80 cm/sec (surface-water velocity at center of channel) and are highest during maximum ebb-tides, however flood-tidal currents are nearly as energetic. The current speeds are undoubtedly higher in the channel thalweg but were not measured due to poor accessibility. Salinity measurements were taken during rising-tide conditions in the late spring to early summer (April to July), and were located near the study area and 1.5 km up river. The corresponding values found at these locations ranged from 27 ppt near the study area to 16 ppt at the landward locale. The waters at the Shepody river locale have a high sediment load held in suspension and were found to be in excess of 21 g/L. The tidal point-bar deposits are dominated by the accumulation of fine-grained sediment and are composed of dipping, interbedded mud, silt and slightly sandy beds. The IHS beds are laterally continuous and are present throughout the extent of the exposure, over a

horizontal distance of about 26 m. Analysis of two grab samples showed that the channel thalweg sediment is dominated by silt (mean values: 68% silt, 19% sand, and 13% clay). Depositional surfaces are generally bioturbated and traces of animal activity can be observed in underlying layers. Cut banks that expose historical layers (up to 14 years old) allow scrutiny of the interred beds.

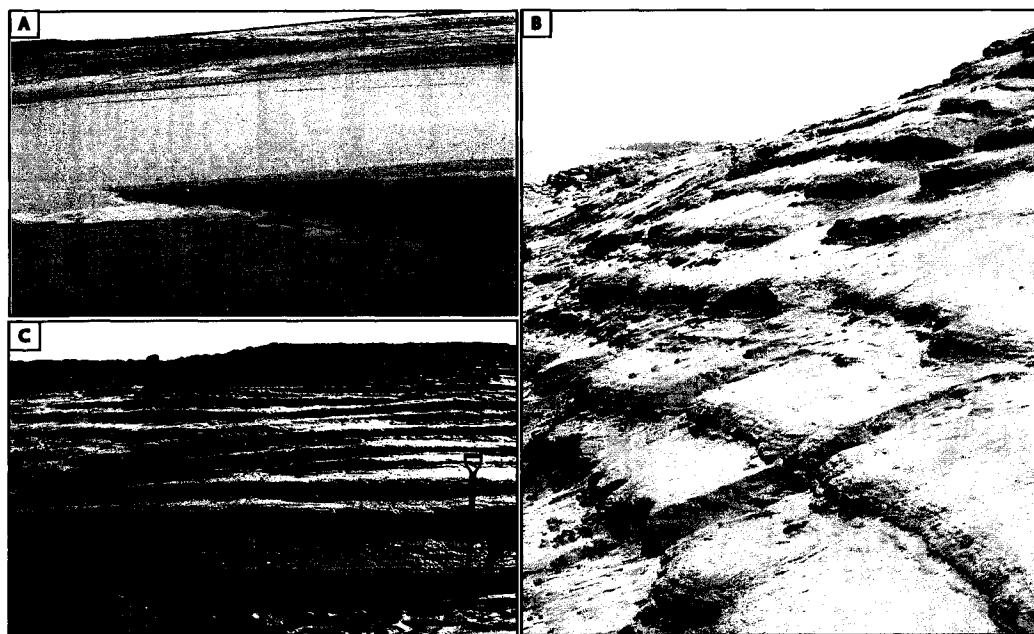


**Figure 2-3:** Different scales of view for muddy, main channel point bars. (A) Point-bar deposits exposed during low tide. (B) Side profile of Shepody most basinward (cut bank) exposure. Deposits are stepped and each step represents a single (seasonal) unit. (C) Front view of Shepody outcrop. Deposits are laterally continuous across the point bar. Scale =1.2 m (Shovel).

## 2.2 MAIN CHANNEL POINT-BAR DEPOSITS

### 2.2.1 General Sedimentology and Ichnology of the Study Area

In the Shepody area the point bars are composed of vertically stacked silty- and sandy-mud. These beds are stepped and have an apparent dip to the NW (Fig. 2-3B,C). The upper 5 to 20 cm of substrate is unconsolidated sediment with a soft to locally fluid consistency (Fig. 2-3A). Below the soft substrate the sediment is comparatively firm. This change in cohesiveness is abrupt and the point at which it occurs varies in depth

from 0 to 20 cm across the study area. The upper-subtidal to lower-intertidal portion of the point bar is characterized by planar, horizontal bedding; the middle-intertidal zone is predominantly low-angle, planar-bedded; and the upper-intertidal zone reverts back to planar, horizontal bedding. The firmer sediment supports open and unlined burrows, whereas the softer sediment contains burrows that are kept open with the aid of mucus linings and constant animal maintenance. These above characteristics result in a trace assemblage that reflects characteristics of both stiffground and restricted softground ichnofacies (Lettley et al. 2005 *in press*).

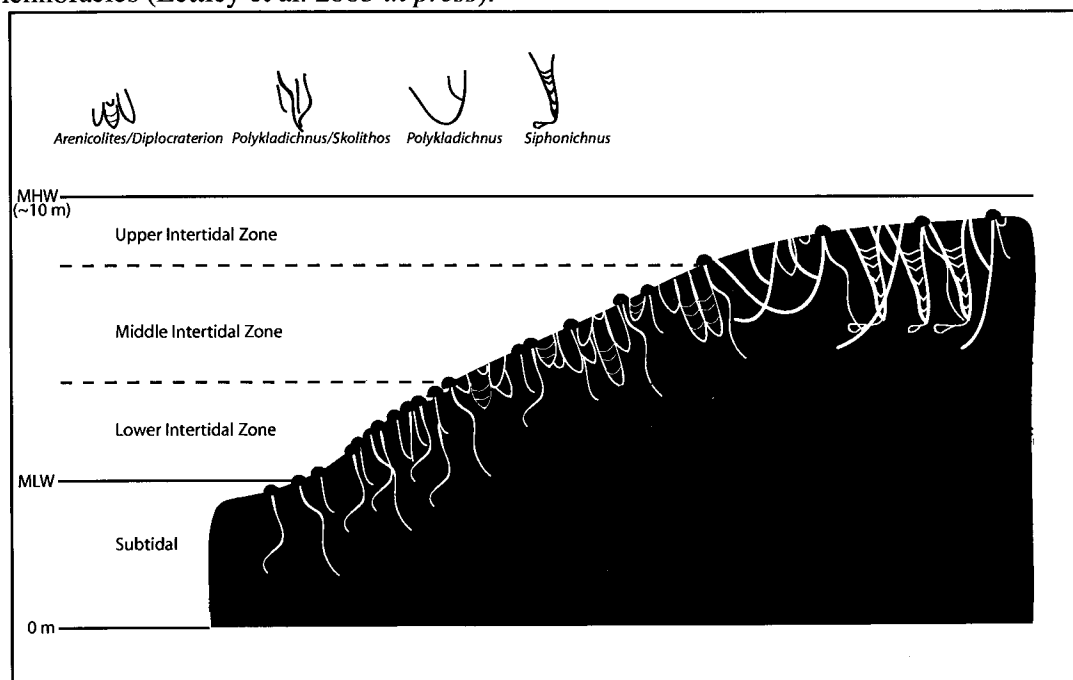


**Figure 2-4:** Schematic diagram of an intertidal point-bar assemblage (substrate silty- to sandy-mud) at Shepody River. The trace assemblage shown represents the dominant bioturbators present in an intertidal point bar within the Shepody River. The upper-intertidal zone is characterized by the activity of the nereid worm *Nereis virens*, *N. diversicolor* and the bivalve *Macoma balthica*. *Nereis* produces *Polykladichnus*-like traces; while *Macoma* makes *Siphonichnus*-like burrows. The middle-intertidal zone is dominated by the amphipod *Corophium volutator*, which creates the traces similar to the ichnogenera *Arenicolites* and *Diplocraterion*. The upper-subtidal to lower-intertidal zones are typified by *Polykladichnus*- and *Skolithos*-like burrows, which are the result of the work of the capitellid polychaete *Heteromastus*. The lower, more stressed portion of the point bar has the highest preservation potential.

The deformed portions of the section are characterized by the occurrence of both small- and large-scale features. Small-scale deformational features occur on the centimetre scale and are prevalent throughout all the deposits at Shepody. Most individual units, whether laminated or bioturbated, have some soft sediment deformation within them. Large-scale slumping occurs on the metre scale and most commonly occurs in areas of the main channel point bars that are dissected by tributaries.

The depositional surfaces of the Shepody point bars, excepting freshly slumped surfaces and small patches of fluid mud, are characterized by persistent bioturbation from the upper-intertidal zone (~Mean High Water: henceforth MHW) to one meter below Mean Low Water (hereafter denoted as MLW) (Fig. 2-4). Bioturbation intensity is generally moderate to abundant (BI 3-5), meter-scale patches are present that have only sparse infaunal traces (BI 1). These sparse patches are associated with previously scoured or slumped zones. A preponderance of infaunal traces referable to the ichnogenera *Siphonichnus* and *Polykladichnus* characterize the upper-intertidal zone and the adjacent tidal flats (Fig. 2-4, 2-5B). These biogenic structures are created by the small bivalve *Macoma balthica* and the polychaete *Nereis virens*, respectively. Some floundering traces are found on depositional surfaces within this zone; these are produced by flatfish fins and could be considered to be a type of *Undichnia* (Fig. 2-5C). The middle portion of the intertidal zone (Fig. 2-4) is colonized by the amphipod *Corophium volutator*, the nereid polychaete *Nereis virens* (occasionally *N. diversicolor*), the capitellid polychaete *Heteromastus*, and rare *Cerebratulus lacteus* (nemertean worm). Burrow counts in this area found the density of *Corophium* locally to range between 10,000 to 60,000 individuals/m<sup>2</sup>. Each *Corophium* resides in an *Arenicolites*- or *Diplocraterion*-like trace (Fig. 2-5D). Due to the extremely high population densities the U-shaped burrows are closely spaced, and generally dominate the ichnofabric. As with the upper-intertidal zone, *Nereis* construct Y-shaped burrows consistent with *Polykladichnus*. Many of the *Nereis* burrows have extensive horizontal networks at around 10 cm depth, which commonly

resemble the ichnogenera *Planolites* and *Palaeophycus* (Fig. 2-5E). *Cerebratulus* also constructs structures consistent with *Planolites* (although the traces do not appear to be backfilled) and *Palaeophycus* but these have larger burrow diameters than those made by *Nereis* (5-8 mm versus 2-6 mm). The threadworm, *Heteromastus* typically constructs *Skolithos*, *Trichichnus* and *Polykladichnus*-like burrows (Fig. 2-5A): these forms are pervasive in the upper-subtidal and lower-intertidal (Fig. 2-4) portions of the point-bar deposits. Below MLW, bioturbation is sparse (BI 1) and is inferred to decrease towards the channel thalweg.

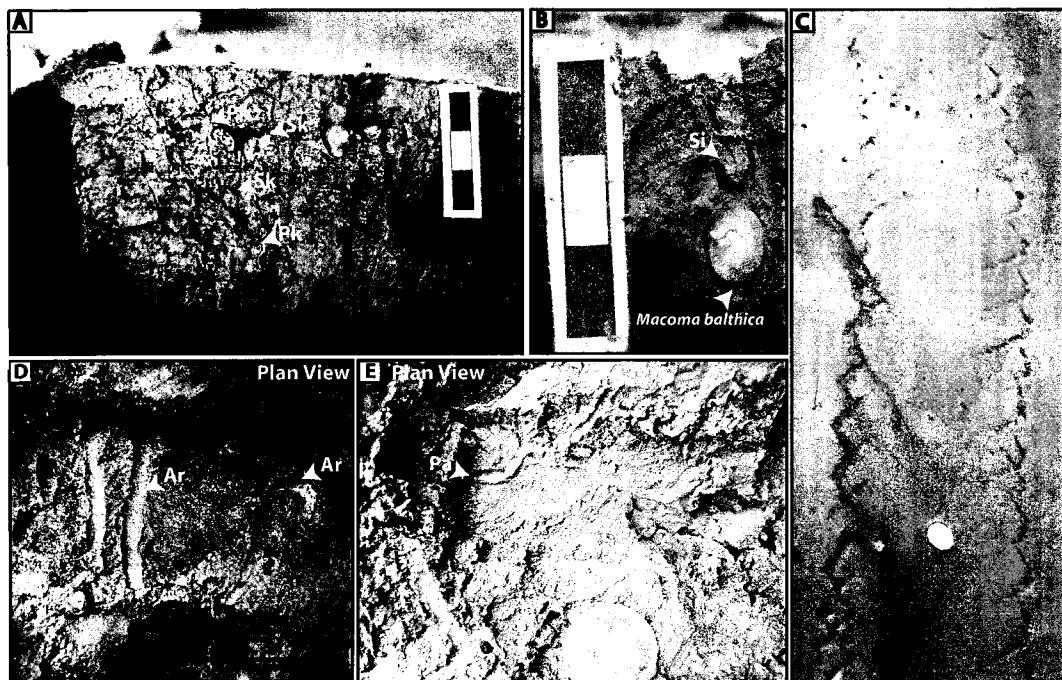


**Figure 2-5:** Ichnogenera observed in the Shepody River sediments. (A) *Skolithos* (Sk) and *Polykladichnus* (Pk), made by *Heteromastus*, vertical face, scale in centimetres. (B) *Siphonichnus* (Si), created by *Macoma balthica* (shown), vertical face, scale in centimetres. (C) Fin trace (?*Undichnia*), plan view, scale = 2.5 cm (quarter). (D) *Arenicolites* (Ar), generated by *Corophium volutator*, plan view, scale = 3 cm. (E) *Palaeophycus* (Pa), produced by *Nereis virens*, plan view, scale = 1.8 cm (dime).

Overall, the infauna consists primarily of opportunistic organisms, while the traces represent a low-diversity suite that is diminutive: less than 3 mm diameter in most cases. Trace-makers include *Heteromastus*, *Corophium volutator*, *Macoma balthica*, *Nereis virens*, and *Cerebratulus lacteus*. The resulting ichnocoenosis is tiered and

includes moderate-depth (1-12 cm) *Arenicolites* and *Diplocraterion*, shallow-depth (1-5 cm) *Siphonichnus*, and moderate depth *Skolithos* and *Polykladichnus* (Fig. 2-5).

### 2.2.2 Detailed Sedimentology and Ichnology of the Cut-bank Sections

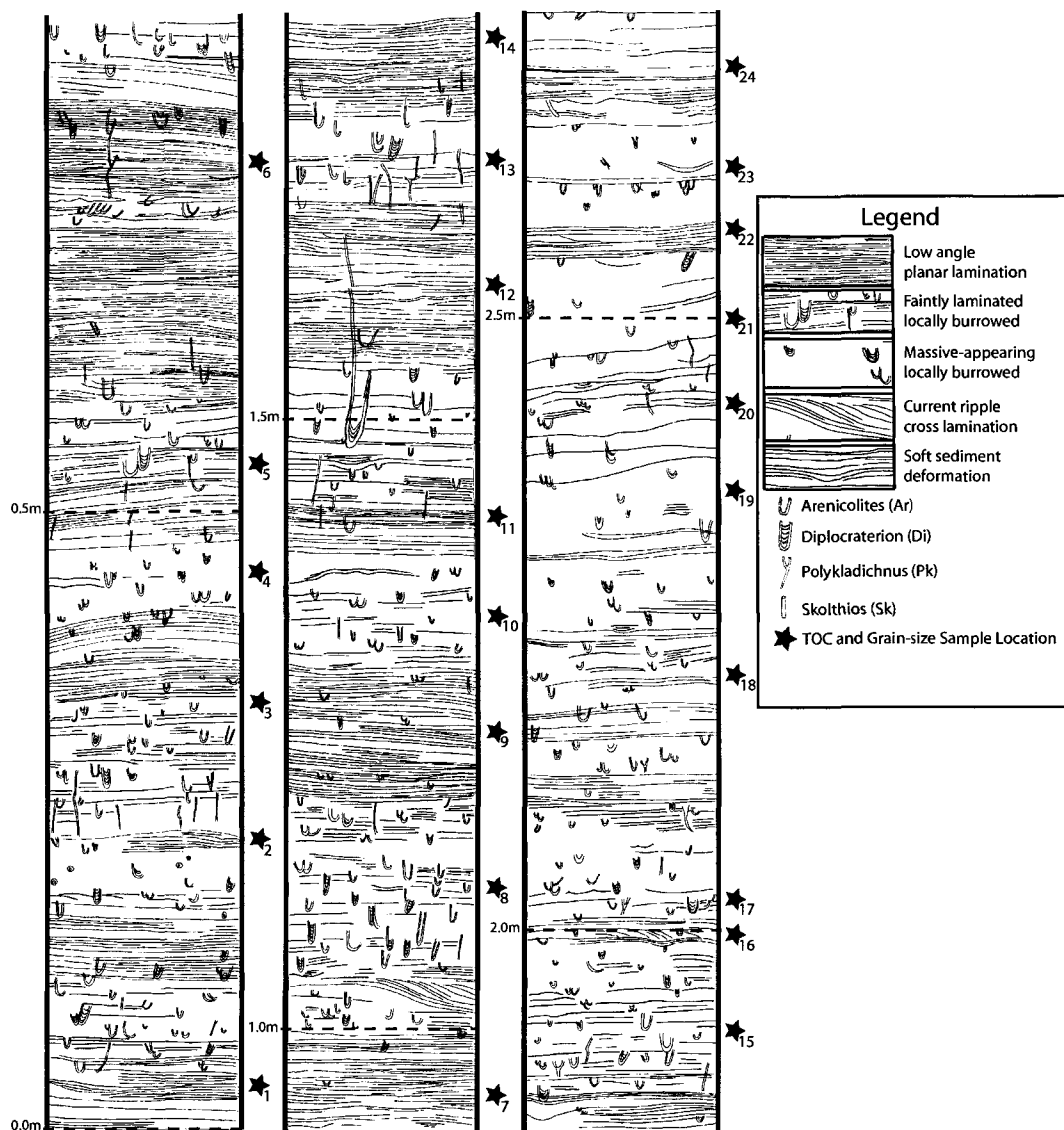


**Figure 2-6:** Vertical section of Shepody low-tide exposure showing the sedimentological and ichnological characteristics. Base is at lower-left and top at the upper-right. Note massive versus laminated interbeds—these are interpreted to be the result of variable seasonal processes.

Within the study area, point bars are characterized by interlaminated and thinly interbedded silty- and sandy-mud. The composition of sedimentary microfacies, outlined in figure 2-6, is taken to represent mud-dominated IHS. As stated above observations were made at multiple points along the Shepody River. The different locations are sedimentologically similar, so the best-exposed (i.e. most complete) cut bank, which is the most basinward section, was chosen to provide the following detailed description (Fig. 2-1B star). The cut-bank sections are characterized by an alternation between laminated and bioturbated beds. Burrowed beds range in thickness from 3.5 to 34 cm (Fig. 2-3B, C). The laminated units range in thickness between 4 and 34 cm (average 13 cm) with a general decrease in thickness up section (Fig. 2-6). Laminated beds are locally characterized by low-angle, planar-laminated tidal couplets (Fig. 2-7A). Individual laminae housed within couplets show only small variations in their thickness: the silty portion of the couplet commonly reaches thicknesses of 1 cm, whereas the sandy portion rarely exceeds 2 mm. Laminae thickness is cyclically variable (Fig. 2-7A). Sandy laminae are fine grained, well sorted and show no grading. Several other sedimentary structures are present; the most common is convolute bedding found at both small- and large-scales. Similar to features reported by Dalrymple et al. (1991) the convolutions consist of sharp-crested anticlines separated by broad synclines. The relief of the convolutions dissipates upwards into the overlying laminated sediment. Unlike Dalrymple et al.'s (1991) example, no basal erosional contact was observed marking this deformation. Current and climbing ripples are rare and coincident with portions of the outcrop that have an increased sand content. Current ripples are observed between 1.0 and 1.1 m and at 2.0 m on the vertical section (Fig. 2-6). Ripple foresets dip to the NW and indicate flood-dominated sediment transport, at least at this locale. Overall, beds are sharp-based and are locally crinkled. Burrowed zones locally reach down to sedimentary contacts and obscure those contacts. Bedding dip falls between 10° to 12° and has limited variance (less than 2°) across the entire exposure. The laminated beds within the IHS are typified by variable

bioturbation intensities, ranging from BI 0 to 3, typically 1. The specific traces found within this unit are dependant on which portion of the intertidal zone they were deposited in (discussed below).

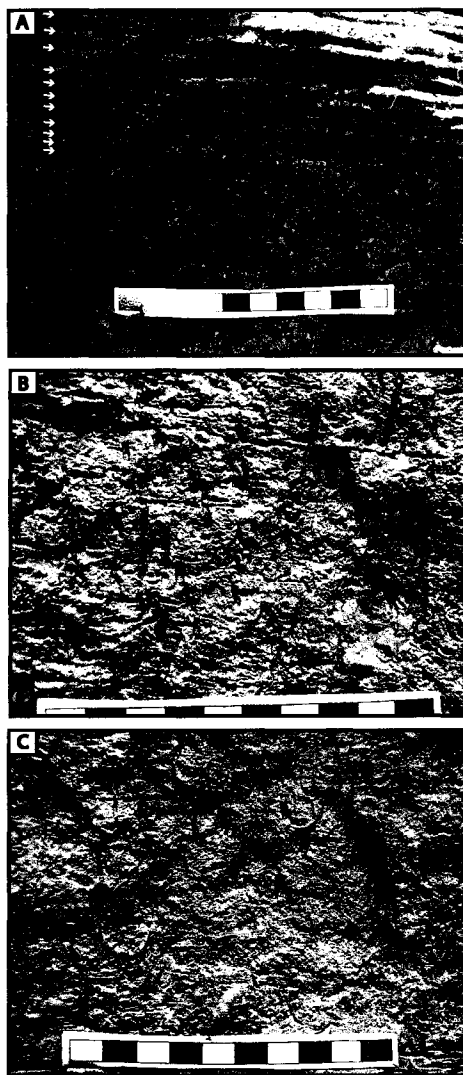


**Figure 2-7:** Seasonal deposits of the Shepody River. (A) Spring deposits typified by parallel-laminated silty mud and little or no bioturbation (BI 0 to 1). Arrows highlight the variation in laminae thickness. (B) Transition from spring to summer deposition with variable bioturbation intensities (BI 0 to 3, typically 2). (C) Summer and fall deposits characterized by pervasive bioturbation (BI 2 to 6, commonly 5). Scale is in centimetres.

Bioturbated beds have a gradational or burrowed contact with underlying laminated beds (Fig. 2-6, 7B). The bioturbated units generally increase in thickness up section (Fig. 2-6). The beds are characterized by more or less pervasive bioturbation. Intensities range from BI 2 to 6, and are normally 5 (Fig. 2-7C). Where the bioturbation intensity is low, biogenic structures are sporadically distributed. Very little organic debris is preserved within the burrowed beds.

Sandier beds are stained orange by iron oxide, and black by manganese oxide. The manganese oxide commonly occurs in deposits characterized by an abundance of organic detritus. The basal portion of many of these units has a granule/pebble lag. This lag is laterally discontinuous and occurs in isolated patches across the exposure. Commonly found distributed within these lags are sparse shell (generally *Macoma balthica*) and terrestrially derived plant debris.

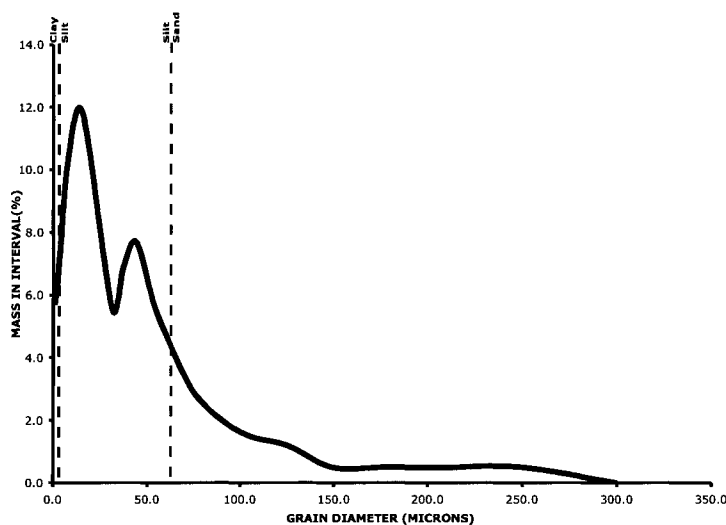


**Figure 2-8:** Typical grain diameter distribution found in a single seasonal deposit (summer to fall) in the Shepody River.

### 2.2.3 Total Organic Carbon and Grain-Size Analysis

The grain-size distribution and TOC were assessed for each laminated and bioturbated unit. Grain-size analyses show that the typical texture is (Fig. 2-8): silt

(66%), clay (24%), and sand (10%). The overall grain-size trend coarsens upwards; i.e. the percentage of coarse silt increases upwards (Fig. 2-9). However, the channel thalweg, though still dominantly muddy, contains the coarsest sediment locally (mean values: 68% silt, 19% sand, and 13% clay).

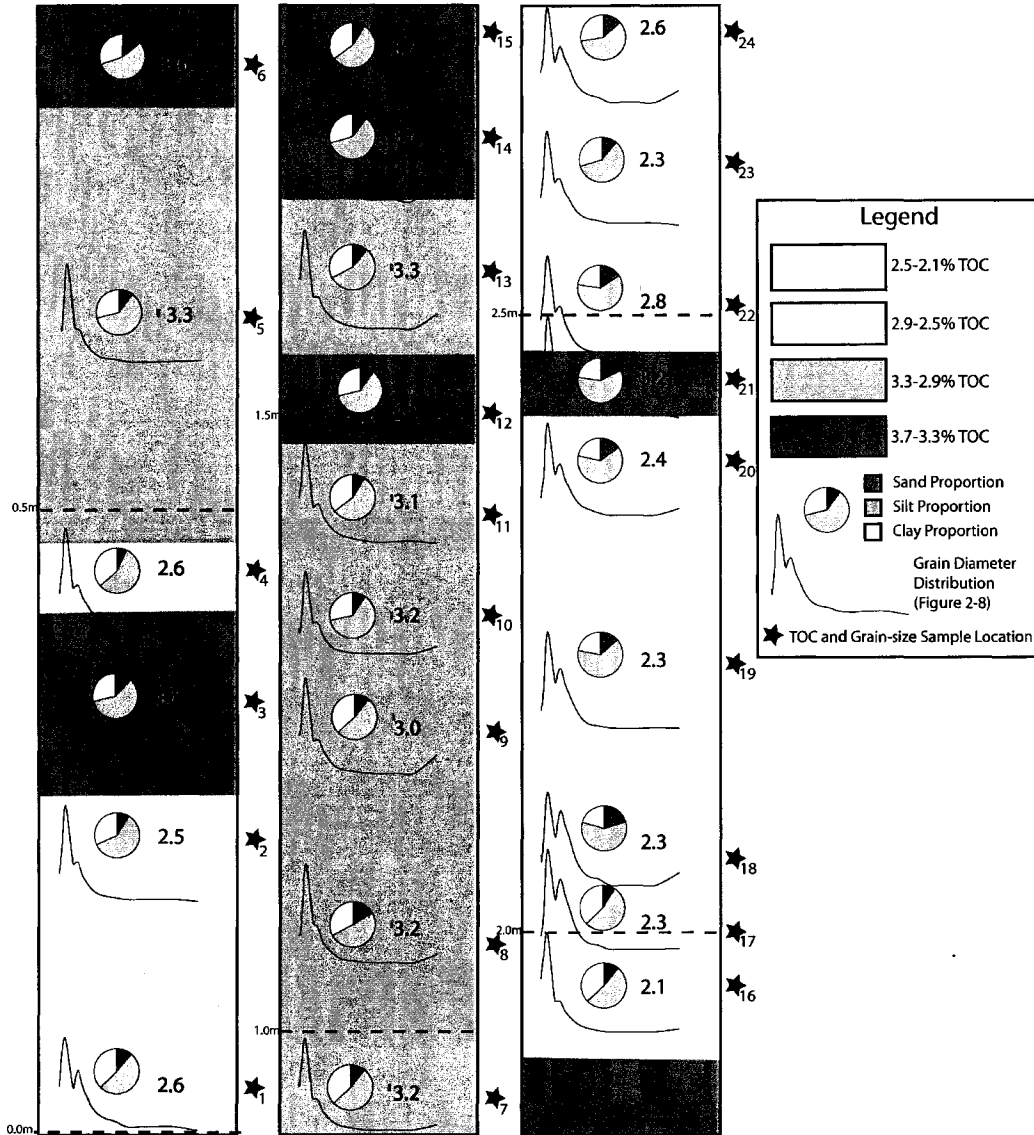


**Figure 2-9:** Vertical section of Shepody outcrop shows the distribution of total organic carbon (TOC) and grain-size. Note while TOC decreases, the proportion of silt and sand increases upwards. See Fig. 2-8 for typical grain distribution.

The TOC averaged 2.9%, with a maximum value of 3.7% and a minimum of 2.1%. TOC values generally decrease upwards (Fig. 2-9, 2-10). Laboratory measurements

showed little difference in either the grain-size distribution or the TOC percentages between the laminated and bioturbated beds; any differences in grain-size constituted less than 5% between clay, silt and sand percentages while changes in the TOC were less than 0.5%.

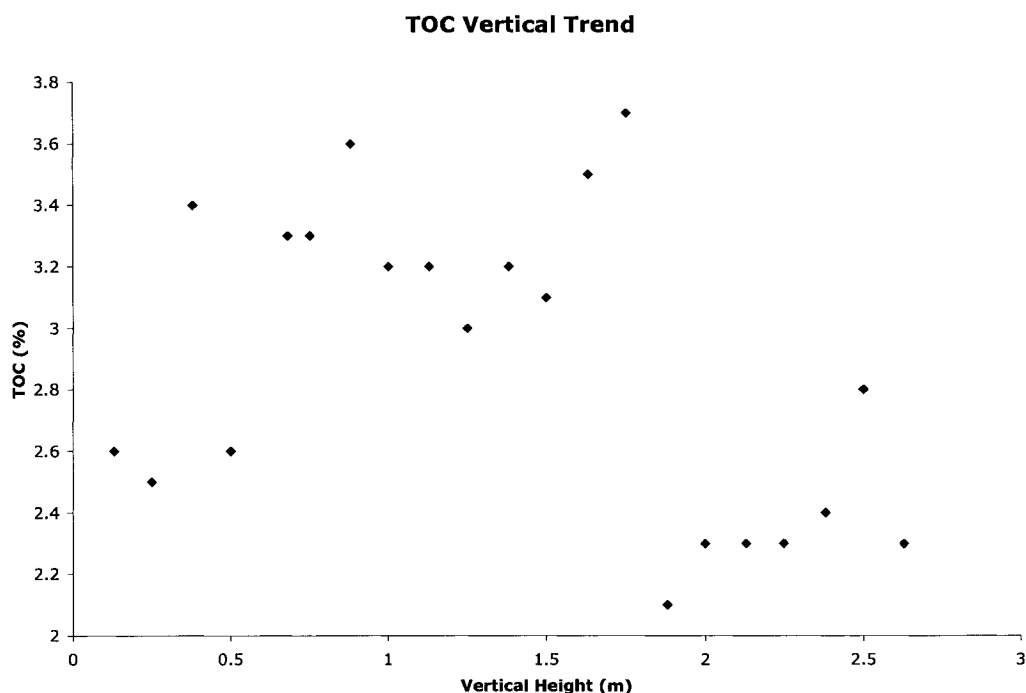


**Figure 2-10:** Total organic carbon scatter plot. Note the initial increase in TOC values up the exposure but as grain-size increases (Fig. 2-9) the TOC percentages decrease.

## 2.3 INTERPRETATION

### 2.3.1 Preservation of a Tidal Signal

The outcropping strata represent fine-grained sediment deposition within a marginal-marine channel. More specifically, the IHS beds represent lateral accretion associated with tidally-modified channel flow (Thomas et al. 1987; Smith 1987, 1988, 1989; Bann et al. 2004). The lack of typical tidal physical sedimentary structures (flaser, lenticular, or wavy bedding) and lack of grain-size contrast is attributed to the unequal proportion of silty- and sandy-mud (9:1), the overall preponderance of silt, and the near absence of sand-dominated beds present within the depositional system. Moreover,

the study locale is dominated by flocculated sediment, which overwhelms or masks coarse-grained sediment that may travel in the traction load. Individual laminae record deposition from successive tidal cycles and these correspond to subtle changes in the caliber of sediment carried. We attribute cyclic variation in laminae thickness found in the Shepody units to neap-spring tidal cyclicity. Progressive thickening of the beds is related to tidal-range increase from the neap to spring tides, whereas thinning-up units reflect the converse (Tessier 1993). Changes in the thickness of individual laminae within the neap-spring bundles are likely altered both by a change in the caliber of sediment (sand versus silt) and diurnal inequality—i.e. the inequality in the strength of successive high and low tides (De Boer et al. 1989; Nio and Yang 1991; Hovikoski et al. 2005). In short, the presence of rhythmic silty- and sandy-mud couplets, likely neap-spring bundles, and asymmetric current ripples attest to the preservation of tidal sedimentary structures within the tidal point bars.

### **2.3.2 The Significance of Convolute Bedding and Pebbly Lags**

Convolute bedding is attributed to sediment loading, ice-loaded deformation, and penecontemporaneous slumping. Also, Van Leussen and Cornelisse (1992) documented that rapid sedimentation of flocculated material is often observed during periods of decelerating currents or around slack tide. This rapid sedimentation (termed “rapid settling”) has the ability to trap water or gas in the generously sized spaces between the settling flocs (Van Leussen and Cornelisse 1992). As this sediment is subsequently loaded the water or gas escapes causing small-scale deformational features. Notably, biogenic methane seeps are common on the Shepody point bars, so gas induced deformation cannot be discounted.

Following initial deposition, dewatering increases the sediment cohesiveness, resulting in a comparatively firm substrate. The firm sediment is most influenced by ice-induced deformation (dragging and loading: the ice can exceed 2 m thickness at the

point-bar tops). The presence of the laterally discontinuous granule/pebble lags, blocks of transported salt marsh, shale clasts, and *Macoma* shells are evidence of ice-assisted transport. The patchy distribution of these deposits, and their position within laminated and directly overlying the bioturbated units suggests that sediment derived from the lower supratidal zone was brought into the channel by multiple processes. It is likely that periods of increased runoff (early spring), increased turbulence related to storms (late fall and winter) and winter ice rafting most contribute to the exotic detritus observed therein (Dalrymple et al. 1991, Dashtgard and Gingras 2005).

### **2.3.3 Mud Deposition at the Shepody River**

The muddy texture of the exposure presents a conundrum: were depositional rates slow and from suspension or high and from traction of flocculated material? Or, is it a combination of both? Amos and Mosher (1985) postulated that the effects of pelletization, flocculation, and interparticulate reactions could cause fine-grained material to settle in a manner other than that determined by Stoke's Law. Several other authors (Johnson 1983; Van Leussen and Cornelisse 1992; Lick 1994; Stone and Droppo 1994; Pejrup 2003) suggest that once fine-grained sediment flocculates, it exhibits hydrodynamic behavior more akin to grains of sand. The deposition of flocculated material is controlled by numerous factors: flow velocity, temperature, dissolved oxygen, pH, sediment concentration, water column height, total dissolved and suspended solids, and likely many more parameters not considered herein (Stone and Droppo 1994). In tidal environments hydraulic energy has the largest effect on sediment deposition and this energy is neither constant nor evenly distributed. It is likely that during the flood- and ebb-current stages—i.e. when hydraulic energy was high—deposition was derived primarily from flocculated material and (secondarily) sand in traction. Formerly it was accepted that under conditions of higher flow velocities the fragile flocculated material would break up due to turbulence, however, Stone and Droppo (1994) proposed

that these conditions in thicker water columns actually promote flocculation through particle collisions. This is apparently supported by Van Leussen and Cornelisse (1992), who observed an entire tidal cycle in the Ems Estuary and found that an abundance of large flocs (200-700  $\mu\text{m}$ ) had survived the high flow velocities associated with the dominant flood- and ebb-tides. Our own observations in mildly turbulent water, shows the accumulation and aggregation of 'flocs' is not inhibited by mildly turbulent water. However, the depositional infilling of excavations made on the tidal flat is even and aggrading, not asymmetric, suggesting that sediment accumulation is primarily from suspension during slack tides and not dominantly during full-flood or -ebb (from traction).

The formation of flocculated material in waters with high hydraulic energy is dependant on multiple factors: (1) suspended sediment load; (2) the presence of a binding agent such as mucopolysaccharides produced by bacteria, algae and higher plants; and (3) water-column height (Van Leussen and Cornelisse 1992; Stone and Droppo 1994; Dalrymple and Choi 2003). The waters at the Shepody river locale have a high sediment load held in suspension (as much as 21 g/L). Also, Shepody exposures are commonly covered in diatomaceous foam that could act as binding agents for the flocculated material. This material may aid in the ability of the larger flocs to withstand the turbulence associated with the higher hydraulic energy of subsequent tides, partly solving the problem of enhanced falling-tide bed shear and resulting floc breakage (Stone and Droppo 1994). Moreover, the higher water column and subsequent decrease in bed shear during the later stages of rising tide and the initial stages of falling tide provide the ideal conditions necessary for floc formation (Dalrymple and Choi 2003). Slack-water stages, which have lower (or no) hydraulic energy, permit deposition of non-flocculated material mainly from suspension and flocculated material through "rapid settling" (Van Leussen and Cornelisse 1992), processes we favor for our interpretation of the Shepody sediments.

#### 2.3.4 Interpretation of IHS Sedimentological and Ichnological Variability

The laminated/bioturbated alternation of the deposits found at the Shepody River results from markedly different summer/winter depositional conditions. Laminated sediment accumulates in the early winter through to the early spring months, both during and following the generation of the sediment deformational features. At these times infaunal population densities are too low to significantly rework the sediment (Dalrymple et al. 1991). With spring runoff, the amount of fine-grained sediment introduced into the river system increases. Discharge data shows an overall increase in freshwater input within the river systems in Chignecto Bay. This increase begins in March (mean value of 7.82 m<sup>3</sup>/s) and reaches a maximum value in April (mean value of 11.58 m<sup>3</sup>/s)(Water Survey of Canada 2005). The increase in sedimentation rates and the inferred salinity change associated with fresh-water input produces conditions that are not amenable to substrate colonization. Bioturbated sediment, which overlies these deposits, therefore represents late-spring colonization. Subsequent bioturbation of the substrate continues as sediment accumulates during the summer and fall months when salinity, oxygen, and temperature conditions are more amenable to substrate colonization. As noted above, sediment deformation observed capping the bioturbated sediment is attributable to ice rafting and ice loading during the late winter and early spring months; these contacts generally coincide with the position of the patchy granule/pebble lags (also reported in Dalrymple et al. 1991).

Biogenic structures are present in the muddy point-bar deposits and bioturbation intensity ranges from sparse to complete (BI 1-6). The return to favorable colonizing conditions during the late spring and summer months is characterized by an increase in the abundance of burrow openings and surficial locomotion trails up the point bar. This increase is indicative of an infaunal community that is thriving beneath the surface. The infaunal traces reported above (*Arenicolites* (abundant), *Diplocraterion*

(abundant), *Skolithos* (common), *Polykladichnus* (common), *Siphonichnus*, *Planolites*, and *Palaeophycus* in rare to moderate abundance) are similar to those described by Howard and Frey (modern environment: 1975), Pemberton and Wightman (Cretaceous strata: 1992), MacEachern and Pemberton (Cretaceous strata: 1994), Gingras et al., (modern environment: 1999) and Pemberton et al. (range of rock-record examples: 2001) as characteristic of the ichnogenera associated with brackish-water environments. All of those examples are reported with high-certainty—i.e. well supported by biological and sedimentological criteria—within well-known brackish-water environments. Likewise, the assemblage reported herein was shaped by overall low salinities (16 to 27 ppt) and notable fluctuations in several environmental parameters. Overall low ichnodiversity, high trace densities, simple structures, diminutive trace fossils, and infaunal assemblage of vertical and horizontal traces characterize the resulting ichnocoenosis. Several parameters likely played a role in limiting the size and diversity of burrowing infauna: lower or fluctuating salinity levels, changes in oxygenation, overall high turbidity, high sedimentation rates, soft to soupy substrate consistencies, prolonged intertidal exposure times and daily through seasonal temperature fluctuations. Moreover, fluctuations in temperature are known to result in subsequent variations in the dissolved oxygen and salinity levels expected within the river waters. This example underscores the fact that diminution of infaunal size, overall low diversities, and the recruitment of opportunistic species are easily assigned to brackish-water conditions (Gingras et al. 1999; Pemberton et al. 2001). This typical brackish-water ichnological signature results from a composite of stresses that are prevalent in bays and estuaries (Gingras et al. 1999; Pemberton et al. 2001).

The sedimentological and ichnological contrasts found between the upper-subtidal, lower-, middle- and upper-intertidal zones are gradational but distinct (Fig. 2-11). The upper-subtidal and lower-intertidal zones are characterized by: (1) moderate to high TOC values (2.5 to 3.4%); (2) fine silt to clay sediment; (3) BI ranging from 2 to

5, commonly 3; and (4) *Polykladichnus*- and *Skolithos*-like traces. The middle-intertidal portion of the point bar is typified by: (1) low to high TOC values (2.1 to 3.7%); (2) fine silt to clay sediment (; (3) BI ranging from 4 to 6, typically 5; and (4) *Arenicolites*-

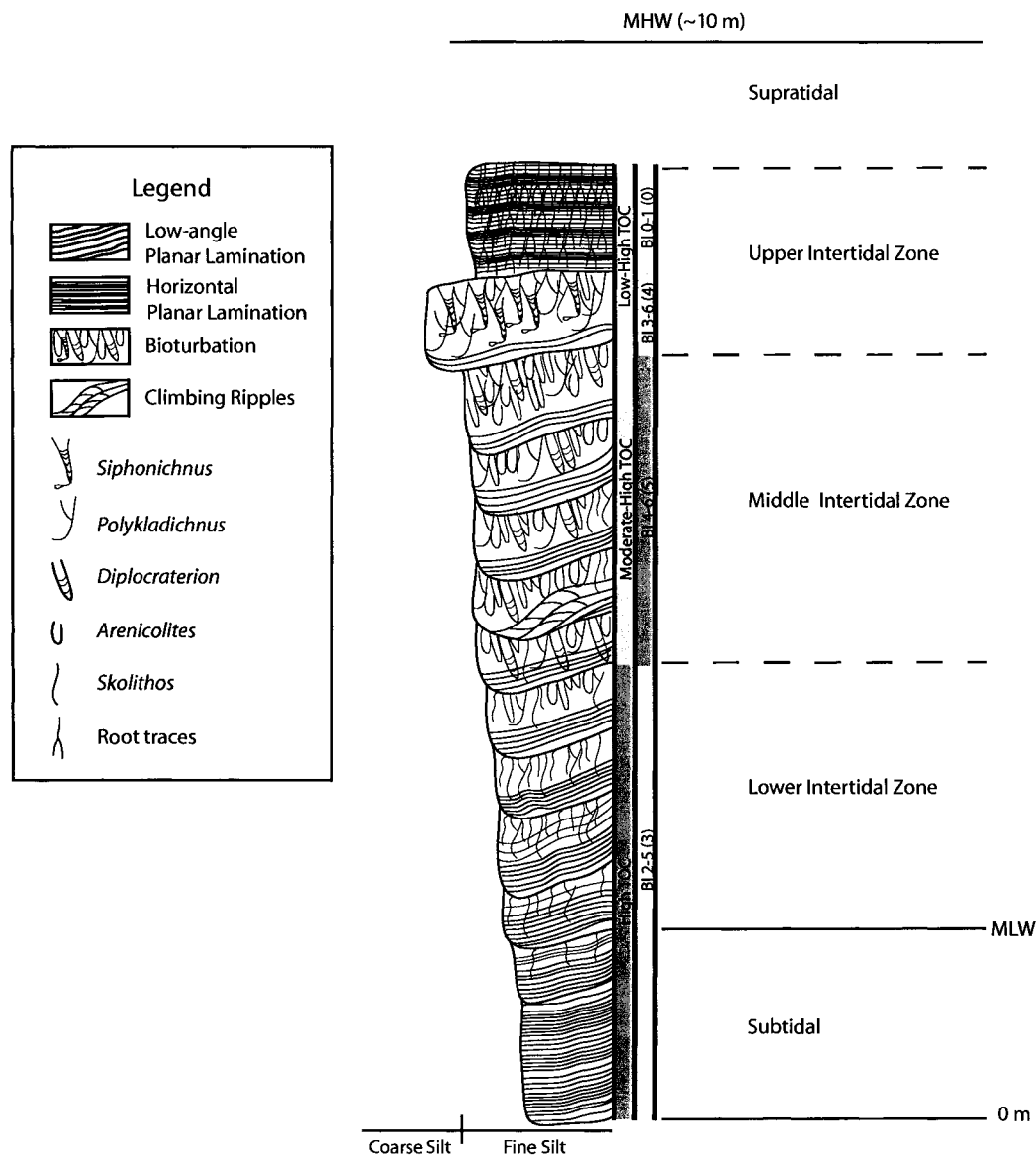


**Figure 2-11:** Schematic diagram showing the facies transitions within a Shepody low-tide exposure. Note the vertical trends in the sedimentology, ichnology, and TOC values.

, *Diplocraterion*-, *Polykladichnus*-, *Palaeophycus*-, and *Planolites*-like burrow forms.

The upper-intertidal zone is epitomized by: (1) low TOC values (2.3 to 2.8%); (2) coarse silt to clay sediment; (3) BI ranging from 3 to 6, usually 4; and (4) *Siphonichnus*-, *Polykladichnus*-, and *Undichnia*-like traces.

The vertical trends observed are the result of changes in the sedimentological and ecological controls within the Shepody River. Grain-size increase up section is due to the locally higher velocity ebb currents that are generated within the thin intertidal cross-section during falling tide. The sand is likely enriched due to mild winnowing of other grains and is the result of typical hypertidal conditions. The percentage of TOC in the deposits decreases up section and is attributable to the same processes. TOC may also be reduced with higher degrees of bioturbation, the result of organisms processing the food resources found *in situ* within the intertidal zones.

The lower BI found in the upper-subtidal to lower-intertidal is the result of slightly higher sedimentation rates and higher sediment creeping rates. The increase in the BI from the lower- to middle-intertidal environments is linked directly to the higher sediment stability observed in these areas.

## 2.4 SUMMARY

Detailed analysis of the fine-grained deposits associated with the estuarine mouth of the Shepody River, New Brunswick, Canada permitted the characterization of the ichnological and sedimentological characteristics of estuarine point bars and the adjacent tidal flats. The neo-ichnology of these depositional subenvironments provided useful criteria for distinguishing the various parts of the point-bar deposit: *Polykladichnus*- and *Skolithos*-like traces characterized the upper-subtidal and lower-intertidal zones of the point bars; *Arenicolites*-, *Diplocraterion*-, *Polykladichnus*-, *Palaeophycus*-, and *Planolites*-like forms were pervasive in the middle-intertidal portions of the point bars; and, *Siphonichnus*- and *Polykladichnus*-like burrows typified the upper-intertidal point

bars and the adjacent tidal flats. The size and diversity of the burrowing fauna is largely affected by seasonal variations within the general composition of the river waters. This assemblage was characterized by a low diversity of traces that were present in high abundance, a pattern that has been commonly noted in brackish-water environments.

Rhythmic bedding characterized both point bars and tidal flats. Bedding was defined by interlaminated and thinly interbedded silty- and sandy-mud. On the point bars, bedding was parallel to the depositional surfaces (i.e. dip towards the channel) and represented mud-dominated inclined heterolithic stratification. Rhythmic bedding observed in the point-bar deposits represented the operation of tidal- and seasonal- processes. Tidal processes were recorded in the laminated beds as rhythmic lamination and rare preserved starved ripples. The (laminated) tidal deposits resulted from the deposition of flocculated material and traction-borne sediment during the flood- and ebb-tide and to a larger extent the slack-water accumulation of fines from suspension and flocculated material from “rapid settling”. Cyclic variation in laminae thickness was likely the result of neap-spring variation in tidal current strength. Although the burrowed interbeds were exposed to the same tidal conditions in which the laminated beds accumulated, biogenic reworking eradicated the tidal sedimentary signature. Intercalated laminated/burrowed beds reflect seasonal variations in the depositional system. The laminated beds characterize early winter and (primarily) spring sediments, while the bioturbated beds typify summer and fall deposits. These deposits are the result of the seasonal variations in the river water composition. These beds are strongly affected by temperature fluctuations.

## 2.5 REFERENCES

Amos, C.L., 1987, Fine-grained sediment transport in Chignecto Bay, Bay of Fundy, Canada: *Continental Shelf Research*, v. 7, p. 1295-1300.

Amos, C.L., and Mosher, D.C., 1985, Erosion and deposition of fine-grained sediments from the Bay of Fundy: *Sedimentology*, v. 32, p. 815-832.

Bann, K.L., Fielding, C.R., MacEachern, J.A., and Tye, S.C., 2004, Differentiation of estuarine and offshore marine deposits using integrated ichnology and sedimentology: Permian Pebbly Beach Formation, Sydney Basin, Australia, *in* McIlroy, D., ed., *The Application of Ichnology to Paleoenvironmental and Stratigraphic Analysis*: Geological Society, London, Special Publications, v. 228, p. 179-211.

Choi, K.S., Dalrymple, R.W., Chun, S.S., and Kim, S.P. 2004, Sedimentology of modern, inclined heterolithic stratification (IHS) in the macrotidal Han River Delta, Korea: *Journal of Sedimentary Research*, v. 74, no. 5, p. 677-689.

Dalrymple, R.W., Knight, R.J., Zaitlin, B.A., and Middleton, G.V., 1990, Dynamics and facies models of a macrotidal sand-bar complex, Cobequid Bay-Salmon River Estuary, Bay of Fundy: *Sedimentology*, v. 37, p. 577-612.

Dalrymple, R.W., Makino, Y., and Zaitlin, B.A., 1991, Temporal and spatial patterns of rhythmic deposition on mud flats in the macrotidal Cobequid Bay-Salmon River Estuary, Bay of Fundy, Canada, *in* Smith, D. G., Zaitlin, B. A., Reinson, G. E., & Rahmani, R. A., eds., *Clastic Tidal Sedimentology*, Canadian Society of Petroleum Geologists, Calgary, Alberta, Memoir 16, p. 137-160.

Dalrymple, R.W., Zaitlin, B.A., and Boyd, R., 1992, Estuarine facies models: conceptual basis and stratigraphic implications: *Journal of Sedimentary Petrology*, v. 62, p. 1130-1146.

Dalrymple, R.W., and Choi, K., 2003, Sediment transport by tides, *in* Middleton, G.V., ed., *Encyclopedia of Sediments and Sedimentary Rocks*: Klywer Academic Publishers, Dordrecht, Netherlands, p.606-609.

Dashtgard, S.E., and Gingras, M.K., 2005, Facies architecture and ichnology of recent salt-marsh deposits: Waterside Marsh, New Brunswick, Canada: *Journal of Sedimentary Research*, v. 75, p. 594-605.

De Boer, P.L., Oost, A.P., and Visser, M.J., 1989, The diurnal inequality of the tide as a parameter for recognizing tidal influences: *Journal of Sedimentary Petrology*, v. 59, p. 912-921.

Desplanque, C., and Mossman, D.J., 2001, Bay of Fundy tides: *Geoscience Canada*, v. 28, p. 1-11.

Eberth, D.A., 1996, Origin and significance of mud-filled incised valleys (Upper Cretaceous) in southern Alberta, Canada: *Sedimentology*, v. 43, p.459-477.

Gingras, M.K., Pemberton, S.G., Saunders, T., and Clifton, H.E., 1999, The ichnology of modern and Pleistocene brackish-water deposits at Willipa Bay, Washington: variability in estuarine settings: *Palaios*, v. 14, p. 352-374.

Gingras, M.K., Rasanen, M., and Ranzi, A., 2002, The significance of bioturbated

inclined heterolithic stratification in the southern part of the Miocene Solimoes Formation, Rio Acre, Amazonia Brazil: *Palaios*, v. 17, p. 591-601.

Heiri, O., Lotter, A.K., and Lemcke, G., 2001, Loss on ignition as a method for estimating organic and carbonate content in sediments: reproducibility and comparability of results: *Journal of Paleolimnology*, v.25, p. 101-110.

Hovikoski, J., Rasanen, M. Gingras, M.K., Roddaz, M., Brusset, S., Hermoza, W., and Romero Pittman, L., 2005, Miocene semidiurnal tidal rhythmites in Madre de Dios, Peru: *Geology*, v. 33, no. 3, p. 177-180.

Howard, J.D., and Frey, R.W., 1975, Regional animal-sediment characteristics of Georgia estuaries: *Senckenbergiana Maritima*, v. 7, p. 33-103.

Johnson, L.R., 1983, The transport mechanism of clay and fine silt in the north Irish Sea: *Marine Geology*, v. 52, p. 33-41.

Lettley, C.D., Gingras, M.K., Pearson, N.J., and Pemberton, S.G., 2005 (*in press*), The repeated development of burrowed firmgrounds on estuarine point bars—modern and ancient examples, and criteria for their discrimination from firmgrounds developed along omission surfaces: *SEPM, Short Course Notes*.

Lick, W., 1994, The flocculation, deposition and resuspension of fine-grained sediments: *in* DePinto, J.V., Lick, W., and Paul, J.F., eds., *Transport and Transformation of Contaminants Near the Sediment-Water Interface*: Lewis Publishers, Boca Raton, p. 35-57.

MacEachern, J.A., and Pemberton, S.G., 1994, Ichnological aspects of incised valley fill systems from the Viking Formation of the Western Canada Sedimentary Basin, Alberta, Canada *in* Boyd, R., Dalrymple, R. W. & Zaitlin, B. A., eds., *Incised Valley Systems: Origin and Sedimentary Sequences*, SEPM, Special Publications, Tulsa, Oklahoma, v. 51, p. 129-157.

MacEachern, J.A., Stelk, C.R., and Pemberton, S.G., 1999, Marine and marginal marine mudstone deposition: paleoenvironmental interpretations based on the integration of ichnology, palynology and foraminiferal paleoecology *in* Bergman, K. A., & Snedden, J. A., eds., *Isolated Shallow Marine Sand Bodies: Sequence Stratigraphic Analysis and Sedimentological Implication*, SEPM, Special Publications, Tulsa, Oklahoma, v. 64, p. 205-225.

Nio, S.D., and Yang, C.S., 1991, Diagnostic attributes of clastic tidal deposits: a review, *in* Smith, D. G., Zaitlin, B. A., Reinson, G. E., & Rahmani, R. A., eds., *Clastic Tidal Sedimentology*, Canadian Society of Petroleum Geologists, Calgary, Alberta, Memoir 16, p. 3-28.

Pejrup, M., 2003, Flocculation, *in* Middleton, G.V., ed., *Encyclopedia of Sediments and Sedimentary Rocks*: Klywer Academic Publishers, Dordrecht, Netherlands, p. 284-285.

Pemberton, S.G, Flach, P.D., and Mossop, G.D., 1982, Trace fossils from the Athabasca Oil Sands, Alberta, Canada: *Science*, v. 217, p. 825-827.

Pemberton, S.G., and Wightman, D.M., 1992, Ichnological characteristics of brackish water deposits: *in* Pemberton, S.G., ed., *Applications of Ichnology to Petroleum Exploration, A Core Workshop*, SEPM, Core Workshop Notes, v. 17, p. 141-167.

Pemberton, S.G., Spila, M.V., Pulham, A.J., Saunders, T., MacEachern, J.A., Robbins, D., and Sinclair, I., 2001, Ichnology and Sedimentology of Shallow to Marginal Marine Systems: Ben Nevis and Avalon Reservoirs, Jeanne D'Arc Basin: Geological Association of Canada, Short Course Notes, no. 15, 343 p.

Reineck, H.E, 1963, Sedimentgefüge im bereichder südlichen nordsee: Abhandlungen der Senchenbergische Naturforschende Gesellschaft, p. 505.

Shrader, H., and Monsen, S., [http://hjs.geol.uib.no/hovedlab/instrument\\_sedigraph\\_operation\\_eng.html](http://hjs.geol.uib.no/hovedlab/instrument_sedigraph_operation_eng.html), Department of Earth Sciences, University of Bergen, September 9, 2005.

Smith, D.G., 1987, Meandering river point bar lithofacies models: modern and ancient examples compared, *in* Ethridge, F. G., Flores, R. M., Harvey, M. D., & Weaver, J. N., eds., Recent Developments in Fluvial Sedimentology, SEPM, Special Publication, Tulsa, Oklahoma, v. 39, p. 83-91.

Smith, D.G., 1988, Modern point-bar deposits analagous to the Athabasca Oil Sands, Alberta, Canada, *in* De Boer, P. L., Van Gelder, A., & Nio, S. D., eds., Tide-Influenced Sedimentary Environments and Facies: Sedimentology and Petroleum Geology, p. 417-432.

Smith, D.G., 1989, Comparative sedimentology of mesotidal (2 to 4 m) estuarine channel point-bar deposits from modern examples and ancient Athabasca Oil Sands (Lower Cretaceous), McMurray Formation, *in* Reinson, G. E., ed., Modern and Ancient Examples of Clastic Tidal Deposits. A Core and Peel Workshop, Canadian Society of Petroleum

Geologists, Calgary, Alberta, p. 60-65.

Stone, M., and Droppo, I.G., 1994, Flocculation of fine-grained suspended solids in the river continuum, *in* Oliver, L.J., Loughran, R.J., and Kesby, J.A., eds., *Variability in Stream Erosion and Sediment Transport*. IAHS-AISH Publication, v. 224, p. 479-489.

Taylor, A., Goldring, R., and Gowland, S., 2003, Analysis and application of ichnofabrics: *Earth Science Reviews*, v. 60, p. 227-259.

Tessier, B., 1993, Upper intertidal rhythmites in Mont-Saint-Micheal Bay (NW France): perspectives for paleoreconstruction: *Marine Geology*, v. 110, p. 355-367.

Thomas, R.G., Smith, D.G., Wood, J.M., Visser, J., Calverley-Range, E.A., and Koster, E.H., 1987, Inclined heterolithic stratification-terminology, description, interpretation, and significance: *Sedimentary Geology*, v. 53, p. 123-179.

Van Leussen, W., and Cornelisse, J.M., 1992, The role of large aggregates in estuarine fine-grained sediment dynamics *in* Mehat, A.J., ed., *Nearshore and Estuarine Cohesive Sediment Transport*. Australian Institute of Mining and Met Parkville, Victoria, Australia, v. 42, p. 75-91.

Water Survey of Canada, [http://www.wsc.ec.gc.ca/statflo/flow\\_daily.cfm](http://www.wsc.ec.gc.ca/statflo/flow_daily.cfm), Environment Canada, September 14, 2005.

### **3.0 A SEDIMENTOLOGICAL AND ICHNOLOGICAL FACIES MODEL FOR MUD-FLAT DEPOSITS**

#### **3.1 INTRODUCTION**

##### **3.1.1 Research Rationale**

Mud-flat deposits represent a significant component of both modern and ancient marginal-marine depositional environments, but their physical *and* biological characteristics are seldom studied together. Much of the previous research completed in estuarine settings (Amos and Mosher 1985; Amos 1987; Dalrymple et al. 1990, 1991, 1992) has demonstrated the importance of the physical sedimentological criteria but has understated the potential that biogenic structures have in interpreting estuarine deposits. Ichnology has been employed (e.g. Reineck 1963; Howard and Frey 1975; Pemberton et al. 1982; Pemberton and Wightman 1992; Gingras et al. 1999; MacEachern et al. 1999; Gingras et al. 2002) to assist in the recognition of lateral variation and identification of key subenvironments within marginal-marine deposits. The development of an ichnological characterization of these deposits is necessary in order to approach a more detailed paleogeographic model for application to the estuarine rock record.

The deposits at Mary's Point, Bay of Fundy, New Brunswick, Canada present an opportunity to integrate ichnological data into a well-understood sedimentological framework. This study focuses on describing the physical and biological structures found in the transition from the lower- to upper-intertidal environments. At this transition, beds displaying evidence of tidal rhythmicity are exposed by creek dissection of tidal point-bar and tidal-flat deposits. As discussed below, the rhythmic beds represent a composite of seasonal and tidal processes. Many beds are locally bioturbated with much of the physical sedimentary character preserved; providing a record of the biological and physical processes for scrutiny. Variations in individual bed thickness, both vertically and laterally, are related to the primary hydraulic processes that influence mud deposition within the mud flat environment. The specific objectives of this research is to: (1) describe the physical and biological structures within the tidal deposits, and (2) identify significant

ichnological trends across the mud flat.

### 3.1.2 Methods

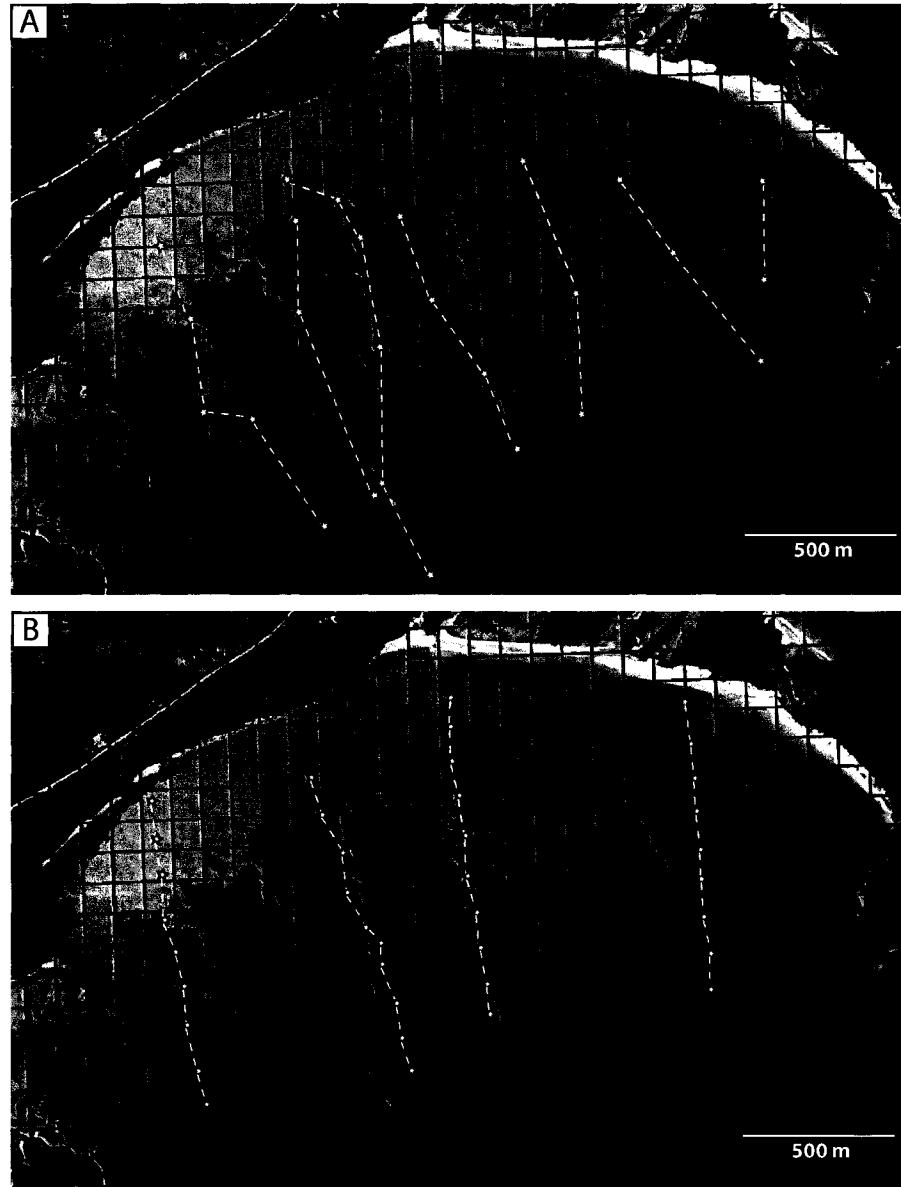


**Figure 3-1:** Schematic diagram of the sampling transects across Mary's Point. (A) Diagram shows the locations of the 26 exposures that were examined for the sedimentological and ichnological characteristics. These sections lie on 7 transects completed across the intertidal flat. (B) Diagram displays the location of the 38 stations that TOC and grain-size data was gathered. These lie on 4 transects completed across the intertidal flat. Note that the map grid was taken from an NTS map, each square is 100 X 100 m.

Exposure of tidal-flat and point-bar deposits were logged (Fig. 3-1), along with box core sampling, and X-ray analysis. X-ray plates were taken from 1 cm thick sediment slices using a Soyee SY-31-100P portable X-ray unit with a fixed time station of 10 mA / 90 kVp. The aforementioned methods allowed the grain diameters, sedimentary structures, nature of bedding contacts and lateral variability to be documented.

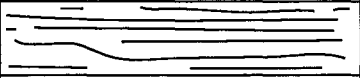
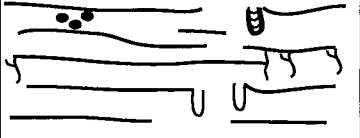
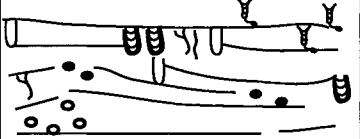
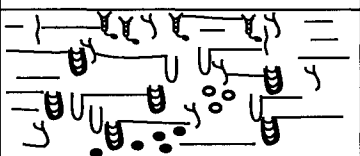
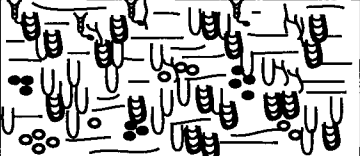
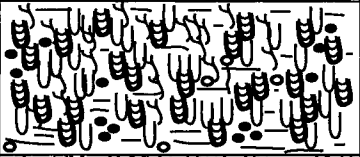
Ichnological observations focused on the identification of individual ichnogenera, the bioturbation intensity, as well as the diversity and abundance of individual insipient ichnofossils. Other data collected included the presence of plant- and shell-debris (e.g. seaweed, logs, *Macoma balthica* shells, etc.) hosted within the silty- or sandy-mud laminae, the presence of pebble/shell lags and *in situ* clasts.

Collection of physical data was limited by the unlithified nature of the sediment. In particular, problems arose when trying to identify individual ichnogenera within historical deposits and in tracing bedding contacts. This difficulty was exacerbated within zones dominated by sediment deformation and fluid-mud accumulation.

Some of the ichnological data were subjectively collected, for example: (1) the bioturbation intensity (hereafter denoted as BI) varies from absent to complete, and (2) trace fossil size was recorded as diminutive (1-5 mm) to moderate (5-8 mm). Measurement of the bioturbation intensity was adapted and modified from Reineck 1963; Taylor et al. 2003; and Bann et al. 2004 (Fig. 3-2).

Laboratory work consisted of sample preparation for the determination of grain-size trends and the percentage of total organic carbon (TOC). The first step in sample preparation was the dehydration of the sediment by heating it at 105°C for 24 hours. Disaggregation of the dry samples was accomplished using a mortar and pestle. Grain-size analysis was conducted using a Sedigraph 5100. The Sedigraph 5100 measures the sedimentation rate using a finely collimated beam of low energy X-rays, which pass through a sample cell. The distribution of particle mass at various points in the cell affects the number of X-ray pulses reaching the detector, which are used to derive the

particle-size distribution and is expressed as a percentage of mass of assigned particle diameters (Shrader and Monsen 2005). The TOC was determined following the method of Heiri et al. (2001), which consists of: (1) assessing the initial mass of the sample; (2) baking samples for 4 hours at 550°C (to incinerate the organic carbon); and (3) measuring the final mass of the sample directly after baking. The difference between the initial and final masses was determined and the result was then recorded as a percentage of the total sample.

Grade	Classification	Visual Representation
0	Bioturbation Absent	
1	Sparse bioturbation, bedding distinct, few discrete traces	
2	Uncommon bioturbation, bedding distinct, low trace density	
3	Moderate bioturbation, bedding boundaries sharp, traces discrete, overlap rare	
4	Common bioturbation, bedding boundaries indistinct, high trace density with common overlap	
5	Abundant bioturbation, bedding completely disturbed (just visible)	
6	Complete bioturbation, total biogenic homogenization of sediment	

**Figure 3-2: Bioturbation intensity (BI).** Measurement of the intensity of bioturbation in the Mary's Point deposits; adapted and modified from Reineck (1963), Taylor et al. (2003), and Bann et al. (2004).

### 3.1.3 Geological Setting

The Bay of Fundy is a macrotidal estuary on the southeastern coast of New Brunswick, Canada. It is a funnel-shaped bay that is approximately 270 km in length and 80 km in width at its head. A tidal range that commonly exceeds 13 m and a tidal prism that exceeds 104 km<sup>3</sup> characterizes the bay (Desplanque and Mossman 2001). The bay's head is split into two smaller bays, Chignecto Bay and the Minas Basin. Chignecto, which is beside our study locale, is a "muddy" estuary due to the nature of its sediment sources, the eroded cliffs that surround the bay and the exhumed seabed. These comprise Paleozoic mudstone and sandstone, and Holocene silt and clay, respectively (Amos 1987). Mary's Point is located in the upper northeast portion of Chignecto Bay (Fig. 3-3) and covers an area of approximately 12 km<sup>2</sup> at mean high tide.

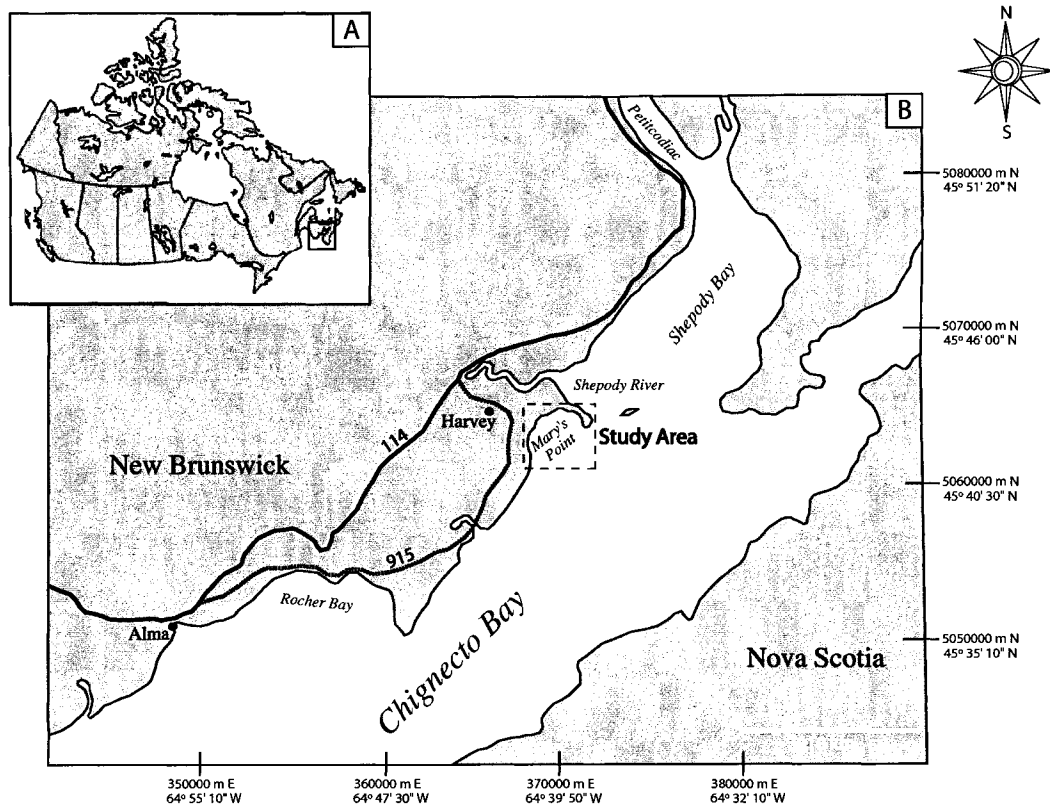


**Figure 3-3:** Location map of Chignecto Bay and Mary's Point, Bay of Fundy, New Brunswick, Canada. (A) Map of Canada with the Bay of Fundy marked by the solid box. (B) Schematic diagram of Chignecto Bay, and the location of the study identified by the dashed box.

This study focused on cut-bank exposures of modern tidal-flat and point-bar deposits established at Mary's Point (5065000 m N, 0370000 m E; N45°43'45", W64°39'50"): Fig. 3-3). The sedimentological and ichnological observations are from 26 cut-bank sections from 7 transects (Fig. 3-1A); while the grain-size and TOC data were collected from 38 stations found on 4 transects across the exposed mud flats (Fig. 3-1B). Sections are well exposed, with low-tide creek bank exposures ranging in height from 0.17 (upper-intertidal) to 1.4 m (lower-intertidal). Low-tide water depths in the thalweg generally range between 0.10 (upper-intertidal) to 0.75 m (lower-intertidal) at times of low river flow. The tidal-flat and point-bar deposits are dominated by the accumulation of fine-grained sediment composed dominantly of silt and clay (mean values: 65% silt, 25% clay and 10% sand). The point-bar deposits are composed of dipping, parallel, interbedded silty- and sandy-mud beds; while the tidal-flat deposits are composed of horizontal, parallel interbedded silty- and sandy-mud beds. The dipping beds are henceforth denoted as "inclined heterolithic stratification" (IHS *sensu* Thomas et al. 1987). The IHS beds are laterally continuous and present throughout the extent of the point-bar exposures, over distances found in excess of 17 m. The tidal creek thalweg sediment was observed to have a higher percentage of sand and granules within it— however no tests were run on this to determine the exact texture.

An infaunal assemblage consisting of bivalves (primarily *Macoma balthica*), worms (*Nereis virens*, *Nereis diversicolor*, *Cerebratulus lacteus*, *Heteromastus*, and *Glycera dibranchiata*), and amphipods (*Corophium volutator*) colonize the depositional surfaces at Mary's Point. Their traces pass into the mud-flat strata and incipient trace fossils produced by similar infauna can be observed in underlying layers. Cut banks that expose historical layers allow examination of the interred beds.

## 3.2 TIDAL-FLAT AND TIDAL-CREEK POINT-BAR DEPOSITS

### 3.2.1 General Sedimentology and Ichnology

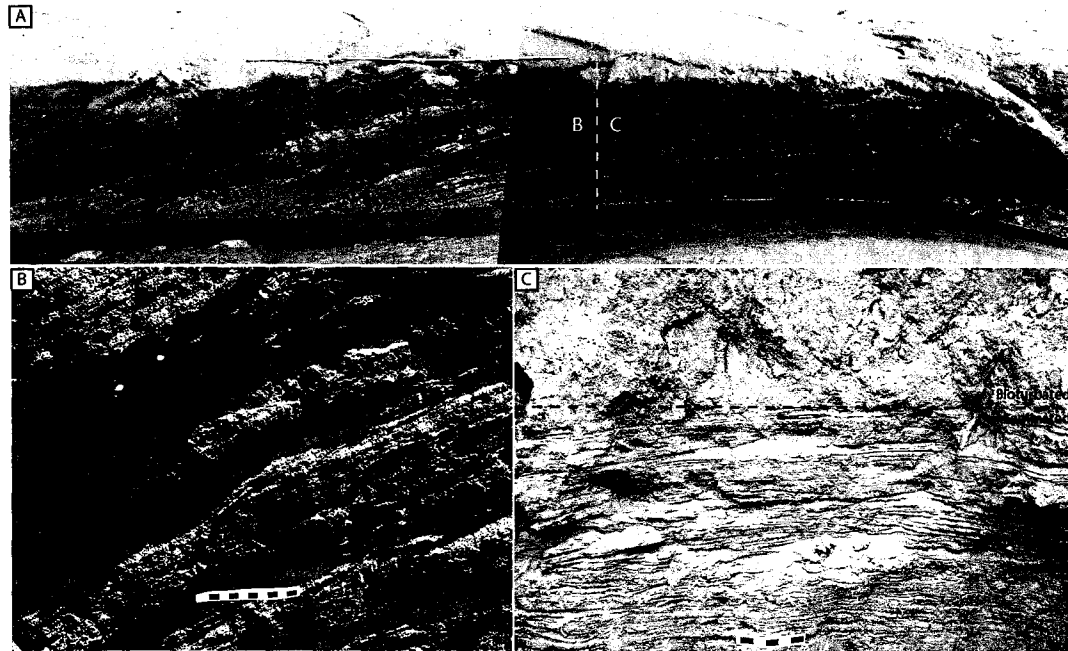


**Figure 3-4:** Sedimentary structures present in the deposits at Mary's Point. (A) Cut bank exposure showing the transition from horizontal, planar-bedded deposits in the upper point bar down into the low-angle, planar-bedded deposits of the lower point bar. The dashed line marks the transition point between these deposits. Scale = 2 m (ruler). (B) Lower point-bar deposits characterized by low-angle, planar-bedding. (C) Upper point-bar deposits typified by horizontal, planar bedding. Units found in this section display a seasonal nature, which is marked by the transition from laminated (early winter and spring) to bioturbated (summer to fall).

At Mary's Point the point bars and tidal flats comprise vertically stacked silty- and sandy-mud. The cohesiveness of the surficial sediment varies considerably across the mud-flat surface. The upper 1 to 11 cm of substrate comprises unconsolidated sediment with a soft to locally fluid consistency. Below the soft substrate the sediment is comparatively firm. This change in cohesiveness is abrupt and fluctuates in depth from 0 to 11 cm across the study area. The tidal-flat portion of the mud flat is characterized by planar, horizontal bedding, and the tidal-creek point-bar sections are predominately low-angle, planar-bedded (Fig. 3-4A). The firmer sediment supports open and unlined burrows, whereas the softer sediment contains burrows that are kept open with the

aid of mucus linings. These characteristics result in a trace assemblage that possesses characteristics of both stiffground and restricted softground ichnofacies (Lettley et al. 2005 *in press*).

The deformed portions of the tidal-creek sections are characterized by the occurrence of both small- and large-scale features (Fig. 3-5A, B). Small-scale deformational features occur on the centimeter scale and are prevalent throughout all the deposits at Mary's Point (Fig. 3-5B). Most individual units, whether laminated or bioturbated, have some soft-sediment deformation within them. Occurrences of large-scale slumping are in areas with high slopes (increase slope instability) or where tidal creeks intersect, this slumping is on the meter-scale (Fig. 3-5A).

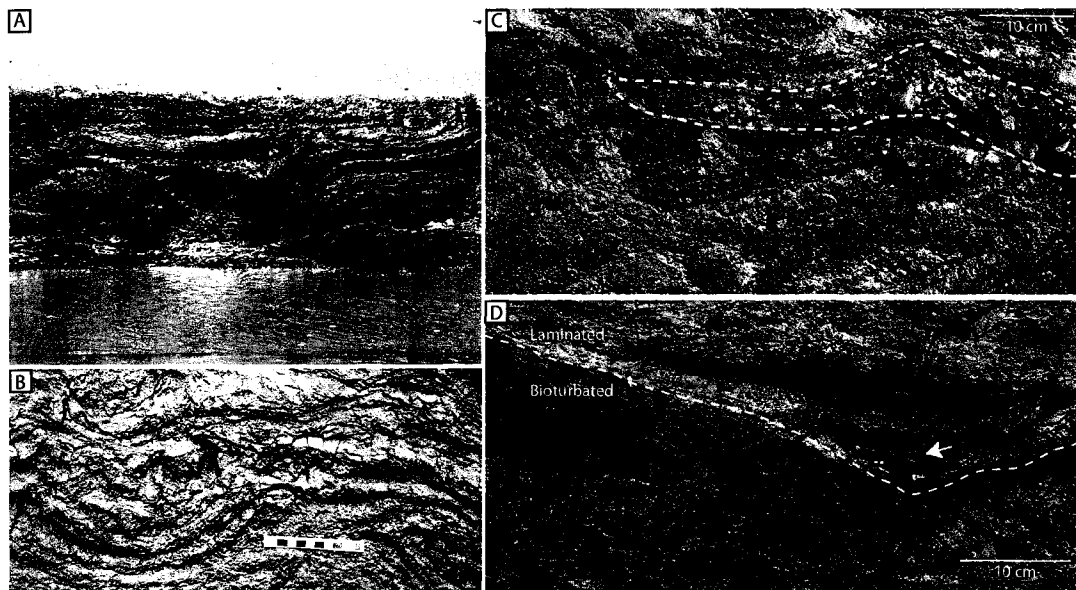


**Figure 3-5:** Different scales of view for convoluted bedding found at Mary's Point. (A) Large-scale deformation found in the upper portion of a point bar. Shovel for scale. (B) Small-scale deformation found in a laminated deposit. Most beds at Mary's Point display this scale of deformation. Scale is in centimeters. (C) Deformation marked by the presence of the patchy pebble/gravel lag. Note the wavy nature of the deformation. The pebble/gravel clasts are accumulating in the synclines of the deformed sediment. (D) Placement of the pebble/gravel lags tends to occur above the bioturbated and below the laminated beds. The arrow points to the pebble/gravel clasts in the syncline of the deformed sediment.

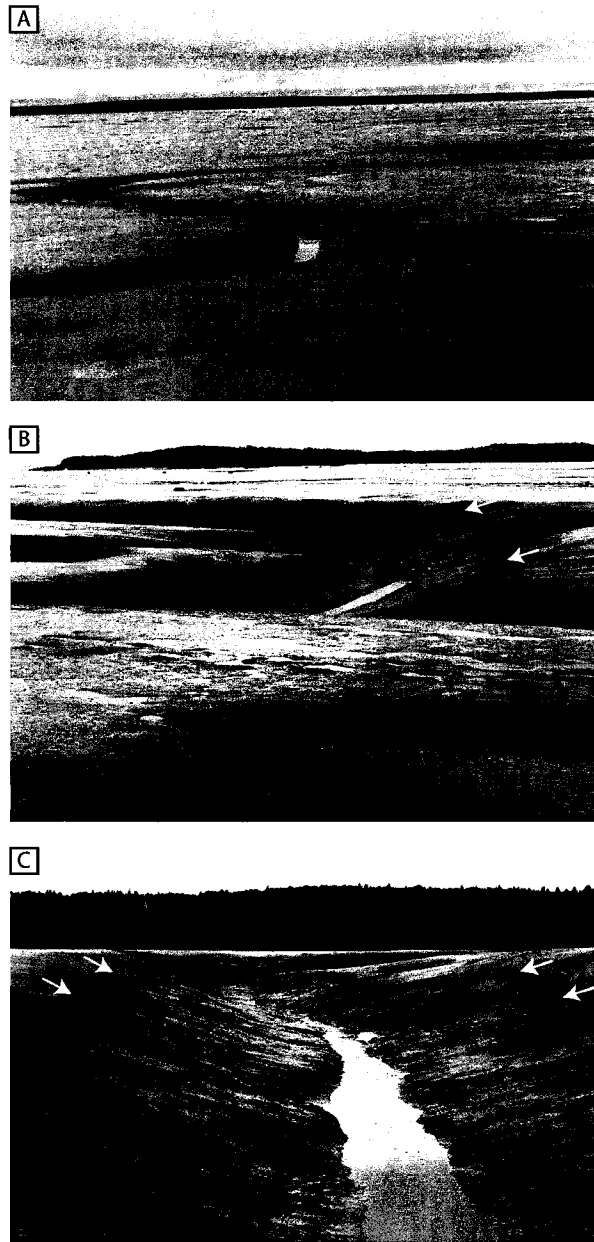


**Figure 3-6:** Morphological features of Mary's Point. (A) Photo shows a shallow, tidal creek in the upper-intertidal zone. Within this zone tidal creeks have broad meanders and creek depths ranging up to 17 cm. Note the right-angle meander-bends and small point bars developed in the foreground. (B) Photo of a tidal creek in the middle-intertidal zone. Noteworthy is the difference in channel depth and width observed from the upper-intertidal to the middle-intertidal zones. Within this zone, tight meanders and channel depths greater than 1.4 m characterize the tidal creeks. Arrows point to areas displaying rotational slumping. (C) Down channel view of a tidal creek in the middle-intertidal zone. Arrows highlight areas where slumping is common. Note that in areas near the creek bend slumping increases and displays characteristics of rotational slumping.

The term “tidal flat” is an inaccurate description of the depositional surface found at Mary’s Point due to the variability in local morphology (Wells et al. 1990). A dendritic network of small tidal creeks dissects the mud flat generating a hummocky intertidal surface. The tight-meandering creeks are the most distinctive morphologic feature in the intertidal zone; they are oriented roughly perpendicular to the coastline and increase in depth towards the bay (Fig. 3-6A, B). Average creek depths range between 17 cm in the upper-intertidal to 2.0 m in the lower-intertidal zones producing varying degrees of intertidal relief over a distance of a few hundred meters. Rotational slides were observed on the flanks of many of the cut-bank sections (Fig. 3-6B). In agreement with Bridges and Leeder’s (1976) observations from the Solway Firth in Scotland the slumps were found on the point-bar slopes of narrow, deeper channels and on the slopes of deeper cut-bank surfaces (Fig. 3-6B, C). Two of the tidal-creeks had point-bar deposits that displayed stepped terracing (Wells et al. 1990). The elevation change from one point-bar terrace to the next was observed to not exceed 20 cm.

The depositional surfaces at Mary’s Point, excepting freshly slumped surfaces and small patches of fluid mud, are characterized by persistent bioturbation from the upper-intertidal zone (~Mean High Water: MHW) to one meter below Mean Low Water (hereafter denoted as MLW). Although bioturbation intensity is generally uncommon to complete (BI 2-6), meter-scale patches are present that have only sparse infaunal traces (BI 1). These sparse patches are normally associated with previously scoured or slumped zones. Infaunal traces referable to the ichnogenera *Siphonichnus* (Fig. 3-7F), *Arenicolites*, *Diplocraterion* (Fig. 3-7E), and *Polykladichnus* (Fig. 3-7A) characterize the upper-intertidal zone (Fig. 3-8C). Surface traces and trackways generated by the interface feeding of *Macoma* (Fig. 3-7B) and *Corophium* (Fig. 3-7 D) are abundant and add to the overall texture of the mud flat surface. These biogenic structures are created by the small bivalve *Macoma balthica* (Fig. 3-7F), the amphipod *Corophium volutator*, and the nereid polychaete *Nereis virens* respectively. Infaunal population counts completed within this

zone ranged between 2300 and >5000 individuals / m<sup>2</sup> (mean value: 4275 individuals / m<sup>2</sup>). *Corophium volutator*, *Nereis virens* and *N. diversicolor*, *Heteromastus*, and rare *Cerebratulus lacteus* (nemertean worm) colonize the middle portion of the intertidal zone (Fig. 3-8B). Within this zone *Arenicolites*-, *Diplocraterion*-, *Polykladichnus*-, *Skolithos*-, *Planolites*-, *Palaeophycus*-, and *Siphonichnus*-like traces are the observed. Here infaunal populations counts locally ranged between 300 to >5000 individuals / m<sup>2</sup> (mean value: >5000 individuals / m<sup>2</sup>). U-shaped burrows dominate the ichnofabric in this zone due to the extremely high population densities of *Corophium* and the close spacing of the burrows. Similar to the upper-intertidal zone, *Nereis* construct Y-shaped burrows referable to the ichnogenera *Polykladichnus*. Many of the *Nereis* burrows have extensive horizontal networks at around 10 cm depth, which commonly resemble the ichnogenera *Planolites* and *Palaeophycus* (Fig. 3-7D). *Cerebratulus* also construct structures consistent with *Planolites* and *Palaeophycus* but these have larger burrow diameters than those made by *Nereis* (5-8 mm versus 2-6 mm). The capitellid polychaete *Heteromastus* typically constructs *Skolithos*-, *Trichichnus*- and *Polykladichnus*-like burrows, and these forms are common in the middle intertidal and are pervasive in the lower-intertidal zone (Fig. 3-8A). Various worms (*Heteromastus*, *Nereis virens*, *Nereis diversicolor*, *Cerebratulus lacteus*, and *Glycera dibranchiata*) are found in the lower intertidal zone. Within this zone infaunal population counts decrease significantly and range from 100 to >5000 individuals / m<sup>2</sup> (mean value: 2100 individuals / m<sup>2</sup>). Below MLW bioturbation is sparse (BI 1) and is inferred to decrease basinward.

Feeding and foraging pits are found on many of the depositional surfaces within each of the aforementioned zones; these are produced by the feeding behavior of the Atlantic sturgeon and are referable to the ichnogenera *Piscichnus* (Fig. 3-9B). The prevalence of this trace in each zone is linked directly to infaunal population density (discussed at length in Chapter 4). Fin traces that descend from areas of intense feeding down into the tidal-creeks are common and are a form of *Undichnia* (Fig. 3-9D). Some

sort of flatfish leaves behind another form of *Piscichnus*, which is outlined by the fish's body impression (Fig. 3-9C). In this instance another type of fin trace (*Undichnia*) can be found leading from the tidal flat surface down into adjacent tidal-creeks (Fig. 3-9A). Other traces found on the flats include the vertebrate trackways of birds (Great Blue Heron: Fig. 3-9E, Canada Goose, and various gulls), and raccoons.

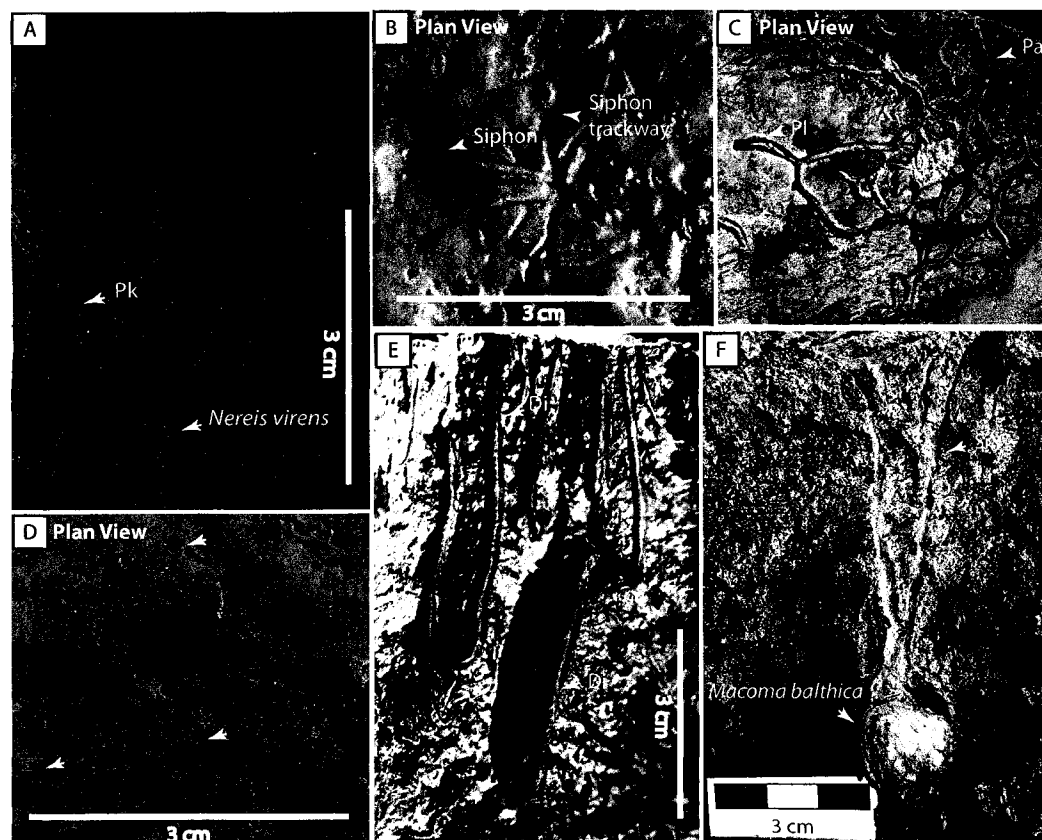


**Figure 3-7:** Infaunal traces observed in the Mary's Point sediment. (A) *Polykladichnus* (Pk), made by *Nereis virens*, vertical face, scale = 3 cm. (B) Surface trace made by *Macoma balthica* while interface feeding. The 'star-like' appearance of this trace is the result of the *Macoma's* siphon probing the sediment (shown in photo). Image is in plan view; scale = 3 cm. (C) Extensive horizontal network of *Nereis virens*. The traces resemble the ichnogenera *Planolites* (Pl) and *Palaeophycus* (Pa). Image is in plan view, scale is in centimetres. (D) Surface trace made by *Corophium volutator* while interface feeding. The grooves leading to the burrow opening are the result of *Corophium* scraping the sediment with their antennae. Arrows point to individual examples of this trace. Image is in plan view, scale = 3 cm. (E) *Diplocraterion* (Di), generated by *Corophium volutator*, vertical face, scale = 3 cm. (F) *Siphonichnus* (Si), generated by *Macoma balthica* (shown), vertical face, scale is in centimetres.

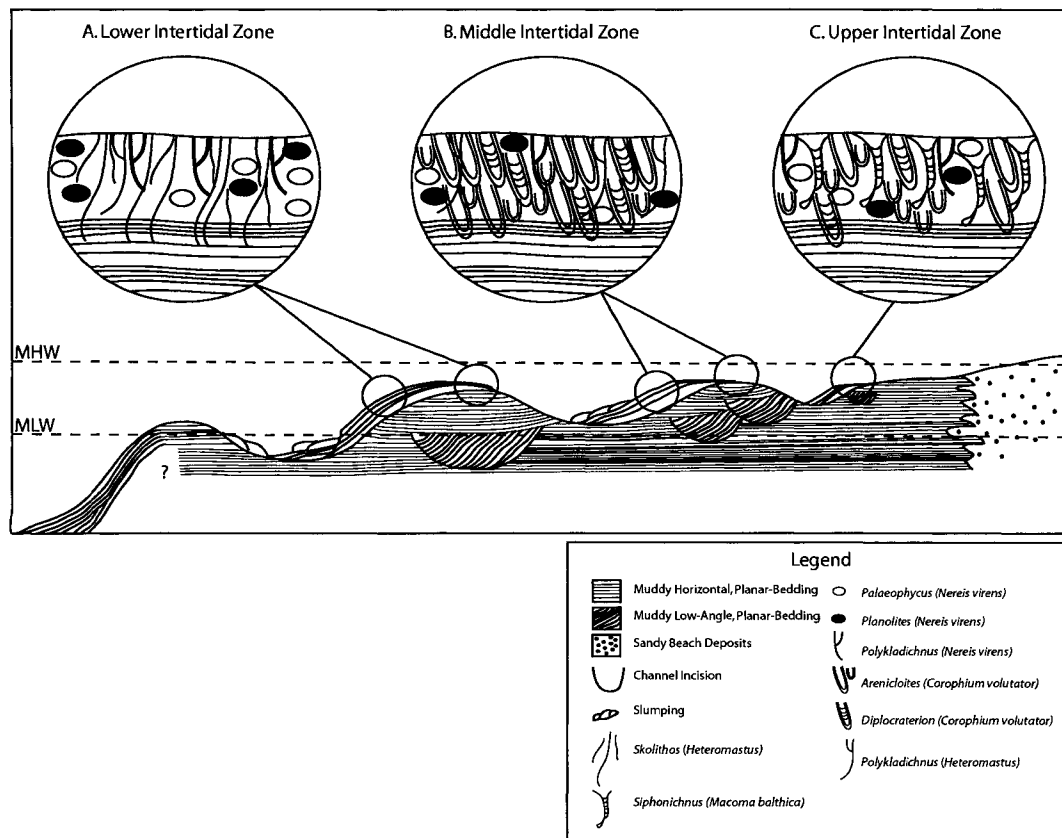


**Figure 3-8:** Schematic diagram of an intertidal point-bar assemblage (substrate is silty-sandy-mud) at Mary's Point. The trace assemblage shown represents the dominant bioturbators present in an intertidal point bar within Mary's Point. (A) The lower-intertidal zone is typified by *Polykladichnus*, *Palaeophycus*, *Planolites* and *Skolithos* burrows. These are the work of *Heteromastus*, *Nereis virens*, *Cerebratulus lacteus*, and *Glycera dibranchiata*. (B) The middle-intertidal zone is dominated by the amphipod *Corophium volutator*, which creates the traces *Arenicolites* and *Diplocraterion*. Other bioturbators present within this zone are *Nereis virens* and *N. diversicolor*, which make *Polykladichnus*, *Planolites*, and *Palaeophycus*; and the bivalve *Macoma balthica*, which produces the trace *Siphonichnus*. (C) The upper-intertidal zone is characterized by the activity of *Nereis virens* and *diversicolor*, *Macoma balthica*, and *Corophium volutator*. *Nereis* produces *Polykladichnus*, *Palaeophycus*, and *Planolites* traces; *Macoma balthica* makes *Siphonichnus* burrow forms; and *Corophium* generates *Arenicolites* and *Diplocraterion* traces.

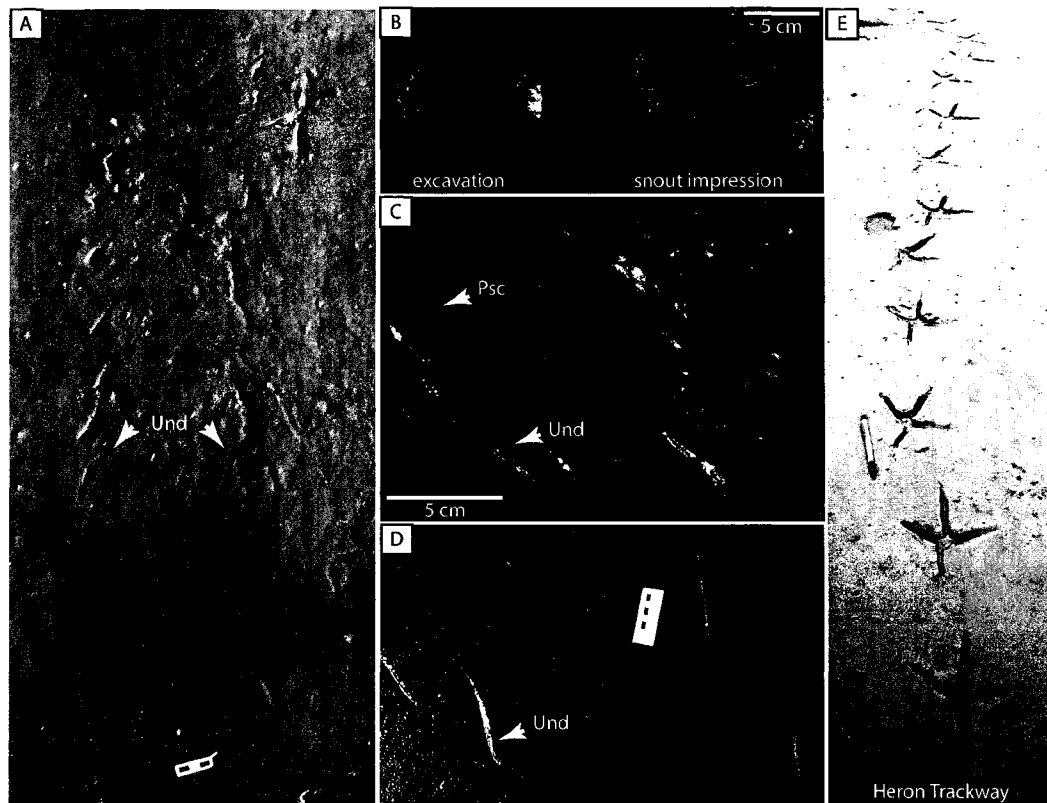


**Figure 3-9:** Traces found on the depositional surface at Mary's Point. (A) *Undichnia* (Und), made by a flat-fish, scale is in centimeters. (B) *Piscichnus*, made by an Atlantic sturgeon, scale = 5 cm. The position of the snout impression in relation to the excavation pit correlates to the anatomical arrangement of the Atlantic sturgeon's snout and protractile mouth. (C) *Piscichnus* (Psc) and *Undichnia* (Und), made by a flatfish, scale = 5 cm. (D) *Undichnia* (Und), made by an Atlantic sturgeon, scale in centimetres. (E) The trackway of a Great Heron, scale = 15 cm (pencil).

Overall, opportunistic organisms characterize the infaunal assemblage, and the resulting ichnocoenosis comprises a low diversity assemblage consisting primarily of diminutive traces: less than 3 mm in diameter in most cases. Trace-makers include *Macoma balthica*, *Corophium volutator*, *Nereis virens*, *Nereis diversicolor*, *Heteromastus*, *Cerebratulus lacteus*, and *Glycera dibranchiata*. The resulting ichnocoenosis is tiered and includes moderate-depth (1-12 cm) *Arenicolites*, *Diplocraterion*, *Skolithos* and *Polykladichnus*, and shallow-depth (1-5 cm) *Siphonichnus*.

### 3.2.2 Detailed Sedimentology and Ichnology of the Cut-bank Sections

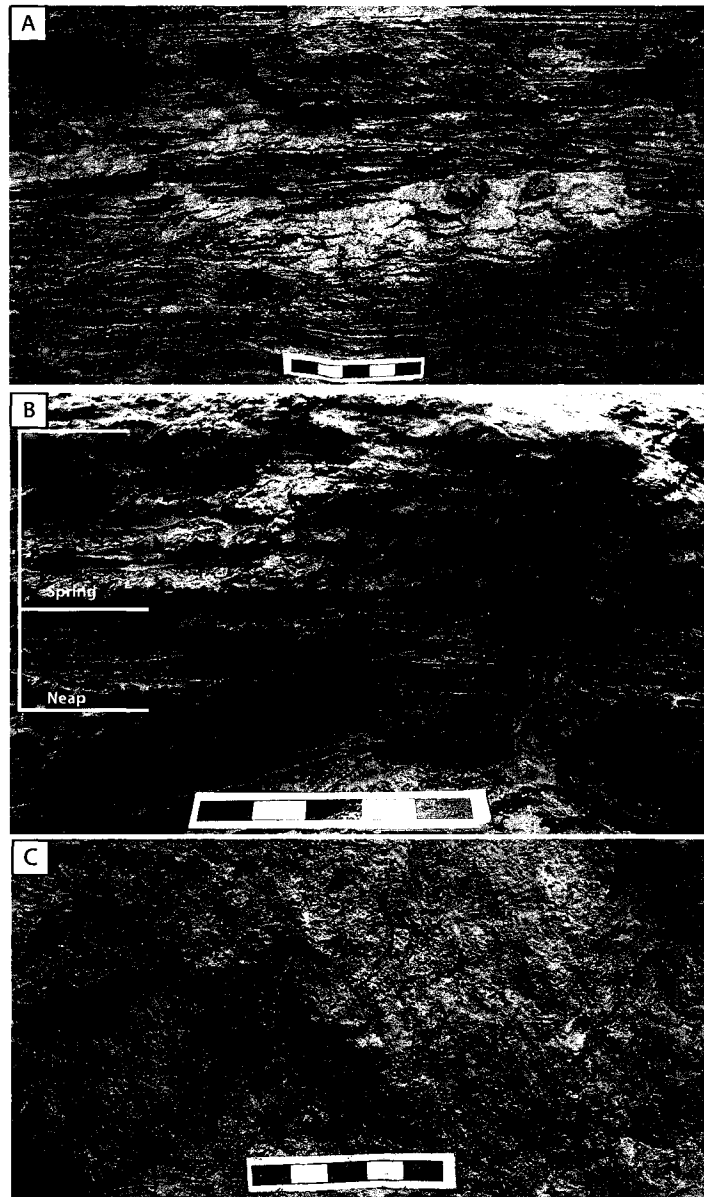


**Figure 3-10:** Seasonal deposits at Mary's Point. (A) Spring deposits typified by horizontal, planar laminated silty- and sandy-mud, and little or no bioturbation (BI 0-2, typically 1). (B) Laminated unit characterized by horizontal, planar-bedding. Within this unit alternations in individual bed thickness were documented; thinner deposits are characteristic of neap tidal cycles (shown), while thicker deposits are from spring tidal cycles (shown). (C) Summer to fall deposits characterized by pervasive bioturbation (BI 2-6, commonly 5).

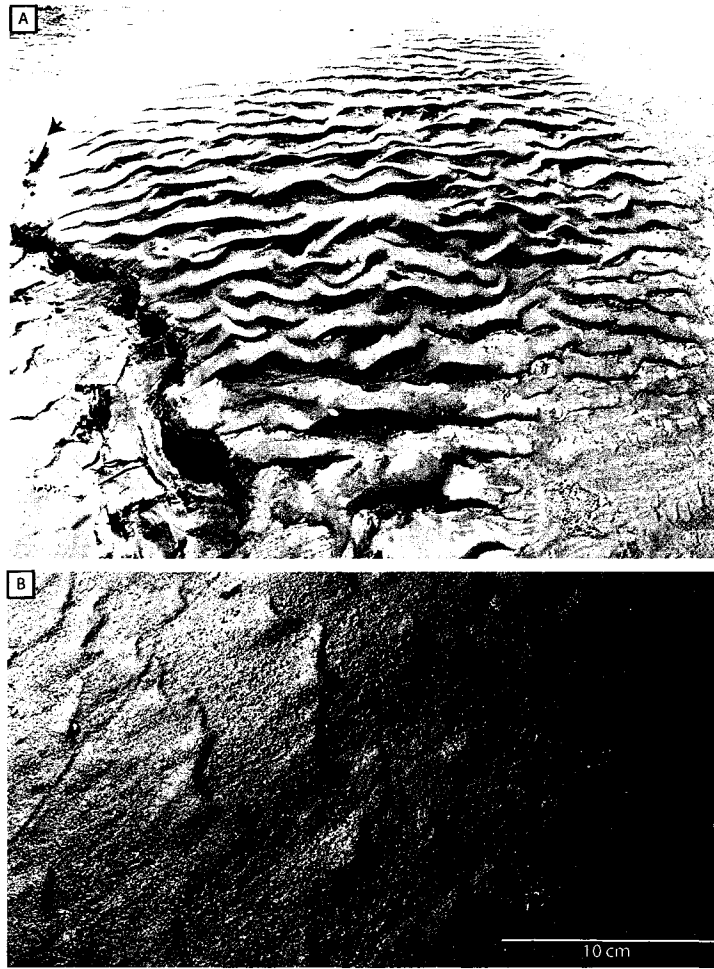


**Figure 3-11:** Isolated occurrences of current ripples on the present day intertidal surface. (A) Sand lens found on the foreground of a point bar. This sand was likely transported from the supratidal zone by ice rafting in the early spring. Ripple foresets dip to the west indicating flood-dominated transport. Scale = 20 cm (arrow). (B) Coarse silt lens found on the intertidal flat. Silt is abundant on the intertidal surface and when coarse enough, current ripples are observed. Ripple foresets dip to the southwest indicating flood-dominated transport.

Within the study area, deposits are dominated by interlaminated and thinly interbedded silty- and sandy-mud. As stated above, observations were made at multiple points across Mary's Point. The different locations are sedimentologically similar, so the best-exposed (i.e. most complete) cut banks were chosen to provide the following detailed description. Point-bar deposits show a gradation from (top) horizontal, planar-bedded to low-angle, planar-bedded tidal couplets (Fig. 3-4A). The low-angle, planar beds are the most prominent and account for almost 75% of the point-bar deposit (Fig.

3-4A, B). The horizontal, planar-bedded deposits characterize the upper portion of the point bar and are the main components of the adjacent tidal-flat deposits (Fig. 3-4A, C). The underlying deposits of the tidal flat are low-angle, planar-bedded deposits of previously migrating point bars. The cut-bank sections are characterized by an alternation between laminated and bioturbated beds (Fig. 3-4C). Burrowed beds range in thickness from 1 to 15 cm (average 6 cm: Fig. 3-10C). The laminated units range in thickness from 1 to 22 cm (average 7 cm) with a general decrease in thickness up section (Fig. 3-10A, B). Individual laminae housed within the couplets show only small variations in their thickness; the silty portion of the couplet commonly reaches 1.5 cm, whereas the sandy portion rarely exceeds 2 mm. Laminae thickness is cyclically variable (Fig. 3-10B). Sandy laminae are fine-grained, well sorted and show no grading. Several other sedimentary structures are present; the most common is soft sediment deformation found at both small- and large-scales (Fig. 3-5A, B). Similar to features reported by Dalrymple et al. (1991) the convolutions consist of sharp-crested anticlines separated by broad synclines (Fig. 3-5C). The relief of the convolutions dissipates upwards into the overlying laminated sediment. Unlike Dalrymple et al's (1991) example, no basal erosional contact was observed marking this deformation; however out-sized clasts up to 30 cm in diameter and/or shell debris were found in troughs of deformed beds (Fig. 3-5C, D). Many of the convolutions are marked by a granule/pebble or shell lag. This lag is laterally discontinuous and occurs sporadically across the sections (Fig. 3-5C). The occurrence of current ripples is rare and coincident with portions of the section that have an increase in silt- or sand-content. Ripples are found on the present-day depositional surface (Fig. 3-11) and intermittently within the historical layers. Desiccation cracks were observed on many of the exposed sections within the middle- and upper-intertidal zone, but were not found on the exposed tidal-flat. Overall, beds are sharp-based and appear crinkled. Burrowed zones may extend down to the sedimentary contacts and obscure those contacts. Point-bar bedding dips vary from 10° to 14° with little variance

(less than 2°) across the entire mud flat. The laminated beds are variably bioturbated, with BI values ranging from 0 to 3, typically 1. The specific traces found within this unit are dependent on which intertidal zone they are contained in (discussed below). An increase in bioturbation usually marks the transition into the bioturbated unit.

Bioturbated beds have a gradational or burrowed contact with the underlying laminated beds. The bioturbated unit generally increases in thickness up section. The beds are characterized by more or less pervasive bioturbation, with intensities ranging from BI 2 to 6 (normally 5). Where the BI is low, biogenic structures are sporadically distributed. Very little organic debris is preserved within the burrowed beds.

### **3.2.3 Total Organic Carbon and Grain-size Analysis**

The grain-size distribution and TOC were assessed for the intertidal flat surface at Mary's Point. Grain-size analyses show that the typical texture is silt (65%), clay (25%), and sand (10%). The overall grain-size trend coarsens baywards; i.e. the percentage of coarse silt increases towards Chignecto Bay (Fig. 3-12B, C).

The TOC averaged 3.1%, with a maximum value of 4.2% and a minimum value of 1.9%. The TOC values generally increases landward (Fig. 3-12A). A small decrease in grain-size and increase in TOC values were found following the transition from the lower- to middle-intertidal zones.

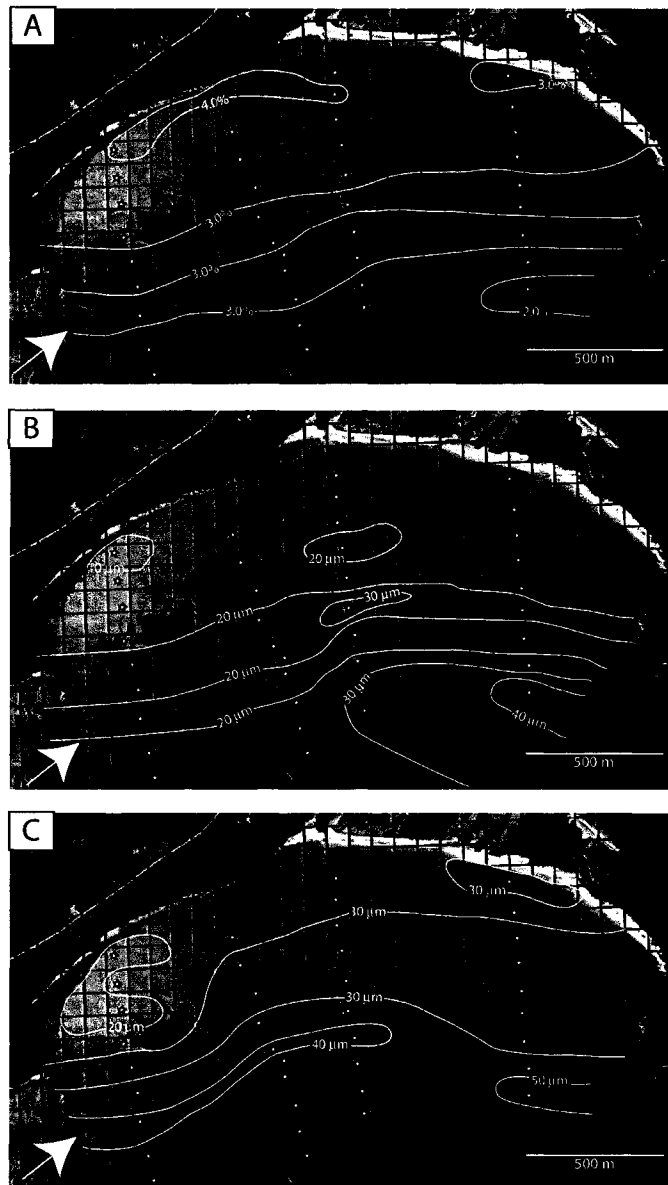


**Figure 3-12:** TOC and grain-size trends measured on the present day intertidal surface at Mary's Point. Note the arrow pointing in the direction of fetch. (A) TOC values. There is an increase in TOC values in the landward direction, with the larger values occurring in areas sheltered from wave action. (B) Mean grain-size values. There is a decrease in grain-size in the landward direction, with the larger values found in areas dominated by wave reworking. Note that the TOC contours occur in the same areas as the mean grain-size contours. (C) Modal grain-size values. Similar to the mean grain-size values these values also decrease in the landward direction and are greatest in areas characterized by wave action.

### 3.3 INTERPRETATIONS

#### 3.3.1 Preservation of a Tidal Signature

Mary's Point mud flats result from fine-grained sediment accumulation within a marginal-marine setting. Specifically, the point-bar deposits (IHS) represent lateral accretion associated with tidally modified channel flow (Thomas et al. 1987; Smith 1987, 1988, 1989; Bann et al. 2004; Choi et al. 2004); and the horizontally laminated deposits of the mud flat represent sediment accumulation under upper-flow regime conditions. The lack of typical tidal physical sedimentary structures (flaser, lenticular, herringbone or wavy bedding) and grain-size contrast is attributed to the overall preponderance of silt, and the near absence of sand-dominated beds. As sand settles out of (intermittent) suspension much more rapidly than silt and clay, its distribution on the mud flats is strongly dependent on local current velocities and proximity to the source (Dalrymple et al. 1991). This is reflected in the mean and modal grain-size distribution documented across the Mary's Point (Fig. 3-12B, C). The larger more coarse material is found nearest to the bay where the fetch/wave action is greatest, and an overall fining is observed in a landward direction. The areas with the smallest recorded mean and modal grain-size distributions correspond to the locations that are sheltered most from wave action. This is consistent with Dalrymple and Choi's (2003) findings that there is a net landward migration of the particles in suspension and as such there is a resulting tendency for fine-grained sediment to accumulate near the landward margin of tidal flats. The rhythmic laminae record deposition from successive tidal cycles and these correspond to subtle changes in the caliber of sediment carried. We attribute cyclic (textural) variation in laminae thickness found in the units at Mary's Point to neap-spring tidal cyclicity (Fig. 3-10B). Progressive thickening of the beds is related to tidal-range increase from the neap to spring tides, whereas thinning-up units reflect the converse (Tessier 1993). Changes in thickness of individual laminae within the neap-spring bundles are likely altered by both

a change in the caliber of sediment (sand versus silt) and diurnal inequality (De Boer et al. 1989; Nio and Yang 1991; Flemming 2003; Hovikoski et al. 2005: seen in Fig. 3-10B). In short, the presence of rhythmic silty- and sandy-mud couplets, likely neap-spring bundles, and asymmetric current ripples attest to the preservation of tidal sedimentary structures within the mud flat.

### **3.3.2 The Significance of Convolute Bedding and Pebble Lags**

Convolute bedding is abundant at Mary's Point and attributed to sediment loading, ice deformation, and penecontemporaneous slumping. Van Leussen and Cornelisse (1992) documented that rapid sedimentation of flocculated material is often observed during periods of decelerating currents or around slack tide. This rapid sedimentation (termed "rapid settling") can trap water in the pore spaces between the settling flocs (Van Leussen and Cornelisse 1992) and create excess pore fluid pressures (Collinson 2003). The muddy sediment is characterized by low permeability, which inhibits the escape of pore waters triggering over-pressured conditions (Collinson 2003). As the sediment is subsequently loaded and compacted this trapped water is released producing small-scale deformational features (Fig. 3-5B). In many of the point-bar sections the muddy sediment is sloping, and commonly the down-slope gravitational component is sufficient to overcome the sediment's cohesive strength (Collinson 2003). The loss of cohesion is one of the causes of the observed large-scale deformation, which is punctuated by the detachment of sections of the sloping sediment (Fig. 3-5A). The rotational slides increase erosion in the channels as sediment is transported from the slump into the basin with subsequent tidal phases. Subsequently, the channel widths increase rapidly (Bridges and Leeder 1976).

Following initial deposition, dewatering increases the sediment cohesiveness, resulting in a comparatively firm substrate. The firm substrate is most influenced by ice deformation (dragging and loading). The presence of the laterally discontinuous

granule/pebble lags, out-sized clasts, and *Macoma* shells are evidence of ice-assisted pebble transport (Fig. 3-5C, D). The patchy distribution of these deposits, and their position within laminated, and directly overlying the bioturbated unit suggests that sediment derived from the lower supratidal zone was brought onto the mud-flat surface by sediment-laden drift ice (Fig. 3-5D). It is probable that periods of increased runoff (spring), increased turbulence associated with storms (late fall and winter), and ice rafting (winter) would most contribute to deposits with this patchy morphology (Dalrymple et al. 1991; Dashtgard and Gingras 2005).

### **3.3.3 Deposition and Accumulation of Muddy Sediment at Mary's Point**

Deposition of the silt-dominated sediment at Mary's Point is accredited to both the suspension settling of silt and clay, as well as traction-dominated deposition of flocculated material and sand. Research has shown that through pelletization, flocculation, and interparticulate reactions, fine-grained material can settle in a manner other than that described by Stoke's Law (Johnson 1983; Amos and Mosher 1985; Van Leussen and Cornelisse 1992; Lick 1994; Stone and Droppo 1994; Pejrup 2003). The occurrence and deposition of flocculated material is controlled by various factors including flow velocity, temperature, dissolved oxygen, pH, suspended-sediment concentration, water-column height, and total dissolved/suspended solids. It is important to note that in a tidal setting, hydraulic energy is neither constant nor evenly distributed. It is expected that during the flood- and ebb-current stages—i.e. when flow velocities are higher—deposition be mainly derived from flocculated material and (to a lesser degree) sand in traction. Previously it was believed that under conditions of higher flow velocity the fragile flocculated material would break up due to turbulence; however, Stone and Droppo (1994) proposed that these conditions in water columns characterized by high suspended sediment concentrations promote flocculation through particle collision. This is supported by Van Leussen and Cornelisse (1992), who observed an entire tidal cycle

in the Ems Estuary and found an abundance of large flocs (200-700  $\mu\text{m}$ ) survived the high flow velocities associated with the dominant flood- and ebb-tides. The Mary's Point waters are mildly turbid with the sediment accumulation on the tidal flat observed to occur in a constant and aggrading manner, not asymmetrically, suggesting that deposition of sediment is primarily from suspension during slack tides and not dominantly from traction during flood- or ebb-tides.

The formation of flocculated material in turbulent waters is dependant on numerous factors. The most significant are: (1) suspended sediment load; (2) the presence of a binding agent such as mucopolysaccharides produced by bacteria, algae, and higher plants; and (3) water column height (Van Leussen and Cornelisse 1992; Stone and Droppo 1994). High-suspended sediment loads characterize the waters at Mary's Point—estimated at 30 g/L (Petitcodiac Environmental Impact Assessment 2005)—and many sections were covered in diatomaceous foam that could easily act as binding agents for the flocculated material. The higher water column and subsequent decrease in bed shear during the later stages of rising tide and the initial stages of falling tide provide ideal conditions for floc formation (Stone and Droppo 1994; Dalrymple and Choi 2003). Slack-water stages, which have little (or no) hydraulic energy, permit deposition of non-flocculated material mainly from suspension and flocculated material through “rapid settling” (Van Leussen and Cornelisse 1992). Rapid settling refers to the rapid sedimentation often observed in periods of decelerating currents or around slack tide (Van Leussen and Cornelisse 1992). This is the set of conditions that we favor for our interpretation of the Mary's Point sediments.

### **3.3.4 Morphology of the Mud Flat**

The processes described above are similar to those active in many of the environments found in the inner estuary (Chapter 2), but the resulting morphology of the Mary's Flats differs significantly. Compared to the main tidal channel systems found

further north of the study area, Mary's Point is best described as having a low-amplitude, hummocky depositional surface. In our study area the intertidal relief changes over a few hundred meters and is understated with relief less than 2 m in most cases. In the larger channel systems the depositional surface has a more pronounced topography, a lower degree of between-channel variability, and channel to tidal flat relief that is commonly greater than 10 m. The sedimentation rates and accommodation space on the tidal flat are lower than those found in the larger tidal channel system. This combined with the absence of a fluvial source of sediment results in thinner deposits on the mud flat than those housed in the main-channel system and are the primary reasons why large channel point bars are not present (Dalrymple et al. 1991).

### **3.3.5 Sedimentologic and Ichnologic Variability at Mary's Point**

The alternating laminated/bioturbated deposits at Mary's Point result from the disparity in seasonal depositional conditions. Laminated sediment accumulates in the early winter and (primarily) spring months when infaunal population densities are low and as a result the amount of sediment reworking is decreased significantly (Dalrymple et al. 1991; Dashtgard et al. 2004). During spring runoff there is an increase in the amount of fine-grained sediment introduced into the mud flat environment. The increase in sedimentation and the inferred decrease in salinity associated with the fresh water input produces conditions not agreeable for substrate colonization. Bioturbated sediment overlies these deposits and represents late-spring colonization of the substrate. Bioturbation of the substrate continues as sediment accumulates during the summer and fall months when salinity, oxygen and temperature conditions return to levels that encourage biogenic reworking of the sediment. As noted above, sediment deformation observed capping this unit is attributed to ice rafting and ice loading during the late winter and early spring months; these contacts coincide with the position of the patchy granule/pebble or shell lags (also reported in Dalrymple et al. 1991).

Biogenic structures are present in the silt-dominated deposits and bioturbation intensity ranges from sparse to complete (BI 1-6). The return to conditions favorable for colonization during the late spring and summer months are echoed in the increase of burrow openings and surficial locomotion trails on the mud-flat surface. The infaunal burrow-like forms reported above *Arenicolites* (abundant), *Diplocraterion* (abundant), *Skolithos*, *Polykladichnus*, *Siphonichnus*, *Planolites*, and *Palaeophycus* (moderate to common) are similar to those reported by Howard and Frey (modern environment: 1975), Pemberton and Wightman (Cretaceous strata: 1992), MacEachern and Pemberton (Cretaceous strata: 1994), Gingras et al. (modern environment: 1999), Pemberton et al. (range of rock-record examples: 2001), Buatois et al. (modern environment and a range of rock record examples: 2005), and MacEachern and Gingras (modern environment and a range of rock record examples: *in press*) as characteristic of the ichnogenera associated with brackish-water environments. These examples are all reported with high-certainty—i.e. well supported by biological and sedimentological criteria—within well-known brackish-water environments. Similarly, this assemblage was inferably shaped by overall low salinities and notable fluctuations in several environmental parameters. The overall low ichnodiversity, high trace densities, simple structures, diminutive traces, and an infaunal assemblage of vertical and horizontal traces characterize the resulting ichnocoenosis. Numerous factors likely limited the size and diversity of the burrowing community: lower or fluctuating salinity levels, changes in oxygenation, overall high turbidity, high sedimentation rates, soft to soupy substrate consistencies, prolonged intertidal exposure time, and daily through seasonal temperature fluctuations. Moreover, fluctuations in temperature result in subsequent variations in the dissolved oxygen and salinity levels found within bay waters. This research underscores the fact that the diminution of infaunal size, overall low densities, and the recruitment of opportunistic species are assigned to brackish-water conditions without difficulty. However, this typical brackish-water ichnological signature results from a composite of stresses that are present

in bays and estuaries (Gingras et al. 1999; Pemberton et al. 2001).

The sedimentology and ichnology between zones of the intertidal flat changes gradationally but distinctively. The lower-intertidal zone (Fig. 3-8A) is characterized by: (1) low to moderate TOC values (1.9 to 3.8 %); (2) high modal grain-size values (40.3 to 55.9  $\mu\text{m}$ ); (3) BI ranging from 2 to 5, commonly 3; and (4) *Polykladichnus*, *Skolithos*, *Palaeophycus*, and *Planolites* traces. The middle intertidal zone (Fig. 3-8B) has: (1) moderate to high TOC values (3.0 to 3.9 %); (2) moderate modal grain-size values (30.1 to 39.3  $\mu\text{m}$ ); (3) BI ranging from 3 to 6, typically 5; and (4) *Arenicolites*, *Diplocraterion*, *Polykladichnus*, *Skolithos*, *Planolites*, and *Palaeophycus* traces. The upper-intertidal zone (Fig. 3-8C) can be described as having: (1) moderate to high TOC values (2.9 to 4.2%); (2) low modal grain-size values (13.8 to 29.6  $\mu\text{m}$ ); (3) BI ranging from 2 to 5, usually 4; and (4) *Siphonichnus*, *Arenicolites*, *Diplocraterion*, *Polykladichnus*, *Planolites* and *Palaeophycus* traces.

The lateral trends observed are the result of variable ecological and sedimentological controls at Mary's Point. The TOC values decrease seaward and are likely linked to the decrease in grain-size. In Dyer et al.'s (2000) comparison of numerous mud-flat environments he reported an increase in the concentration of organic content with a decrease in grain-size. In figure 3-12 A, B this relationship is accentuated by the coincidence of contours separating the changes in TOC and mean grain-size values. Dyer et al.'s (2000) research punctuates the complexity of the organic/grain-size relationship. Overall, grain-size values decrease landward and result from coarser material settling out as the tidal waters move in across the mud-flat surface. As tidal waters move in across Mary's Point their hydraulic energy is dissipated, which results in a decrease in local current speeds. As such, the coarser-grained material is held in suspension (transported) and it settles. Further, in the areas of Mary's Point (NW) that are sheltered from the wave fetch have the lowest observed grain-size and the highest TOC values. Conversely, the areas that are exposed to the full effects of the fetch (SE) have larger mean and modal

grain-size values and the lowest TOC values. The small change in the grain-size and TOC values observed between the lower- and middle- intertidal transition is attributed to the presence of silt ridges on the mud-flat surface (Fig. 3-12).

The lower BI values found in the lower-intertidal zone are the result of higher sedimentation rates found in closer proximity to the bay. With lower sedimentation rates and greater intertidal exposure time the deposits of the upper-intertidal zone have similar bioturbation intensities. The middle-intertidal zone has an increase in infaunal diversity, which can be attributed to higher sediment stability and moderate intertidal exposure times. The presence of desiccation cracks on the middle- and upper-intertidal point-bar sections is evidence of the increase in exposure time and increase in temperature that the burrowing infauna are subjected to. The organisms found in the upper-intertidal zone are exposed for the longest period of time, and as such need to avoid exposure to extreme temperatures and to replenish oxygenated water (Gingras et al. 1999). This is accomplished by the creation of deeper, vertical burrow-like forms (*Siphonichnus*, *Arenicolites*, *Diplocraterion*, and *Polykladichnus*).

### 3.4 SUMMARY

Observations taken at Mary's Point, New Brunswick, Canada permitted the characterization of the ichnological and sedimentological characteristics of estuarine tidal-creek point-bar and tidal-flat deposits. Due to the lack of sedimentary variability across the mud flat the application of neo-ichnology to these deposits provided useful tools for distinguishing the various parts of the point-bar and adjacent tidal-flat deposits: *Polykladichnus*-, *Skolithos*-, *Palaeophycus*-, and *Planolites*-like traces were indicative of the lower-intertidal zone; *Arenicolites*-, *Diplocraterion*-, *Polykladichnus*-, *Skolithos*-, *Planolites*-, *Palaeophycus*-, and *Siphonichnus*-like burrow forms were pervasive in the middle-intertidal zone; and traces similar to the ichnogenera *Siphonichnus*, *Arenicolites*, *Diplocraterion*, *Polykladichnus*, *Planolites* and *Palaeophycus* typified the upper-intertidal

zone. The size and diversity of the burrowing infauna is largely affected by seasonal variations within the composition of the bay water. This assemblage was characterized by a low diversity of traces that were present in high abundance, a pattern that has been commonly noted in brackish-water environments.

Rhythmic bedding characterized both the point-bar and tidal-flat deposits. Interlaminated and thinly interbedded silty- and sandy-mud defined the bedding. On the point-bars, bedding was parallel to the depositional surface (i.e. dipped towards the channel) and represented mud-dominated inclined heterolithic stratification. On the tidal-flats bedding was dominated by horizontal, parallel bedding and was underlain by previous point-bar deposits of the laterally migrating channels. Rhythmic bedding observed in these deposits represented the operation of both tidal and seasonal processes. Tidal processes were recorded in the laminated beds as rhythmic lamination and rare preserved starved ripples. The (laminated) tidal deposits resulted from the deposition of flocculated material and traction-borne sediment during the flood- and ebb-tide and to a larger extent the slack-water accumulation of fines from suspension and flocculated material from “rapid settling”. Cyclic variations in laminae thickness resulted from neap-spring variation in tidal current strength. Although the burrowed interbeds were arguably exposed to the same tidal conditions in which the laminated beds accumulated in, biogenic reworking eradicated the tidal sedimentary signature. Intercalated laminated/burrowed beds reflect seasonal variations in the depositional system. The laminated beds characterize early winter and (primarily) spring sediment, whereas the bioturbated beds typify summer and fall deposits. These deposits were the result of the seasonal variation in the bay water composition. These beds are largely affected by temperature fluctuations.

### 3.5 REFERENCES

- Amos, C.L., 1987, Fine-grained sediment transport in Chignecto Bay, Bay of Fundy, Canada: *Continental Shelf Research*, v. 7, p. 1295-1300.
- Amos, C.L, and Mosher, D.C., 1985, Erosion and deposition of fine-grained sediments from the Bay of Fundy: *Sedimentology*, v. 32, p. 815-832.
- Bann, K.L., Fielding, C.R., MacEachern, J.A., and Tye, S.C., 2004, Differentiation of estuarine and offshore marine deposits using integrated ichnology and sedimentology: Permian Pebble Beach Formation, Sydney Basin, Australia, *in* Mcilroy, D., ed., *The Application of Ichnology to Paleoenvironmental and Stratigraphic Analysis*: Geological Society, London, Special Publications, v. 228, p. 179-211.
- Bridges, P.H., and Leeder, M.R., 1976, Sedimentary model for intertidal mudflat channels, with examples from the Solway Firth, Scotland: *Sedimentology*, v. 23, p. 533-552.
- Buatois, L.A., Gingras, M.K., MacEachern, J.A., Mangano, M.G., Zonnerveld, J.P., Pemberton, S.G., Netto, R.G., and Martin, A., 2005, Colonization of brackish-water systems through time: evidence from the trace-fossil record: *Palaios*, v. 20, no. 4, p. 321-347.
- Choi, K.S., Dalrymple, R.W., Chun, S.S., and Kim, S.P. 2004, Sedimentology of modern, inclined heterolithic stratification (IHS) in the macrotidal Han River Delta, Korea: *Journal of Sedimentary Research*, v. 74, no. 5, p. 677-689.
- Collinson, J.D., 2003, Deformation of sediments, *in* Middleton, G.V., ed., *Encyclopedia*

of Sediments and Sedimentary Rocks: Klywer Academic Publishers, Dordrecht, Netherlands, p. 190-193.

Dalrymple, R.W., Knight, R.J., Zaitlin, B.A., and Middleton, G.V., 1990, Dynamics and facies models of a macrotidal sand-bar complex, Cobequid Bay-Salmon River Estuary, Bay of Fundy: *Sedimentology*, v. 37, p. 577-612.

Dalrymple, R.W., Makino, Y., and Zaitlin, B.A., 1991, Temporal and spatial patterns of rhythmic deposition on mud flats in the macrotidal Cobequid Bay-Salmon River Estuary, Bay of Fundy, Canada, *in* Smith, D. G., Zaitlin, B. A., Reinson, G. E., & Rahmani, R. A., eds., *Clastic Tidal Sedimentology*, Canadian Society of Petroleum Geologists, Calgary, Alberta, Memoir 16, p. 137-160.

Dalrymple, R.W., Zaitlin, B.A., and Boyd, R., 1992, Estuarine facies models: conceptual basis and stratigraphic implications: *Journal of Sedimentary Petrology*, v. 62, p. 1130-1146.

Dalrymple, R.W., and Choi, K., 2003, Sediment transport by tides, *in* Middleton, G.V., ed., *Encyclopedia of Sediments and Sedimentary Rocks*: Klywer Academic Publishers, Dordrecht, Netherlands, p.606-609.

Dashtgard, S.E., Watson, N.J., and Gingras, M.K., 2004, *Sedimentology and Ichnology at the Bay of Fundy*: ASIRT Consortium Field Trip.

Dashtgard, S.E., and Gingras, M.K., 2005, Facies architecture and ichnology of recent salt-marsh deposits: Waterside Marsh, New Brunswick, Canada: *Journal of Sedimentary Research*, v. 75, p. 594-605.

De Boer, P.L., Oost, A.P., and Visser, M.J., 1989, The diurnal inequality of the tide as a parameter for recognizing tidal influences: *Journal of Sedimentary Petrology*, v. 59, p. 912-921.

Desplanque, C., and Mossman, D.J., 2001, Bay of Fundy tides: *Geoscience Canada*, v. 28, p. 1-11.

Dyer, K.R., Christie, M.C., and Wright, E.W., 2000, The classification of intertidal mudflats: *Continental Shelf Research*, n. 20, p. 1039-1060.

Flemming, B.W., 2003, Tidal Flats, *in* Middleton, G.V., ed., *Encyclopedia of Sediments and Sedimentary Rocks*: Kluwer Academic Publishers, Dordrecht, Netherlands, p. 734-737.

Gingras, M.K., Pemberton, S.G., Saunders, T., and Clifton, H.E., 1999, The ichnology of modern and Pleistocene brackish-water deposits at Willapa Bay, Washington: variability in estuarine settings: *Palaios*, v. 14, p. 352-374.

Gingras, M.K., Rasanen, M., and Ranzi, A., 2002, The significance of bioturbated inclined heterolithic stratification in the southern part of the Miocene Solimoes Formation, Rio Acre, Amazonia Brazil: *Palaios*, v. 17, p. 591-601.

Heiri, O., Lotter, A.K., and Lemcke, G., 2001, Loss on ignition as a method for estimating organic and carbonate content in sediments: reproducibility and comparability of results: *Journal of Paleolimnology*, v.25, p. 101-110.

Hovikoski, J., Rasanen, M. Gingras, M.K., Roddaz, M., Brusset, S., Hermoza, W., and Romero Pittman, L., 2005, Miocene semidiurnal tidal rhythmites in Madre de Dios, Peru: *Geology*, v. 33, no. 3, p. 177-180.

Howard, J.D., and Frey, R.W., 1975, Regional animal-sediment characteristics of Georgia estuaries: *Senckenbergiana Maritima*, v. 7, p. 33-103.

Johnson, L.R., 1983, The transport mechanism of clay and fine silt in the north Irish Sea: *Marine Geology*, v. 52, p. 33-41.

Lettley, C.D., Gingras, M.K., Pearson, N.J., and Pemberton, S.G., 2005 (*in press*), The repeated development of burrowed firmgrounds on estuarine point bars—modern and ancient examples, and criteria for their discrimination from firmgrounds developed along omission surfaces: *SEPM, Short Course Notes*.

Lick, W., 1994, The flocculation, deposition and resuspension of fine-grained sediments: *in* DePinto, J.V., Lick, W., and Paul, J.F., eds., *Transport and Transformation of Contaminants Near the Sediment-Water Interface*: Lewis Publishers, Boca Raton, p. 35-57.

MacEachern, J.A., and Pemberton, S.G., 1994, Ichnological aspects of incised valley fill systems from the Viking Formation of the Western Canada Sedimentary Basin, Alberta, Canada *in* Boyd, R., Dalrymple, R. W. & Zaitlin, B. A., eds., *Incised Valley Systems: Origin and Sedimentary Sequences*, *SEPM, Special Publications*, Tulsa, Oklahoma, v. 51, p. 129-157.

MacEachern, J.A., and Gingras, M.K., (*in press*), Recognition of brackish-water trace

fossil assemblages in the Cretaceous Western Interior Seaway of Alberta: Ichnia Special Publication.

MacEachern, J.A., Stelk, C.R., and Pemberton, S.G., 1999, Marine and marginal marine mudstone deposition: paleoenvironmental interpretations based on the integration of ichnology, palynology and foraminiferal paleoecology *in* Bergman, K. A., & Snedden, J. A., eds., *Isolated Shallow Marine Sand Bodies: Sequence Stratigraphic Analysis and Sedimentological Implication*, SEPM, Special Publications, Tulsa, Oklahoma, v. 64, p. 205-225.

Nio, S.D., and Yang, C.S., 1991, Diagnostic attributes of clastic tidal deposits: a review, *in* Smith, D. G., Zaitlin, B. A., Reinson, G. E., & Rahmani, R. A., eds., *Clastic Tidal Sedimentology*, Canadian Society of Petroleum Geologists, Calgary, Alberta, Memoir 16, p. 3-28.

Pejrup. M., 2003, Flocculation, *in* Middleton, G.V., ed., *Encyclopedia of Sediments and Sedimentary Rocks*: Klywer Academic Publishers, Dordrecht, Netherlands, p. 284-285.

Pemberton, S.G, Flach, P.D., and Mossop, G.D., 1982, Trace fossils from the Athabasca Oil Sands, Alberta, Canada: *Science*, v. 217, p. 825-827.

Pemberton, S.G., Spila, M.V., Pulham, A.J., Saunders, T., MacEachern, J.A., Robbins, D., and Sinclair, I., 2001, Ichnology and Sedimentology of Shallow to Marginal Marine Systems: Ben Nevis and Avalon Reservoirs, Jeanne D'Arc Basin: Geological Association of Canada, Short Course Notes, no. 15, 343 p.

Pemberton, S.G., and Wightman, D.M., 1992, Ichnological characteristics of brackish

water deposits: *in* Pemberton, S.G., ed., Applications of Ichnology to Petroleum Exploration, A Core Workshop, SEPM, Core Workshop Notes, v. 17, p. 141-167.

Petitcodiac Environmental Impact Assessment, <http://www.petitcodiac.com/freq-e.htm>,  
Gouvernement of Canada & the Provincial Government of New Brunswick, November 16,  
2005.

Reineck, H.E, 1963, Sedimentgefüge im bereichder südlichen nordsee: Abhandlungen der  
Senchenbergische Naturforschende Gesellschaft, p. 505.

Shrader, H., and Monsen, S., <http://www.petitcodiac.com/freq-e.htm>, Department of  
Earth Sciences, University of Bergen, September 9, 2005.

Smith, D.G., 1987, Meandering river point bar lithofacies models: modern and ancient  
examples compared, *in* Ethridge, F. G., Flores, R. M., Harvey, M. D., & Weaver, J. N.,  
eds., Recent Developments in Fluvial Sedimentology, SEPM, Special Publication, Tulsa,  
Oklahoma, v. 39, p. 83-91.

Smith, D.G., 1988, Modern point-bar deposits analagous to the Athabasca Oil Sands,  
Alberta, Canada, *in* De Boer, P. L., Van Gelder, A., & Nio, S. D., eds., Tide-Influenced  
Sedimentary Environments and Facies: Sedimentology and Petroleum Geology, p. 417-  
432.

Smith, D.G., 1989, Comparative sedimentology of mesotidal (2 to 4 m) estuarine channel  
point-bar deposits from modern examples and ancient Athabasca Oil Sands (Lower  
Cretaceous), McMurray Formation, *in* Reinson, G. E., ed., Modern and Ancient Examples  
of Clastic Tidal Deposits. A Core and Peel Workshop, Canadian Society of Petroleum

Geologists, Calgary, Alberta, p. 60-65.

Stone, M., and Droppo, I.G., 1994, Flocculation of fine-grained suspended solids in the river continuum, *in* Oliver, L.J., Loughran, R.J., and Kesby, J.A., eds., *Variability in Stream Erosion and Sediment Transport*. IAHS-AISH Publication, v. 224, p. 479-489.

Taylor, A., Goldring, R., and Gowland, S., 2003, Analysis and application of ichnofabrics: *Earth Science Reviews*, v. 60, p. 227-259.

Tessier, B., 1993, Upper intertidal rhythmites in Mont-Saint-Micheal Bay (NW France): perspectives for paleoreconstruction: *Marine Geology*, v. 110, p. 355-367.

Thomas, R.G., Smith, D.G., Wood, J.M., Visser, J., Calverley-Range, E.A., and Koster, E.H., 1987, Inclined heterolithic stratification-terminology, description, interpretation, and significance: *Sedimentary Geology*, v. 53, p. 123-179.

Van Leussen, W., and Cornelisse, J.M., 1992, The role of large aggregates in estuarine fine-grained sediment dynamics *in* Mehat, A.J., ed., *Nearshore and Estuarine Cohesive Sediment Transport*. Australian Institute of Mining and Met Parkville, Victoria, Australia, v. 42, p. 75-91.

Wells, J.T., Adams, Jr., C.E, Park, Y.A., and Frankenberg, E.W., 1990, Morphology, sedimentology, and tidal channel processes on a high-tide range mudflat, west coast of South Korea: *Marine Geology*, v. 95, p. 111-130.

## 4.0 THE SIGNIFICANCE OF ATLANTIC STURGEON FEEDING EXCAVATIONS, MARY'S POINT, BAY OF FUNDY, NEW BRUNSWICK, CANADA

A version of this chapter has been submitted to the journal *Palaios* for publication. Pearson, N.J., Gingras, M.K., Armitage, I.A., and Pemberton, S.G. *in review*.

### 4.1 INTRODUCTION

#### 4.1.1 Research Rationale

Feeding excavations of the Atlantic sturgeon (*Acipenser oxyrinchus*) are common on the intertidal mud flats adjacent to Mary's Point, New Brunswick, Canada. Many of these foraging traces comprise a crescent-shaped depression adjacent to a cylindrical hole (Fig. 4-1). Bigelow and Schroeder (1953, p.83) suggested that the feeding depressions are the work of sturgeon "...rooting in the sand or mud with its snout..." in their search for buried infauna. In fact, the crescent portion of the trace represents the animal's snout, whereas the cylindrical hole was made by the animal's everted mouth.

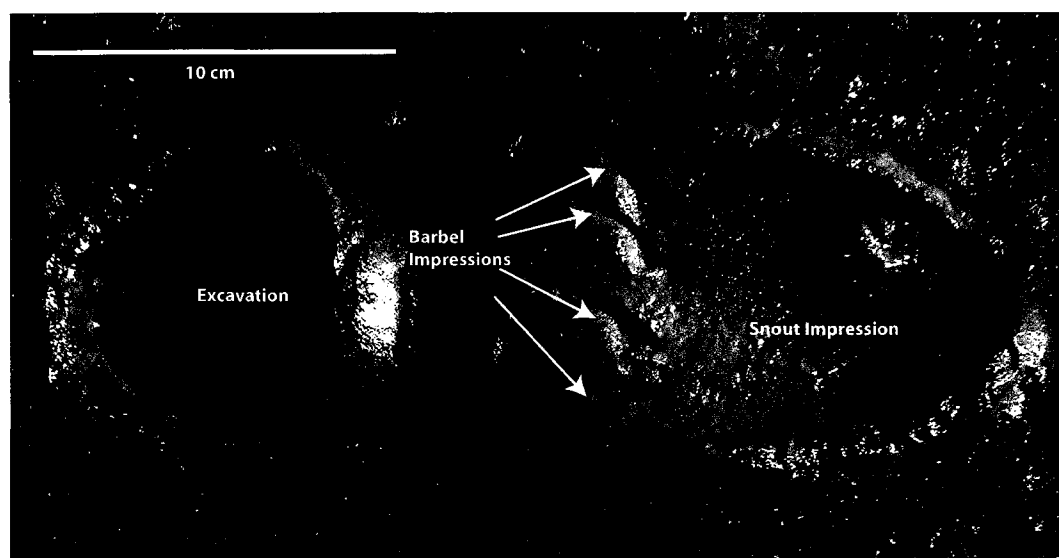


**Figure 4-1:** Typical sturgeon feeding excavation. The shallow, crescent-shaped snout-impression houses the preserved barbel impression and is closely followed by the cylindrical plug-shaped excavation. Substrate is silty- to sandy-mud and excavations are usually 2 to 6 cm in depth. Note that bay water is impounded within the cylindrical excavation.

Research on modern and fossil fish traces (Cook 1971; Howard and Frey 1975; Howard et al. 1977; Gregory et al. 1979; Gregory 1991; Kotake and Nara 2002) suggests that although the individual trace may have little paleoenvironmental significance (i.e. they have no strong ichnofacies association) useful supplementary information can be obtained through the study of such excavations. Such information can include substrate consistency, predator-prey relationships, and ecological structure. Given the paucity of research on ancient and modern fish-feeding traces, developing an ichnological characterization of modern occurrences is useful and should add to our overall understanding of the potential sedimentological and paleoecological applications of *Piscichnus*.

The objectives of this paper are to: (1) describe the geometry and mechanism of excavation of the Atlantic sturgeon feeding pits, (2) associate the occurrence of the traces with the distribution of infauna on the Mary's Points tidal flats, (3) use oriented traces to reveal the animal's orientation at the time of trace emplacement and thereby assess the role that hydraulic currents may have in the orientation of these excavations, and (4) consider the effect that fish-feeding activities have on the erosion and resuspension of sediment on the intertidal mud flat at Mary's Point.

#### **4.1.2 Methods**

The methods used to investigate the foraging activities of the Atlantic sturgeon included trace-density counts, trace orientations, and infaunal identification and density assessments. Transects across Mary's Point were initiated from the beach with the initial station's location coincident with the first occurrence of sturgeon feeding excavations. Transects were generally 1 km in length and followed an oceanward bearing. Stations were erected every 100 m and a 100 m<sup>2</sup> grid was traced on the sediment surface. This grid was divided into four quadrants (NE, SE, SW & NW) and the trace-density counts, trace orientations and determination of infaunal content were completed within each.

*Piscichnus* orientations were measured only if the snout impression was preserved. Without this impression the orientation of the organism at the time of excavation is indeterminate. Orientations were taken such that the medial line of the crescentic impression was bisected through the cylindrical excavation. Because the mouth is behind the snout of the animal, the animal's orientation is towards the crescent-shaped indent (Fig. 4-1).

Infaunal density was derived by counting the number of active burrow openings in a 100 cm<sup>2</sup> area and up-scaling that quantity to square meters. This is a particularly useful scheme when assessing small animals, such as *Corophium*, which are often present in very high population densities (up to 60,000/m<sup>2</sup>). Several randomly selected squares were chosen in each quadrant: their median value is reported.

Other data collected included the presence of plant- and shell-debris (e.g. seaweed, *Macoma balthica* shells, etc.) surrounding or contained within any of the traces, as well as sedimentological observations including bedforms present, substrate consistency, and grain size (determined by Sedigraph).

#### 4.1.3 Geological Setting

The Bay of Fundy is a large, macrotidal estuary on the eastern coast of New Brunswick, Canada. It is a straight-sided, funnel-shaped bay that is 270 km in length and 80 km in width at its head. A tidal range that commonly exceeds 13 m and a tidal prism that surpasses 104 km<sup>3</sup> characterizes the bay (Desplanque and Mossman 2001). The bay's head is split into two smaller bays, Chignecto Bay and the Minas Basin. Chignecto, which is adjacent to our study locale, is a "muddy" estuary due to the nature of its sediment sources: i.e. the eroded cliffs that surround the bay and the eroded seabed. These are composed of Paleozoic mudstone and sandstone, and Holocene silt and clay, respectively (Amos 1987). Mary's Point is located in the upper (NE) portion of Chignecto Bay and covers an area of approximately 12 km<sup>2</sup> at mean high tide (Fig. 4-2).

This study focused on intertidal components of the tidal flats at Mary's Point (N45°43'45", W64°39'50"; 5065000 m N, 0370000 m E: Fig. 4-2). Four transects were completed across the exposed mud flats. The tidal-flat deposits are dominated by the accumulation of fine-grained sediment and are composed primarily of silt and clay (mean values: sand 10%, silt 65%, and clay 25%). Depositional surfaces are generally colonized by an infaunal assemblage comprising bivalves (primarily *Macoma balthica*), worms (nereid, capitellid and glyceriid polychaetes) and amphipods (*Corophium volutator*). Their traces pass into the mud flat strata and incipient trace fossils produced by similar infauna can be observed in the underlying layers.

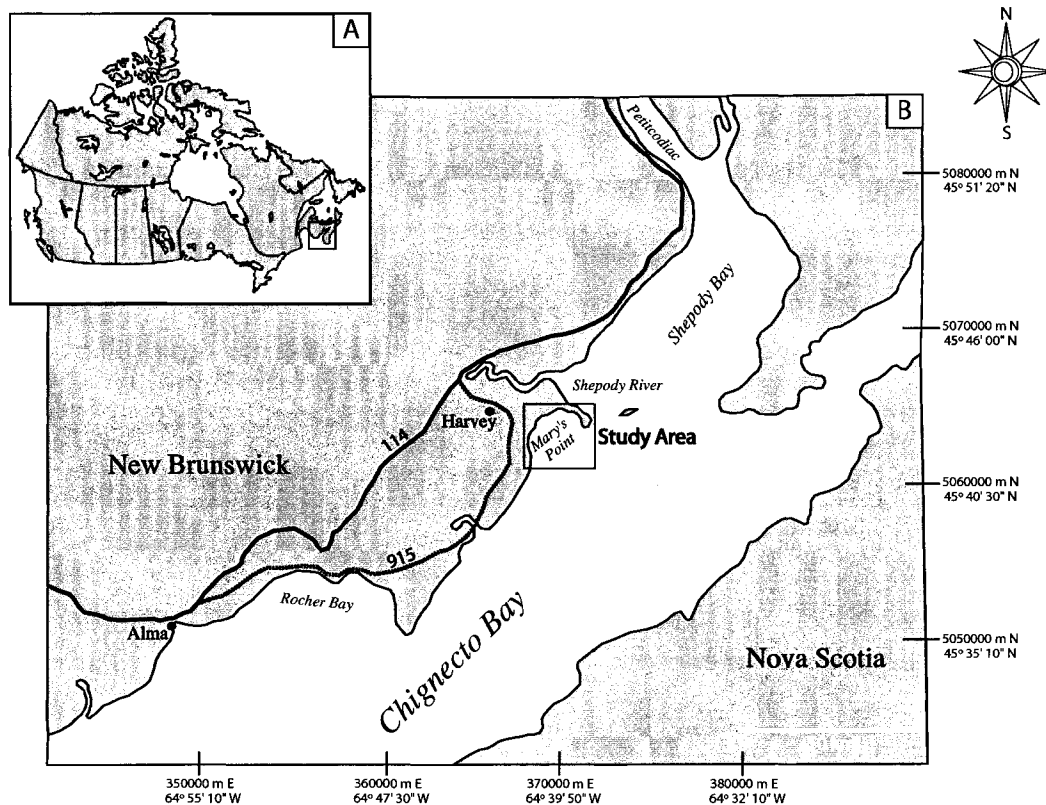


**Figure 4-2:** Location map of Chignecto Bay and Mary's Point, Bay of Fundy, New Brunswick, Canada. (A) Map of Canada with the Bay of Fundy identified by the solid box. (B) Schematic diagram of Chignecto Bay, and the location of the study area (dashed box).

#### 4.2 THE ATLANTIC STURGEON (*ACIPENSER OXYRHYNCHUS*)

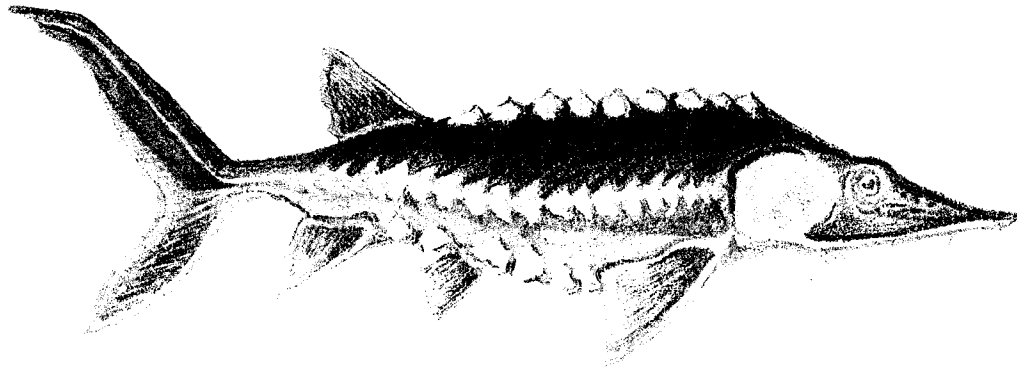


**Figure 4-3:** Sketch of the Atlantic Sturgeon, *Acipenser oxyrinchus*. Sketch by Kar-men Zivkovic.

The Atlantic sturgeon, *Acipenser oxyrinchus*, is common in the Atlantic coastal waters of North America from the north in Ungava Bay, Quebec to their southerly range in eastern Florida (Scott and Crossman 1973). Liem and Scott (1966) describe this fish as elongate, and somewhat cylindrically armed with five rows of bony bucklers. They have hard, elongate, upturned snouts with four ventral barbels ahead of a toothless mouth (Scott and Crossman 1973)(Fig. 4-3). *A. oxyrinchus* is distinguished from other sturgeon by its elongate snout, and two rows of smaller bony plates anterior to the anal fin (Scott and Crossman 1973). Sexually mature sturgeon range in length / mass from 1.8 m / 29 kg (male) to 3.0 m / 115 kg (female) (Scott and Crossman 1973). The largest Atlantic sturgeon documented was found July 1924 at Middle Island, Maugerville, New Brunswick and was female, 4.3 m in length and over 367 kg in mass (Liem and Scott 1966). The sturgeon's diet primarily comprises the amphipod *Corophium volutator*, the bivalve *Macoma balthica*, and assorted worms (*Heteromastus*, *Nereis virens*, *Cerebratulus lacteus*, and *Glycera dibranchiata*) (Fig. 4-4). These organisms are found as a result of rooting through the sediment with the sturgeon's snout and barbels (Bigelow and Schroeder 1953). The prey is extracted from the sediment by a rapid biting motion, which abruptly removes a small substrate cylinder, much of which is passed to the sturgeon's gut.

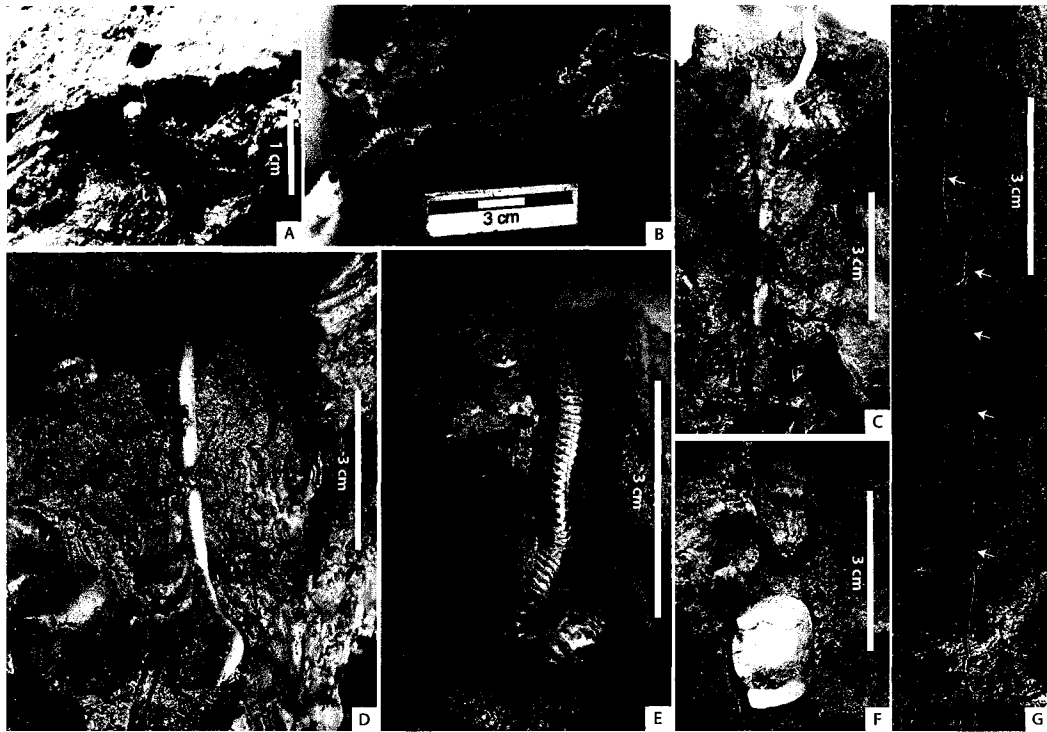


**Figure 4-4:** Infaunal community present within the intertidal sediment at Mary's Point. (A) *Corophium volutator*, scale = 1 cm. (B) *Nereis diversicolor*, scale in centimetres. (C) *Cerebratulus lacteus*, scale = 3 cm. (D) *Glycera dibranchiata*, scale = 3 cm. (E) *Nereis virens*, scale = 3 cm. (F) *Macoma balthica*, scale = 3 cm. (G) *Heteromastus*, scale = 3 cm.

During the months of May to July these large, primitive bony fish are found ascending from coastal waters into their natal freshwater rivers or brackish bays for spawning (Bigelow and Schroeder 1953). While breeding a female sturgeon can lay anywhere from 800,000 to 4,000,000 eggs in a two week period (Liem and Scott 1966). Upon hatching these young sturgeon or juveniles will remain in the fresh or brackish water of their natal rivers/estuaries between one and six years before migrating into the coastal waters (Bigelow and Schroeder 1953).

#### 4.3 FEEDING EXCAVATION OF *ACIPENSER OXYRHYNCHUS*

Numerous foraging and feeding traces have been observed on the intertidal mud flats in the upper reaches of the Bay of Fundy. These divots—found in abundance on Mary's Point—are concentrated on, but not restricted to, the banks of the intertidal

creeks (Fig. 4-5). Here the sturgeon feed on the amphipod *Corophium volutator*, as well as the bivalve *Macoma balthica* and various worms (*Heteromastus*, *Nereis virens*, *Cerebratulus lacteus*, and *Glycera dibranchiata*). These organisms are found at depths between 5-15 cm below the sediment-water interface. Feeding traces are composed of two indentations: a crescent-shaped impression, and a cylindrical, plug-shaped excavation (Fig. 4-1). The morphological configuration of the impression and excavation correspond to the anatomical arrangement of the snout and protractile mouthparts characteristic of the Atlantic sturgeon. Four curved grooves that radiate from the opened portion of the crescentic crest towards the excavation are commonly preserved and represent the impression of the sturgeon's barbels located between the snout and mouthparts (Fig. 4-1). The cylindrical excavations have diameters varying from 5 to 15 cm with corresponding depths that range between 2 and 6 cm. The substrate that these traces occur ranges in consistency from locally fluid to cohesive; is oxidized and brown colored in the upper 1 to 10.5 cm (average 3.9 cm), but suboxic and blue-black in color below. It is composed dominantly of silt and clay with very little sand. The sturgeon traces are never associated with an outline of the fish's body, but rare fin traces (*Undichnia*) are observed (Fig. 4-6). In general the fish does not leave a body impression while feeding.

Tidal processes and sediment from suspension infill the feeding pits but these pits also impound bay water, at least shortly following their excavation. Sturgeon fecal material, which is deposited throughout the tidal flat, consists of very loose sediment, and shell and plant material (Fig. 4-7): the stool breaks apart and is reworked after two tidal cycles.

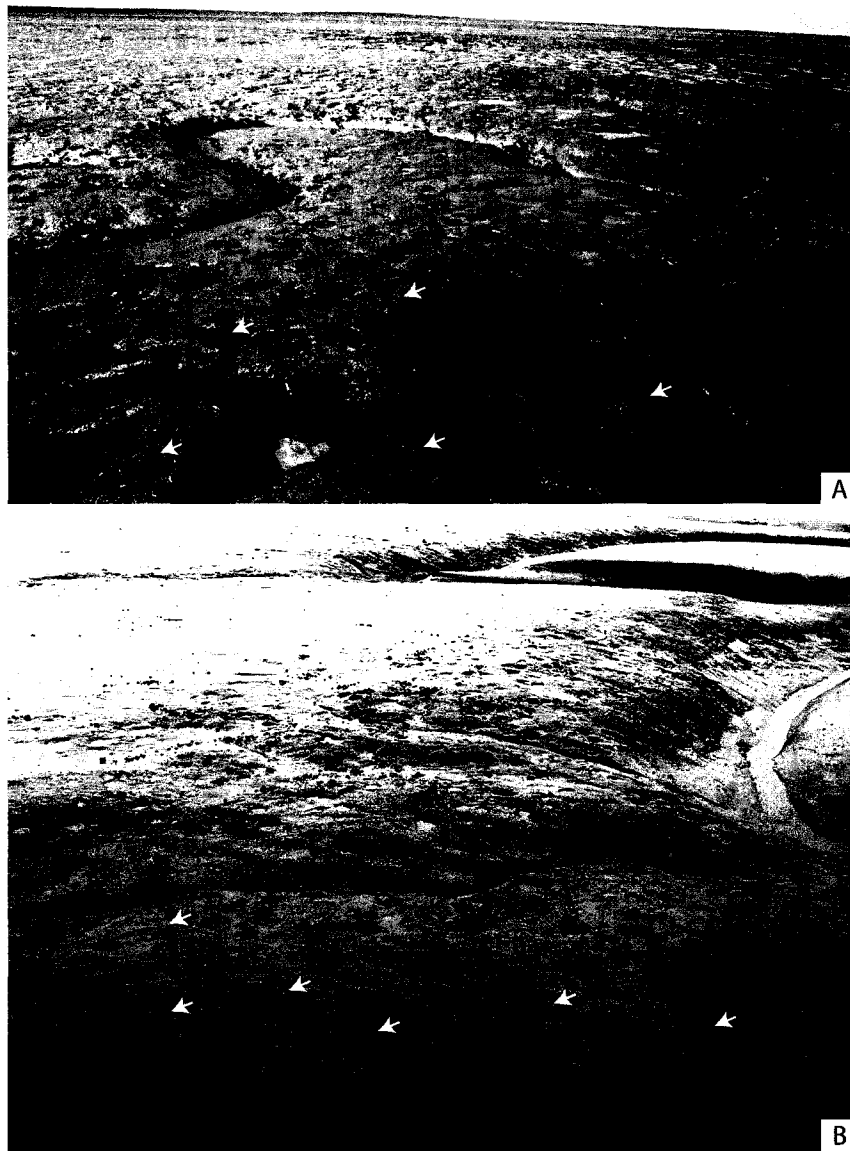


**Figure 4-5:** A comparison between the intertidal mud flat surfaces between May 2003 and July 2004. Arrows highlight individual examples of the sturgeon traces. Note that bay water is pooling in many of the excavations. (A) Sturgeon feeding at the height of spawning season. The intertidal mud flat is completely reworked by their foraging activity. Both the banks of the intertidal creek and the mud flat surfaces adjacent to it are littered with traces. Photo taken in May 2003. (B) Sturgeon feeding frenzy on the bank of the intertidal creek. On this bank there are over 400 individual excavations present. Noteworthy is the lack of feeding pits on the mud flat surfaces adjacent to the intertidal creek. Photo taken in July 2004.



**Figure 4-6:** Atlantic sturgeon fin-trace (*Undichnia*), scale in centimeters.

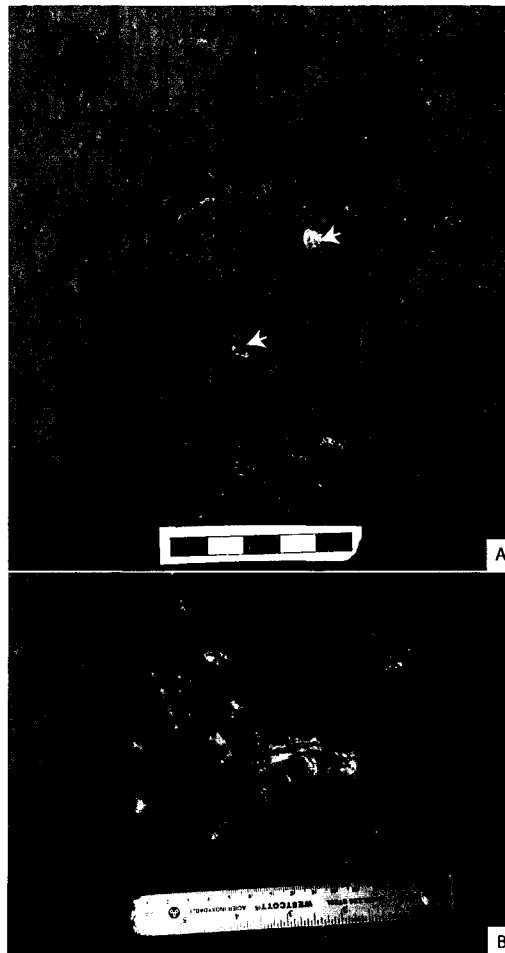


**Figure 4-7.** Atlantic sturgeon fecal material. (A) Example of fecal material broken up by tidal processes. It usually takes at least two tidal cycles to break up this material. Arrows point to shell debris contained in expelled sediment. Scale is in centimetres. (B) Example of fecal material not broken up by tidal processes. Scale is 15 cm.

#### 4.4 ORGANISM AND TRACE DISTRIBUTION

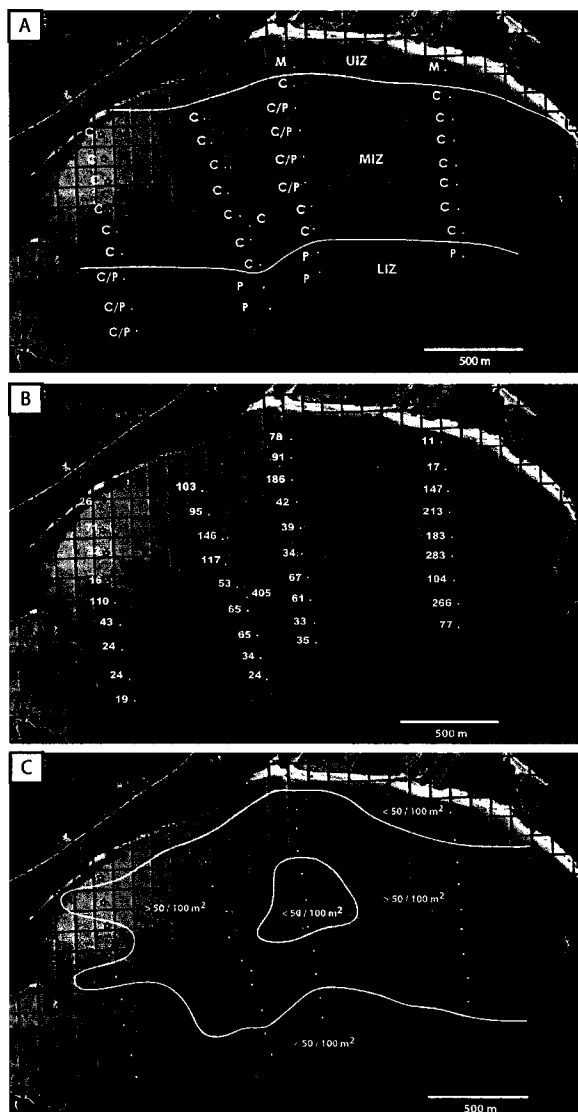


**Figure 4-8:** Schematic diagram showing infaunal distribution and Atlantic sturgeon feeding trends across Mary's Point. (A) Infaunal distribution across Mary's Point. Letters indicate dominant food source for the Atlantic sturgeon at each stations. C= *Corophium volutator*, M= *Macoma balthica*, and P= polychaetes. In instances where the dominant food source is more then one organism both are included. Subdivision of the intertidal mud flat through the distribution of dominant benthos is shown. UIZ= Upper Intertidal Zone, MIZ= Middle Intertidal Zone, and LIZ= Lower Intertidal Zone. (B) Atlantic sturgeon feeding trace distribution across Mary's Point. The number of sturgeon excavations found at each station is shown. (C) This diagram highlights general areas of high (>50 traces / 100 m<sup>2</sup>) and low (<50 traces / 100 m<sup>2</sup>) trace abundance. Note that areas of high sturgeon trace abundance are loosely correlated with areas dominated by the amphipod *Corophium volutator*. The grid was taken from a NTS map, each square is 100 X 100 m.

#### 4.4.1 Observations

At Mary's Point the intertidal mud flat encompasses an area of 12 km<sup>2</sup>. The sediment on these mud flats is colonized by the bivalve *Macoma balthica*, the amphipod *Corophium volutator*, and various worms (*Nereis virens & diversicolor*, *Heteromastus*, *Cerebratulus lacteus*, and *Glycera dibranchiata*). The distribution of the infauna provides a rationale for subdivision of the intertidal flat (Fig. 4-8A). The upper intertidal zone primarily contains *Macoma balthica* and *Corophium volutator*. This zone is characterized by infaunal population densities ranging between 2300 and >5000 individuals / m<sup>2</sup> (average 4275 individuals / m<sup>2</sup>). *Corophium volutator*, *Heteromastus*, *Nereis virens* and *N. diversicolor* characterize the middle intertidal zone. Therein, infaunal population densities are slightly lower and range from 300 to >5000 individuals / m<sup>2</sup> (average >5000 individuals / m<sup>2</sup>). Various worms (*Nereis virens*, *N. diversicolor*, *Heteromastus*, *Cerebratulus lacteus*, and *Glycera dibranchiata*) typify the lower intertidal zone. Within this zone infaunal population densities decrease significantly and extend from 100 to >5000 individuals / m<sup>2</sup> (average 2100 individuals / m<sup>2</sup>).

As shown in Figure 2-8B, C the number of sturgeon excavations in the upper intertidal zone ranges from 11 to 78 excavations / 100 m<sup>2</sup> (average 44 excavations / 100 m<sup>2</sup>). The middle intertidal zone has 53 to 405 excavations / 100 m<sup>2</sup> (average 136 excavations / 100 m<sup>2</sup>). In the lower intertidal zone these erosional divits range in number from 19 to 43 / 100 m<sup>2</sup> (average 32 excavations / 100 m<sup>2</sup>).

#### 4.4.2 Interpretations

The observed changes in the benthos and population density within each intertidal zone apparently correlate to the number of sturgeon traces found across the intertidal mud flat. Specifically, the feeding activity of the Atlantic sturgeon is greatest in the areas that have the maximum concentration of *Corophium*: high densities of *Corophium volutator* are about 500 m from the mean high tide mark, or about 3m below mean high water

(MHW). Although the presence of a richer food resource would certainly entice bottom feeders to attend certain areas of the flat, a reasonable depth of water is required to afford sturgeon space for mobility. Also, the amount of time afforded to subaqueous feeding is increasingly shorter as the intertidal flat is ascended. It is likely that the distribution of intertidal sturgeon is influenced mostly by both the distribution of its prey and the depth of water. In a macrotidal setting, such as Mary's Point, the distribution of food probably represents the primary factor, as the high tides permit movement of large fish onto and off of the intertidal flats.

#### 4.5 ORIENTATION AND TIME OF EXCAVATION

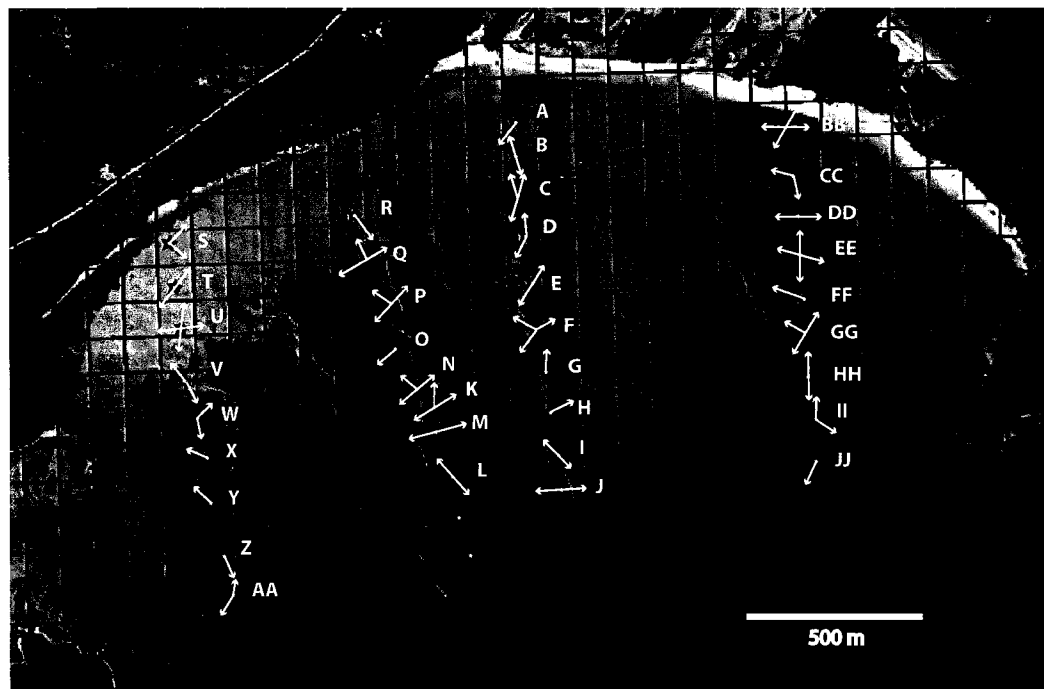


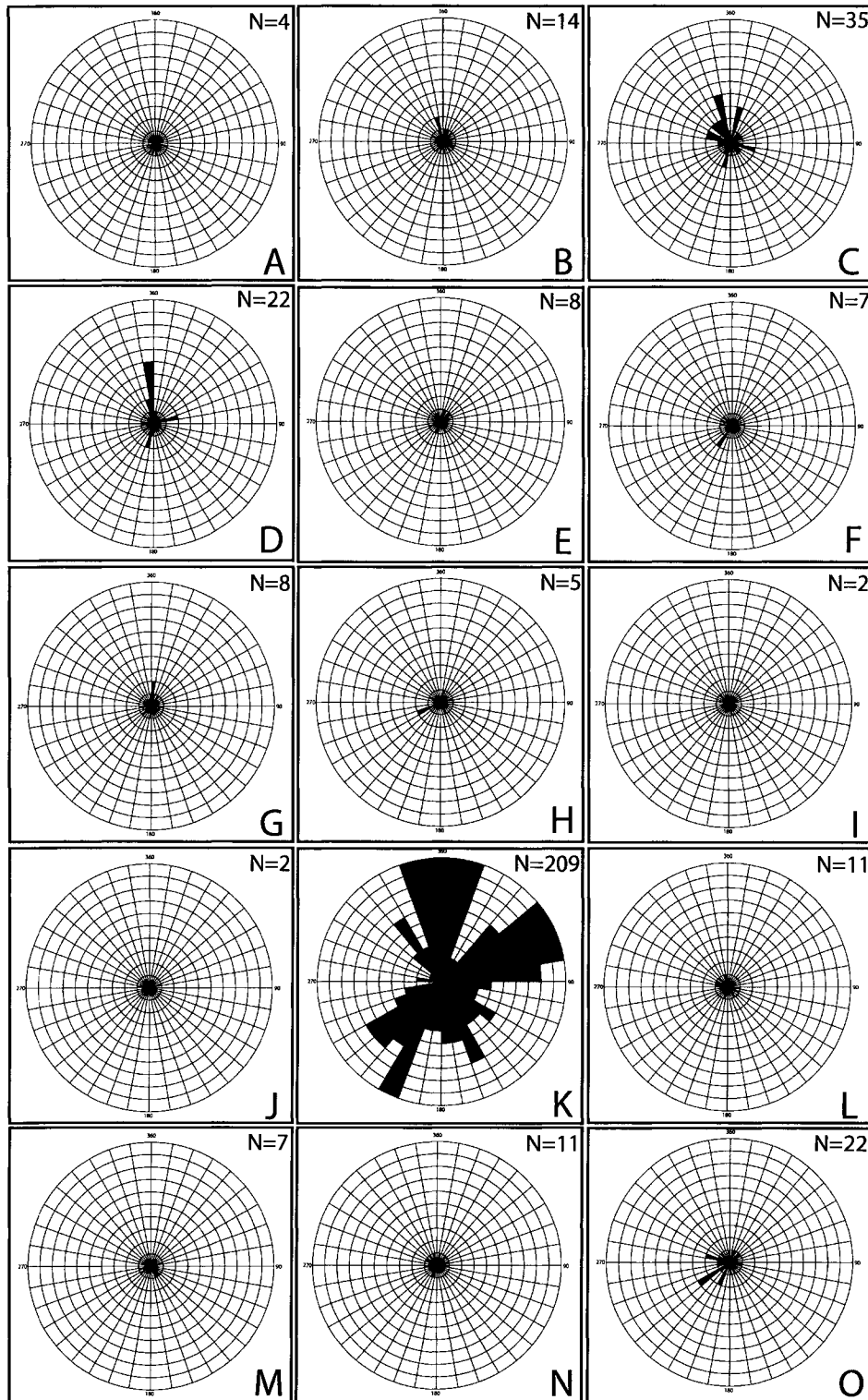
**Figure 4-9:** Schematic representation of average orientation trends at each station at Mary's Point. Arrows highlight the directions the fish are aligning. The grid was taken from a NTS map, each square is 100 X 100 m.

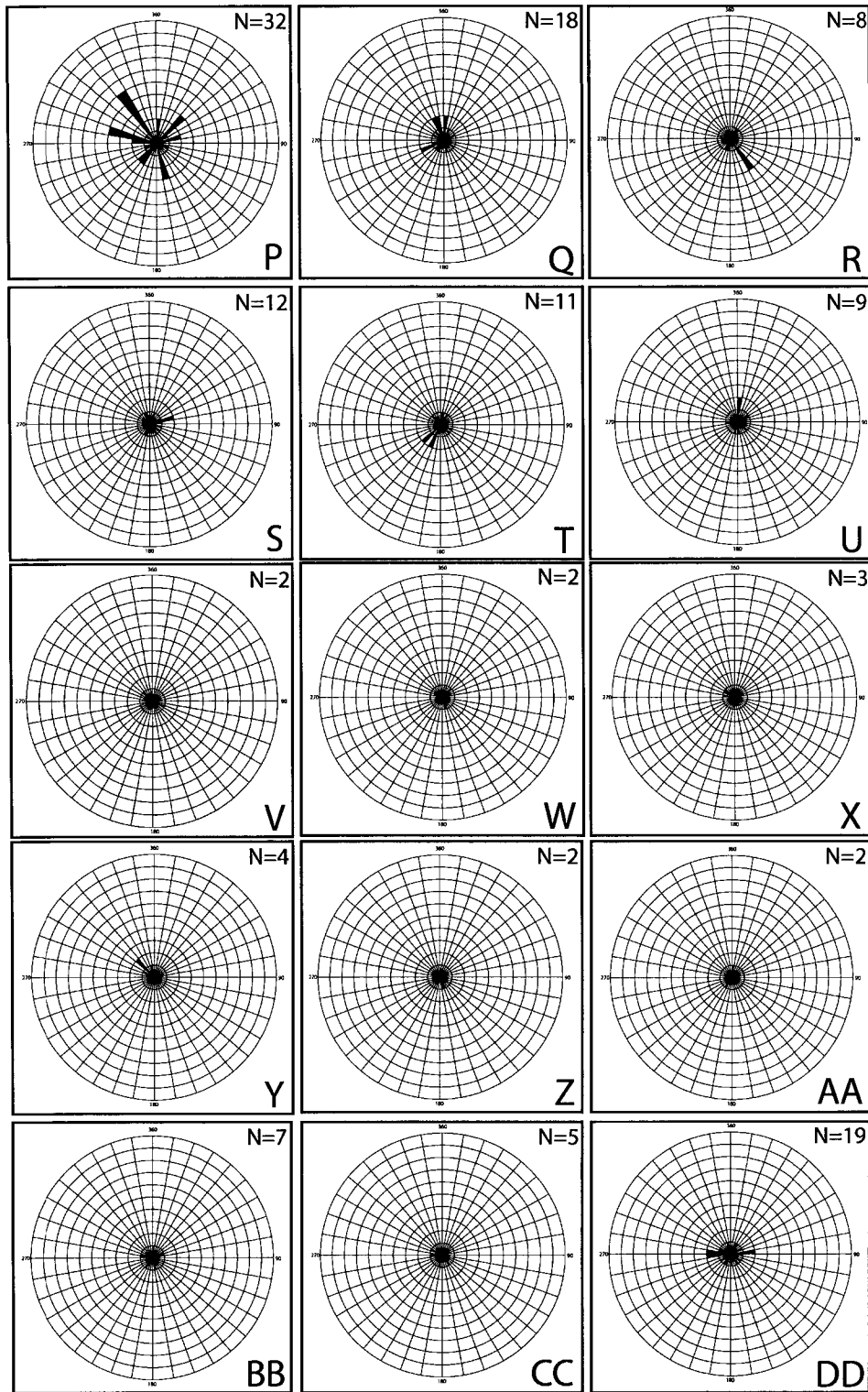
##### 4.5.1 Observations

Howard et al. (1977) and Gregory et al. (1979) noted that the eagle ray of New Zealand excavated a *Piscichnus*-like trace and due to its body size, the rays had to point

into hydraulic currents to remain stable. Due to the sturgeon's size, particularly its length, the fish must also point into hydraulic currents to maintain stability while feeding. Unfortunately, it was impossible to observe sturgeon behavior directly—the turbid water at Mary's Point offers no visibility. However, the orientations of the sturgeon-snout impressions present discernible patterns (Figs. 4-9, 4-10). Figure 4-10 shows the overall orientation and abundance of feeding traces found on the intertidal surfaces of Mary's Point. Within the sturgeon-snout orientation data there were three prevailing azimuth trends (Fig. 4-9): (1) traces oriented from  $200^{\circ}$  to  $260^{\circ}$ ; (2) traces oriented between  $20^{\circ}$  and  $80^{\circ}$ ; and (3) traces oriented from  $0^{\circ}$  to  $20^{\circ}$ ,  $80^{\circ}$  to  $200^{\circ}$ , and  $260^{\circ}$  to  $360^{\circ}$ .

In general, current directions during rising and falling tide could be inferred by observing and walking with the rising tide and observing sedimentary structures produced during the falling tide. Naturally, the dominant flood-tidal currents are generated during rising tide conditions (Fig. 4-11A) the observed dominant flood-current direction was at approximately  $45^{\circ}$  (NE; i.e. associated with snout-trend 1, above). Ebb-tidal currents especially typify the initial to medial stages of the falling tide (Fig. 4-11C): the dominant ebb current occurred at about  $225^{\circ}$  (SW, i.e. associated snout trend 2, above). The final stages of falling tide are dominated by local currents that are directed towards the intertidal creeks (Fig. 4-11D). Local currents near the intertidal creeks vary depending on the position near the creeks and the local tidal creek morphology; the local currents are represented by the more 'random' snout-trend 3, above.





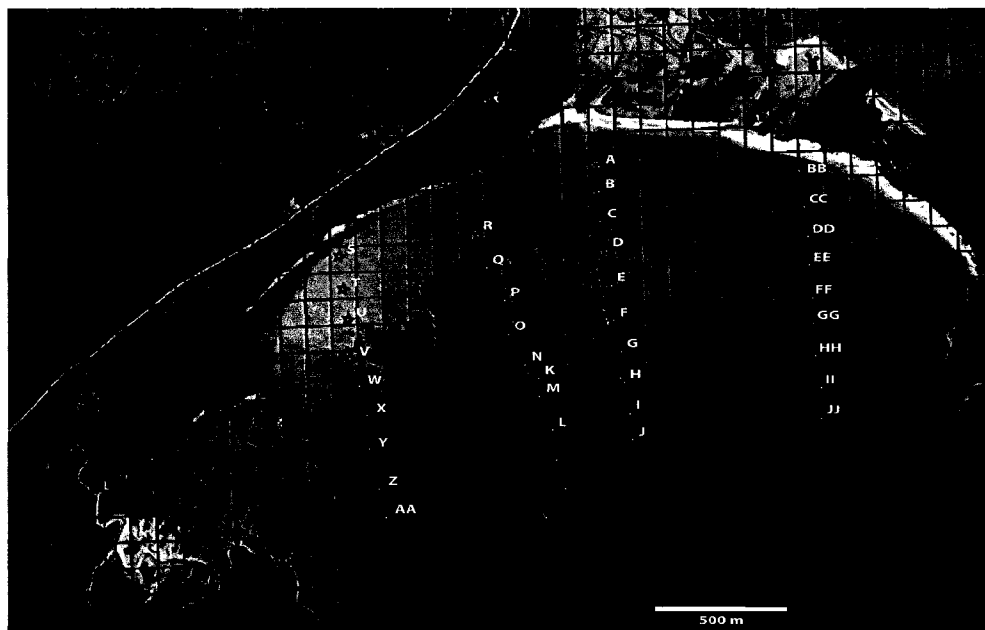
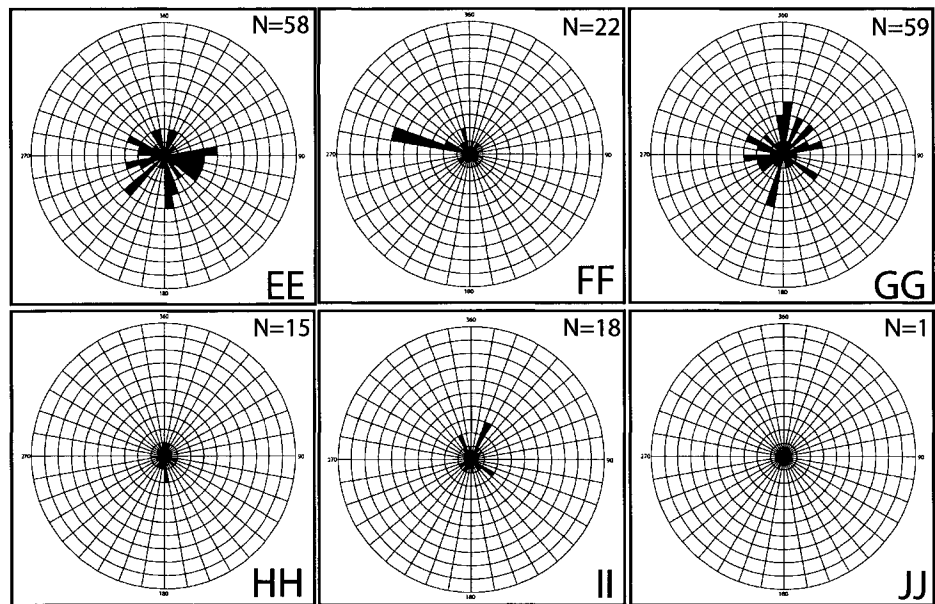


**Figure 4-10.** Rose diagrams constructed for the sturgeon-snout orientations with  $10^\circ$  petals. Letters correspond to individual stations at Mary's Point (inset map). Each rose diagram corresponds to an area of  $100 \text{ m}^2$ . The grid for the inset map was taken from a NTS map, each square is  $100 \times 100 \text{ m}$ .

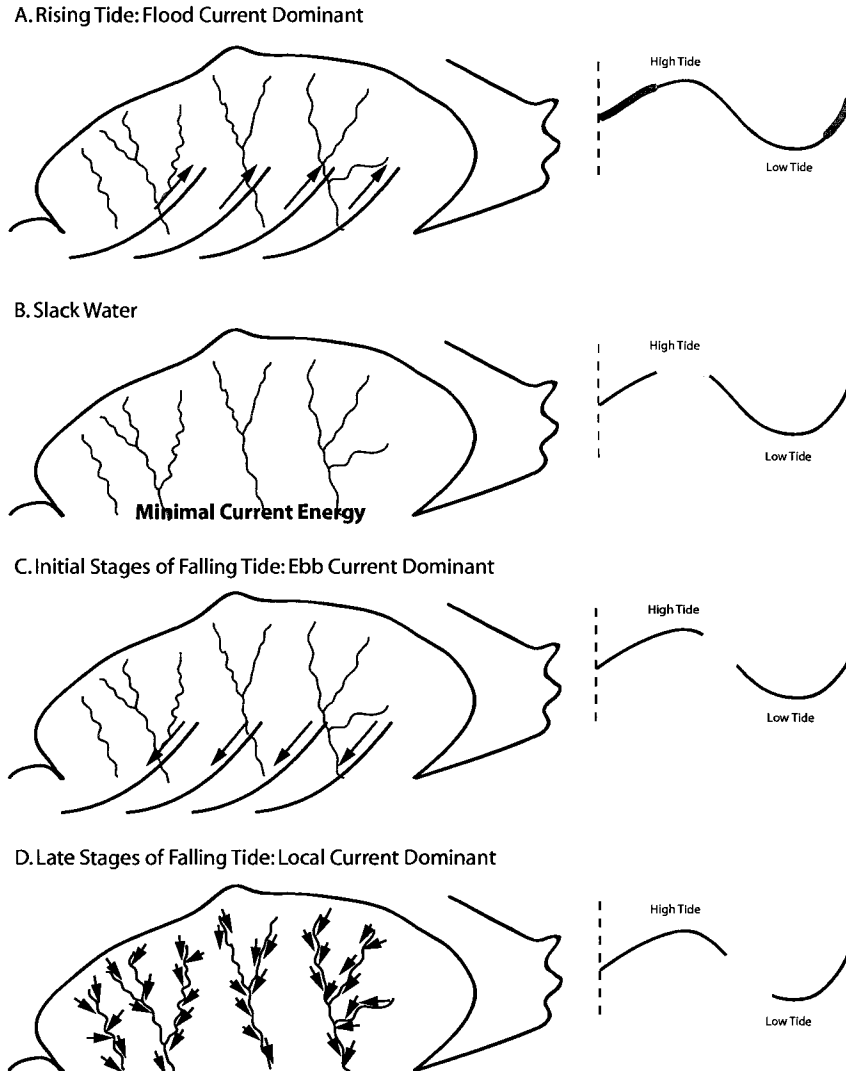


**Figure 4-11.** Schematic diagram demonstrating dominant current directions during the subsequent stages of the tidal cycle at Mary's Point. (A) At rising tide flood currents ( $\sim 45^\circ$ ) are dominant on the intertidal flat. As such, you can expect sturgeon-snout orientations parallel but opposite to this direction ( $200^\circ$  to  $260^\circ$ ). (B) During slack-water conditions minimal current energy is observed. This stage is short ( $\sim 30$  minutes) and orientations of the traces can be in any direction. (C) Initial stages of falling tide are characterized by tidal currents in the ebb direction ( $\sim 225^\circ$ ). Under these circumstances sturgeon-snout orientations will be parallel but opposite to this direction ( $20^\circ$  to  $80^\circ$ ). (D) The final stages of falling tide are dominated by local currents directed towards the intertidal creeks. During this phase trace orientations are found in many directions but can be grouped into the following orientations  $0^\circ$  to  $20^\circ$ ,  $80^\circ$  to  $200^\circ$ , and  $260^\circ$  to  $360^\circ$ . The sturgeon-snout orientations will rely on position near the intertidal creek, tidal creek morphology and which intertidal creek observations are made at. Note: Slack-water phase at low-tide is not depicted.

#### 4.5.2 Interpretations

Extrapolation of the Atlantic sturgeon feeding patterns at Mary's Point was achieved through the analysis of both the orientation and current-direction datasets. This data supports the idea that Atlantic sturgeon feed oriented into the current. During rising tide conditions and the initial stages of falling tide the fish align head into the dominant flood- and ebb-currents (need a word here), and at the final stages of falling tide the sturgeon align parallel but opposite to the local currents near the tidal creeks. Traces that were oriented against local currents likely represent foraging activity outside of the tidal creeks while drainage is capturing the final falling tide. Slack-water conditions should provide random orientation of feeding structures, however due to the short duration of slack tides very little overprinting by a purely random set of orientations occurs.

#### 4.6 BIOEROSION AND REDEPOSITION CAPABILITIES

Within the upper 5 cm of substrate as much as 90% of the total volume constitutes organisms and open-burrow systems; locally as much as 10% of the substrate (by surface area) is disrupted by Atlantic sturgeon in the course of a spawning season. This is a surprisingly high value that reveals the extent of sediment reworking due to bottom-water feeders in the study area.

As noted above, measured values for the cylindrical plug are as follows:

$r_{\min}$  = Minimum Radius of the Feeding Excavation = 2.5 cm

$r_{\max}$  = Maximum Radius of the Feeding Excavation = 7.5 cm

$d_{\min}$  = Minimum Depth of the Feeding Excavation = 2.0 cm

$d_{\max}$  = Maximum Depth of the Feeding Excavation = 6.0 cm

0.10 = Minimum Proportion of Feeding Excavation Volume Composed of Sediment

These values can be used to approximate the volume of sediment that is eroded and resuspended by Atlantic sturgeon in the study area:

$$V_{BE} = \pi r^2 d (0.10) \quad (1.1)$$

$$\begin{aligned} V_{BEmin} &= (3.14)(2.5 \text{ cm})^2(2.0 \text{ cm})(0.10) \\ &= 3.93 \text{ cm}^3 \end{aligned}$$

$$\begin{aligned} V_{BEmax} &= (3.14)(7.5 \text{ cm})^2(6.0 \text{ cm})(0.10) \\ &= 105.98 \text{ cm}^3 \end{aligned}$$

$V_{BE}$  = Volume of Sediment Bioeroded

In other words, Atlantic sturgeon remove and redistribute 3.9 to 105.9 cm<sup>3</sup> of sediment with each bite. The amount of sediment redistributed across Mary's Point as a whole can also be calculated:

$$V_{SR} = V_{BE} A n_{EX} \quad (1.2)$$

$$\begin{aligned} V_{SRmin} &= (3.93 \text{ cm}^3)(12 \text{ km}^2)(96 / 100 \text{ m}^2) \\ &= 44.93 \text{ m}^3 \end{aligned}$$

$$\begin{aligned} V_{SRmax} &= (105.98 \text{ cm}^3)(12 \text{ km}^2)(96 / 100 \text{ m}^2) \\ &= 1220.89 \text{ m}^3 \end{aligned}$$

$V_{SRmin}$  = Minimum Volume of Sediment Redistributed

$V_{SRmax}$  = Maximum Volume of Sediment Redistributed

$V_{BE}$  = Volume of Sediment Bioeroded

A = Area of Mary's Point

$n_{EX}$  = Average number of Feeding Excavations

Overall the Atlantic sturgeon has the ability to erode and resuspend 44.9 to 1220.9 m<sup>3</sup> of sediment across the entire intertidal mud flat at Mary's Point. The above calculations

depend on burrow counts that were collected throughout the summer spawning season. As such they most likely represent the amount of sediment eroded and redistributed over a time span of approximately 6-8 weeks.

#### 4.7 DISCUSSION

Noteworthy in this study are three main points: (1) density of *Piscichnus* can be correlated, at least in part, to the population density of their prey, (2) feeding excavations of larger bottom feeders are likely to be sensitive to the direction of the hydraulic currents, and (3) large vertebrate bottom feeders can be a significant agent of bioerosion—even in clastic depositional settings.

Several marine animals forage within sediment substrates for prey including: elasmobranch fishes (Gregory et al. 1979; Kotake and Nara 2002), fish (Cook 1971), crabs (Zaklan and Ydenberg 1997), sea stars (Fukuyama and Oliver 1985), sea otters (Shimek 1977; Calkins 1978), whales (Nelson and Johnson 1987; Nelson et al. 1987; Klaus et al. 1990), and walruses (Oliver et al. 1983; Fukuyama and Oliver 1985; Gingras et al. in review). Despite the range of animals engaged in this behavior, their trace fossils are not commonly observed in the rock record. Perhaps due to the paucity of fossil *Piscichnus*, associated prey and predator relationships are not commonly reported from the rock record. However, two outstanding occurrences of *Piscichnus* show that bottom feeding traces and trace fossils are likely a response to the presence of prey. The first is Kotake and Nara (2002), who detail high-density *Piscichnus* that are associated with a productive infauna. The second is Gingras et al. (in review), which shows a direct relationship between walrus-generated *Piscichnus* and infaunal bivalves.

The idea that paleocurrents could be deduced from biogenic structures is not completely novel (Howard et al. 1977). However, the sturgeon traces detailed above provide a startlingly good example. In fact, the azimuth-range of tidal currents within the local depositional environment is discernible (Fig. 4-11) from the measured and oriented

traces. This simply has not been observed in the rock record. Unfortunately, many *Piscichnus* traces comprise only a bowl-shaped structure associated with the animal's mouth. Ray traces reported from the Book Cliffs by Komola et al. (1985) are likely oriented concordantly with depositional currents, but research on this subject has not been conducted.

Finally, the activity of invertebrates is known to cause bioerosion, but only a few examples of bioerosion due to marine vertebrates have been reported. Nelson and Johnson (1987) and Nelson et al. (1987) documented that Pacific walruses and California grey whales disturb sea bottom sediment in their attempts to forage for food. The California grey whales ingest both sediment and prey creating large pits on the sea floor (2.5 X 1.5 X 0.1 m) (Nelson and Johnson 1987; Nelson et al. 1987). Ingested sediment is either expelled on the sea floor or more often near the water's surface while they come up for air (Nelson and Johnson 1987; Nelson et al. 1987). The Pacific walruses physically and hydraulically root in the sediment creating linear furrows (47 X 0.4 X 0.1 m) (Nelson and Johnson 1987; Nelson et al. 1987). It has been determined that these two organisms were responsible for the erosion and redistribution of approximately  $195 \times 10^6$  m<sup>3</sup> sediment in one feeding season (Nelson and Johnson 1987; Nelson et al. 1987). In comparison to Nelson and Johnson's (1987) and Nelson et al.'s (1987) findings, with respect to volumetric significance, our sturgeon pale in comparison to the whales and walruses. However, the density of sturgeon traces locally suggests that the sturgeon can be an important sedimentary agent: one that is surely not accounted for in studies of ancient rocks.

#### **4.8 CONCLUSIONS**

The analysis of the feeding excavations found at Mary's Point, New Brunswick, Canada, leads to four key conclusions:

- (1) The feeding excavation morphology (crescent-shaped impression followed by a cylindrical, plug-shaped excavation) corresponds to the anatomical arrangement of the Atlantic sturgeon's snout and protractile mouthparts. The Atlantic sturgeon uses its sensory organs, its barbels, to root around the silty mud for food. Once a food source has been established it is then sucked up into the fish's protractile mouth along with a large quantity of sediment.
- (2) The distribution of feeding excavations on the intertidal mud flat reveals that feeding activity is greatest in the areas that have the maximum concentration of *Corophium volutator*. This area coincides with the middle intertidal zone or within 500 m of the mean high tide mark.
- (3) Analysis of both the trace orientation and current data supports Atlantic sturgeon feeding in a current sensitive manner. During high tide conditions the fish aligns head into the dominant flood- and ebb-current (~45° and 225° respectively), while at initial falling tide it aligns parallel but opposite to the more variable local currents near the intertidal creeks.
- (4) With the aid of volumetric calculations (Equations 1.1 & 1.2) it was determined that the Atlantic sturgeon disrupts and resuspends 3.9 to 105.9 cm<sup>3</sup> of intertidal sediment with each feeding excavation. Overall the Atlantic sturgeon is responsible for the bioerosion of 44.9 to 1220.9 m<sup>3</sup> of sediment across Mary's Point in a 6 to 8 week time period.

With respect to the rock record, we suggest that *Piscichnus* should normally be associated with high infaunal biomass. Where *Piscichnus* are found to be abundant in the rock record, their impact on sedimentary processes should be considered (cf. Kotake and Nara 2002). Finally, the potential utility of subaqueous vertebrate trace fossils to be oriented into hydraulic currents should not be overlooked in rock-record examples. Future work will focus on linking ancient examples to the remarkable modern occurrences outlined above.

#### 4.9 REFERENCES

- Amos, C.L., 1987, Fine-grained sediment transport in Chignecto Bay, Bay of Fundy, Canada: *Continental Shelf Research*, v. 7, p. 1295-1300.
- Bigelow, H.B., and Schroeder, W.C., 1953, *Fishes of the Gulf of Maine: Fishery Bulletin of the Fish and Wildlife Service*, Washington, v. 53, p. 81-84.
- Calkins, D.G., 1978, Feeding behavior and major prey species of sea otter, *Enhydra lutris*, in Montague Strait, Prince William Sound, Alaska: *Fishery Bulletin*, v. 76, p. 125-131.
- Cook, D.O., 1971, Depressions in shallow marine sediment made by benthic fish: *Journal of Sedimentary Petrology*, v. 41, p. 577-602.
- Desplanque, C., and Mossman, D.J., 2001, Bay of Fundy tides: *Geoscience Canada*, v. 28, p. 1-11.
- Fukuyama, A.K, and Oliver, J.S., 1985, Sea star and walrus predation on bivalves in Norton Sound, Bering Sea, Alaska: *Ophelia*, v. 24, p. 17-36.
- Gingras, M.K., Armitage, I.A., Pemberton, S.G., and Clifton, H.E., in review, First fossil evidence of walrus predation traces link ancient walrus herds to the Olympic Peninsula: *Palaios*.
- Gregory, M.R., 1991, New trace fossils from the Miocene of Northland, New Zealand: *Rorschachichnus amoeba* and *Piscichnus waitemata*: *Ichnos*, v. 1, p. 195-205.
- Gregory, M.R., Mallance, P.F., Graham, W.G., and Ayling, A.M., 1979, On how some rays (Elasmobranchia) excavate feeding depressions by jetting water: *Journal of Sedimentary Petrology*, v. 49, p. 1125-1130.

Howard, J.D., and Frey, R.W., 1975, Regional animal-sediment characteristics of Georgia estuaries: *Senckenbergiana Maritima*, v. 7, Estuaries of the Georgia Coast, USA; *Sedimentology and Biology*, p. 1-31.

Howard, J.D., Mayou, T.V., and Heard, R.W., 1977, Biogenic sedimentary structures formed by rays: *Journal of Sedimentary Petrology*, v. 47, p. 339-346.

Klaus, A.D., Oliver, J.S., and Kvitek, R.G., 1990, The effects of gray whale, walrus, and ice gouging disturbance on benthic communities in the Bering Sea and Chukchi Sea, Alaska: *National Geographic Research*, v. 6, p. 470-484.

Komola, D., Pfaff, B., Newman, S.L., Frey, R.W., and Howard, J.D., 1985, Field trip no. 10: Depositional facies of the Cretaceous Castlegate and Blackhawk formations, Book Cliffs, eastern Utah: *SEPM (SSG), Rocky Mountain Sector*, Denver, Colorado, USA, 152p.

Kotake, N., and Nara, M., 2002, The ichnofossils: *Piscichnus waitemata*: a biogenic sedimentary structure produced by the foraging behavior using water jet: *Geological Society of Japan*, v. 108, p. 1-2.

Liem, A.H., and Scott, W.B., 1966, Fishes of the Atlantic Coast of Canada: Fisheries Research Board of Canada, Ottawa, Bulletin no. 155, p. 82-83.

Nelson, C.H., and Johnson, K.R., 1987, Whales and walruses as tillers of the sea floor: *Scientific American*, v. 256, p. 112-117.

Nelson, C.H., Johnson, K.R., and Barber, J.H. Jr., 1987, Gray whale and walrus feeding excavations on the Bering Shelf, Alaska: *Journal of Sedimentary Petrology*, v. 57, p. 419-430.

Oliver, J.S., Slattery, P.N, O'Connor, E.F., and Lowry, L.F., 1983, Walrus, *Odobenus Rosmarus*, feeding in the Bering Sea: A benthic perspective: Fishery Bulletin, v. 81, p.501-512.

Scott, W.B., and Crossman, E.J., 1973, Freshwater Fishes of Canada: Fisheries Research Board of Canada, Ottawa, Bulletin no. 184, p. 92-95.

Shimek, S.J., 1977, The underwater foraging habits of the sea otter, *Enhydra lutris*: California Fish and Game, v. 62, p. 120-122.

Zaklan, S.D., and Ydenberg, R., 1997, The body size-burial depth relationship in the infaunal clam *Mya arenaria*: Journal of Experimental Marine Biology and Ecology, v. 215, p. 1-17.

## 5.0 CONCLUSIONS

(1) The detailed analysis of the fine-grained (mud-dominated) deposits associated with inner estuarine point bars and mud flats found at Mary's Point and the Shepody River allow for subdivision of the intertidal environment based on ichnological and sedimentological trends.

(2) The neo-ichnology of the inner estuarine point bar and mud flat environments provided useful criteria for distinguishing the depositional subenvironments found within each locale. In the Shepody River point-bar deposits: *Polykladichnus*- and *Skolithos*-like traces characterized the upper-subtidal and lower-intertidal zones; *Arenicolites*-, *Diplocraterion*-, *Polykladichnus*-, *Palaeophycus*-, and *Planolites*-like forms were pervasive in the middle-intertidal portion of the point bar; and, *Siphonichnus*- and *Polykladichnus*-like burrows typified the upper-intertidal zone and the adjacent mud flats. In the Mary's Point mud-flat deposits: *Polykladichnus*, *Skolithos*, *Palaeophycus*, and *Planolites* traces were indicative of the lower-intertidal zone; *Arenicolites*, *Diplocraterion*, *Polykladichnus*, *Skolithos*, *Planolites*, *Palaeophycus*, and *Siphonichnus* forms were abundant in the middle-intertidal zone; and *Siphonichnus*, *Arenicolites*, *Diplocraterion*, *Polykladichnus*, *Planolites* and *Palaeophycus* burrows typified the upper-intertidal zone.

(3) The size and diversity of the burrowing fauna were controlled by temperature fluctuations and seasonal compositional variations within the bay waters. The infaunal assemblage was characterized by a low diversity of traces that were present in high abundance—a pattern commonly noted in brackish-water environments. However, the low diversity and high infaunal abundances found within the inner estuary also reflect seasonal opportunism, which seems to be indistinguishable from the brackish-water signature.

(4) Within the inner-estuarine deposits beds are rhythmically laminated. This lamination was defined by thinly interbedded silty- and sandy-mud. Within both the

point-bar and mud-flat deposits bedding was parallel to the depositional surface. In the case of the point bars, beds dip towards the channel and represented mud-dominated inclined heterolithic stratification. On the intertidal-flat surface there was no dip and lamination was horizontal, and planar-bedded.

Rhythmic bedding observed in the inner-estuarine deposits represented tidal- and seasonal-processes. Tidal processes were recorded in the beds as rhythmic lamination and rare preserved starved ripples. Intercalated laminated/burrowed beds reflect seasonal variations in the depositional system. The laminated beds characterize early winter and (primarily) spring sediments, and the bioturbated beds typify summer and fall deposits. Although the burrowed interbeds were deposited under the same tidal conditions in which the laminated beds accumulated in, biogenic reworking eliminated the primary sedimentary signature.

(5) The tidal deposits result from deposition of flocculated material and traction-borne sediment during the flood- and ebb-tide and to a larger extent the slack-water accumulation of fines from suspension and flocculated material from “rapid settling”. Cyclic changes in laminae thickness resulted from neap-spring variation in tidal current strength. Within the neap-spring bundles changes in laminae thickness is attributed to diurnal inequality.

To conclude, the deposits from Mary’s Point and the Shepody River provide excellent modern examples of inner estuarine point bar and mud flat environments. This study is a comprehensive representation of the sedimentological and ichnological characteristics that are found within each of these environments. This study provides tools for more thorough comparisons between modern and ancient muddy estuarine deposits for application in paleoenvironmental reconstruction.